Title

Controlling Complex Systems and Developing Dynamic Technology

Permalink

https://escholarship.org/uc/item/35c10822

Author

Avizienis, Audrius Victor

Publication Date

2013

Peer reviewed|Thesis/dissertation

Controlling Complex Systems
and Developing Dynamic Technology

A dissertation submitted in partial satisfaction

of the requirements for the degree

Doctor of Philosophy in Chemistry

by

Audrius Victor Avizienis

2013

ABSTRACT OF THE DISSERTATION

Controlling Complex Systems and Developing Dynamic Technology

by

Audrius Victor Avizienis

Doctor of Philosophy in Chemistry

University of California, Los Angeles, 2013

Professor James K. Gimzewski, Chair

In complex systems, control and understanding become intertwined. Following Ilya Prigogine, we define complex systems as having *control parameters* which mediate transitions between distinct modes of dynamical behavior. From this perspective, determining the nature of control parameters and demonstrating the associated dynamical phase transitions are practically equivalent and fundamental to engaging with complexity.

In the first part of this work, a control parameter is determined for a non-equilibrium electrochemical system by studying a transition in the morphology of structures produced by an electroless deposition reaction. Specifically, changing the size of copper posts used as the substrate for growing metallic silver structures by the reduction of Ag^+ from solution under diffusion-limited reaction conditions causes a dynamical phase transition in the crystal growth process. For Cu^0 posts $\sim 1\mu m$, local forces promoting anisotropic growth predominate, and the reaction produces interconnected networks of Ag^0 nanowires. As the post size is increased above $\sim 10\mu m$, the local interfacial growth reaction dynamics couple with the macroscopic diffusion field, leading to spatially propagating instabilities in the electrochemical potential which induce periodic branching during crystal growth, producing dendritic deposits. This result is interesting both as an example of control and understanding in a complex system, and as a useful combination of top-down lithography with bottom-up electrochemical self-assembly.

The second part of this work focuses on the technological development of devices fabricated using this non-equilibrium electrochemical process, towards a goal of integrating a complex network as a dynamic functional component in a neuromorphic computing device. Self-assembled networks of silver nanowires were reacted with sulfur to produce interfacial "atomic switches": $Ag^0-Ag_2S-Ag^0$ junctions, which exhibit complex dynamics (e.g. both short- and long-term changes in conductivity) in response to applied voltage signals. Characterization of these atomic switch networks (ASNs) brought out interesting parallels to biological neural networks, including power-law scaling in the statistics of electrical signal propagation and dynamic self-organization of differentiated subnetworks. A reservoir computing (RC) strategy was employed to utilize measurements of electrical signals dynamically generated in ASNs to perform time-series memory and manipulation tasks including a parity test and arbitrary waveform generation. These results represent the useful integration of a complex network into a dynamic physical RC device.

The dissertation of Audrius Victor Avizienis is approved.

Delroy A. Baugh

Suneel Kodambaka

James K. Gimzewski, Committee Chair

University of California, Los Angeles

2013

to Algis

TABLE OF CONTENTS

List of Figures

LIST OF TABLES

focus my excitable and erratic energies on the tasks at hand. Your daily diligent discipline and perseverance set an example that I strive to emulate. From the finer points of chromic acid baths to the arrangement of surfboard fins, our conversations have invariably been interesting and useful.

Į sveikatą!

1997-2001	Regents' and Chancellor's Scholar
	University of California, Berkeley
2001	B.S. (Chemistry)
	University of California, Berkeley
2007	M.S. (Experimental Physics)
	Vytautas Magnus University
	Kaunas, Lithuania.

Publications

Avizienis, A. V.; Martin-Olmos, C.; Sillin, H. O.; Aono, M.; Gimzewski, J. K. & Stieg, A. Z. Morphological Transitions from Dendrites to Nanowires in the Electroless Deposition of Silver. *Crystal Growth & Design*, ACS Publications, 2013, 13, 465-469.

Avizienis, A. V.; Sillin, H. O.; Martin-Olmos, C.; Shieh, H. H.; Aono, M.; Stieg, A. Z. & Gimzewski, J. K. Neuromorphic atomic switch networks. *PloS one*, Public Library of Science, 2012, 7, e42772.

Stieg, A. Z.; Avizienis, A. V.; Sillin, H. O.; Martin-Olmos, C.; Aono, M. & Gimzewski, J. K. Emergent Criticality in Complex Turing B-Type Atomic Switch Networks. *Advanced Materials*, Wiley Online Library, 2012, 24, 286-293.

Sillin, H. O.; Aguilera, R; Shieh, H. H.; Avizienis, A. V.; Aono, M.; Stieg, A. Z. & Gimzewski, J. K. A theoretical and experimental study of neuromorphic atomic switch networks for reservoir computing. *Nanotechnology*, IOP Publishing, 2013, 24, 384004.

Stieg, A. Z.; Avizienis, A. V.; Sillin, H. O.; Shieh, H. H.; Martin-Olmos, C; Aguilera, R; Sandouk, E.; Aono, M. & Gimzewski, J. K. "Self-organization and Emergence of Dynamical Structures in Neuromorphic Atomic Switch Networks" In: *Memristor Networks* (2014), Eds. Adamatzky & Chua, Springer-Verlag, ISBN 978-3-319-02629-9.

Stieg, A. Z.; Avizienis, A. V.; Sillin, H. O.; Martin-Olmos, C.; Aono, M. & Gimzewski, J. K. Self-organized Atomic Switch Networks. In Press: *Japanese Journal of Applied Physics* (2014).

Sillin, H.O.; Sandouk, E.; Avizienis, A. V.; Aono, M.; Stieg, A. Z. & Gimzewski, J. K. Bench-top Fabrication of Memristive Atomic Switch Networks. In Press: *Journal of Nanoscience and Nanotechnology*, 13, (2013), DOI:10.1166/jnn.2013.8636 - arXiv ID: 1304.1243.

CHAPTER 1

Introduction

Science in those days worked in broad strokes! They got right to the point. Nowadays it's always molecule, molecule, molecule.

—The Tick

The world as we find it is a very complex system. We begin to build an intuitive understanding of this unavoidable structure from sensory perceptions, which vary as a function of both the external environment and internal mental states like mood and focus. Associative memory adds layers of abstraction to this process, giving us the means to determine causal relationships and develop theories to predict the future evolution of events. Where these theories deal with the structure, bonding and reactivity of molecules, we find chemistry.

The chemical world of molecules, we learn in our quantum mechanics classes, has very different rules from the quaint, "classical" world we learned to walk around in. Diving deeply into the matter of developing consistent explanations for a growing body of connected observations, our clever forebears extended their physical understanding beyond the intuitive causal relationships established by the senses, to a place where going from point A to point B doesn't necessarily involve passing through the space between. Even if one is skeptical of the implied metaphysics, technological marvels like the smartphone make a persuasive practical argument for accepting the quantum theory that underpins solid state semiconductor-based electronics.

The scientific method of combining experimental observation and mathematical theory, exemplified by the interplay between Faraday and Maxwell, has proven to be one of the great drivers of human progress. Abstract mathematical tools, fabricated from relentless logical

consistency, enable scientists to proceed where physical intuition falters. When experimental observations defy expectations, and neither reasoned reconsideration nor intuitive leaps can explain the discrepancy, purely mathematical models can be built which fit the data with initially arbitrary. By studying the logical structure of the fitting model, and connecting its abstract elements back to tangible quantities in the physical system which it represents, we can convince ourselves of scientific truths that were unfathomable from previous perspectives, as Planck did in establishing quantum theory from empirical fits of radiation curves.

And so it seems almost rude to ask: how about the weather? For a long time before the advent of atomic theory, people have been coping with regular seasonal variations in their environments as well as sudden manifestations of tremendous natural forces during earthquakes, volcanic eruptions and other spectacular weather events. Those familiar with their local landscape and armed with ancestral lore can develop finely tuned intuitions about which sensory observations constitute important meteorological data, how features of that data combine to create regional weather patterns and anticipate future events. It seems curious, then, that adding information from satellites and using advanced data analysis algorithms has not (yet) produced major improvements in the reliability of weather forecasts.

The confounding factor is *complexity*: an appropriately difficult term to define, as the ability to transition between multiple states is a key feature of complex systems. When objects are dynamically interconnected, new properties can *emerge* which belong to the whole without belonging to any particular part. Complex dynamics often emerge in open, dissipative systems, where matter and energy are exchanged with the surroundings. However, there are no obvious *a priori* principles for making useful distinctions between "systems" and their "surroundings", though they can be intuitively clear in context. On a large scale, we understand the Earth as a system bounded by its gaseous atmosphere, with solar energy flowing in from the surrounding space. On a small scale, we recognize living things as systems bounded by membranes of dynamic permeability, which regulate the exchange of ions and more between their internal structures and the surrounding environment. The trouble with predicting the weather lies in determining the relevant context. In a general sense, we can define weather as a manifestation of emergent dynamics in a planetary system,

an example of pattern formation in dissipative non-equilibrium states sustained by incoming energy flows from solar radiation, nuclear fission, and so on. But consider spatiotemporal variations in sea surface temperature: is El Niño a cause or effect of other weather events? The answer, of course, is that "it's complicated." Complex systems typically contain feedback loops, resonances, and other nonlinear features that make it impossible to isolate and analyze individual parts in terms of simpler, reductive categories.

The local strategy for weather prediction produces reasonably accurate forecasts because restricting the context to a limited set of important features makes it easier to determine their temporal correlations with events of interest. There is some risk of making spurious associations, or overlooking behaviors emerging from more subtle global factors that can manifest resonances at particular confluences of previously uncoupled local states, but simple qualitative analysis starting from an intuitive selection of key parameters can produce very good models that accurate describe the local systems normal dynamic range. The global strategy starts from the high-level, generic context of basic balance equations describing the flow of mass, energy and momentum through the system. Since the precise mathematical form of these flows and the complex couplings between them are not well known, the next step is to parametrize and numerically fit using all available data. This is a massive computational undertaking, the product of which is likely to be undermined by the same complexity it aims to model: the data comes from measurements of systems that can transition into turbulent states with chaotic dynamics that are extremely sensitive to initial conditions, making it practically unfeasible to derive meaningful information from them. In the end, there is no clear practical benefit to choosing the comprehensive global context instead of focusing on a less general but more manageable restricted local context. Finding ways to usefully combine these approaches, maximizing the strengths of each, is an active area of complex systems research.

Developments in our understanding of complex systems suggest that we might be due for more mind-bending adjustments to our modern scientific intuitions. In at least some practical sense, different forces exist at different scales. Predicting oceanic currents by running a quantum molecular dynamical simulation of every molecule in the sea is a not possible

given the available computing resources, which implies we must develop other methods simply for practical reasons. But the problem is bigger than that. It may be the case that such a simulation would still be inaccurate, because the molecular dynamics fail to capture important complex dynamics that emerge at larger size scales. The question remains: where could these properties emerge from, if not the underlying quantum world of the constituent molecules? Does this imply the existence of additional, "undiscovered" fundamental forces of nature? The two major breakthroughs defining modern physics, quantum mechanics and relativity, remain unreconciled. The study of complex systems, with their inherently hierarchical structures, is the most promising approach to bridging that gap between size scales and pushing us into a newer, stranger and even more beautiful world.

The bulk of this dissertation consists of previously published material, a product of the modern "write as you go" approach to graduate study in the sciences. The paper in chapter 3 developed from previously unreported observations of nanowire growth during a diffusion-limited reaction using copper metal to reduce silver ions. We had been using the process to grow dendritic silver structures, following recipes established in the 1980s when this reaction was somewhat popular as an experimental test case for diffusion-limited aggregation (DLA) models. At first, while using mm-sized pieces of copper wire and foil, as in the previous works, we reproduced the expected dendritic structures. Then, while doing a summer internship at NIMS in Tsukuba, Japan with Sakurai-sensei, we ran the same reaction using copper microspheres, expecting to produce a distribution of microscale silver snowflakes, and were startled to instead find silver nanowires (somewhat loosely speaking, as the widths were $\gtrsim 100nm$). Since the reaction was supposed to be diffusion-limited based on the concentration of silver ions, which produced dendrites with branching at intervals significantly smaller than a micron, it seemed as though the same DLA mechanism from the models should still be at work. Clearly, it was not.

It took several years of exploring non-equilibrium systems and nonlinear dynamics to develop a reasonable explanation of the observed transition. In short, under these reaction conditions, silver generally favors growth by stacking along the (111). When the nucleation

4

site is small enough, the DLA mechanism is defeated by the advance of the growth front into the bulk solution–small wires grow fast enough to keep growing as wires. When the reaction area is larger, the growth process does couple with the diffusion field, forming a repeating pattern of instabilities that bring on dendritic growth. On a personal note, I feel very fortunate to have been gifted the magical experience of accidental discovering a previously unreported phenomenon, and am proud to have completed the effort detailed in this work: starting with an unexpected, unexplained result–which we utilized in the main research effort described in the other 3 papers–and studying and experimenting and thinking and developing my understanding of the relevant physical processes until I could offer a reasonable explanation of *why* it happens.

The remaining 3 papers are all focused, from different perspectives, on one main subject: Atomic Switch Networks (ASNs). ASNs were developed in collaboration with our colleagues at NIMS, who did the initial work building single "atomic switches": $Ag-Ag_2S$ junctions, which when probed by STM were observed to extrude single-atom Ag wires from the silver sulfide surface layer. Further experiments on single switches found interesting *memory* properties. For example, the time constant of the (high conductance, wire-formed) ON state had a nonlinear dependence on the form of the bias voltage input. Our group took on the challenge of creating a massively interconnected network of these switches, towards the dream of building a metal brain with inorganic synapses.

In more practical terms, we succeeding in fabricating silver-silver sulfide nanowire networks that exhibited many interesting dynamical properties, with some similarities to isolated atomic switches, along with network-specific behaviors. The paper included in chapter 6 came first, chronologically speaking, written partly as an overview of dynamic computing strategies, and serves to outline the overall research effort. It also includes probably the single most interesting result in this dissertation, namely the power-law statistics of metastable ASN conductance state residence times, as analyzed from the overall network current response to applied voltage pulses. The current usually fluctuates between metastable conductance "plateaus" several times per 10ms pulse, but the power-law extends out into the range of seconds, i.e. no fluctuations in conductivity for more than 10 consecutive pulses. This

result connects to the concept of *criticality* (which turns out to be quite a loaded term) and to the self-organized (SOC) variety in particular . Our understanding of the implications is still developing, but it was certainly an indication that the ASN was something like the functional network of nonlinear elements that we had set out to build.

The paper included in chapter 4 is focused on the network-specific properties of ASNs. Since we have yet to find an effective way of directly observing switching events as they happen, we had to infer the degree to which the network connectivity was a causally significant feature. This lack of direct evidence was responsible for a persistent anxiety about the possibility that all the action was happening at the electrode-ASN interface. The IR camera experiment (in chapter 6) had allayed these fears to some degree, but our first opportunity to test the ASN against a theoretical prediction of memristor network behavior came when Oskoee and Sahimi published the results of their simulation of memristor networks (2011). The simplest prediction to test experimentally regarded higher harmonic generation (HHG). Our first experimental attempt at testing for this effect, using a sine wave voltage bias, found HHG in line with the simulated results. This also provided a control against the dynamical activity observed in untreated silver nanowire networks, which can exhibit conductance fluctuations (presumably arcing between wires), but did not show HHG.

The paper include in chapter 5 details our effort to design an ASN-specific computational model. From the experimentalist's perspective, it is often not clear how best to make further progress with these systems. We fabricated new substrates, with more electrodes in different patterns, and were able to reproduce some of the earlier results on them. But we also saw some differences, including new problems getting clear signals, presumably due to the proximity between and/or smaller size of the new electrodes. This is a basic problem when working with dynamic systems, especially self-assembled ones: they can exhibit a wide range of signal dynamics based on device history and other nonlinear factors, and it can be hard to determine whether the observed dynamics are coming from within the network or from e.g. intermittent contact or limiting charge injection kinetics at the electrode-ASN interface. Where there is a clear objective, as there was after the Oskoee simulation was published, we can design an experiment to test it. Therefore, we set about building our own model,

building in features specific to the $Ag-Ag_2S-Ag$ atomic switch as we understood it. The atomic switch differs from a generic (passive) memristor, as the high conductivity state can be relatively far from equilibrium, leading to the observed tendency for switches to turn off over time We tested the model against experimental results, and found the range of model parameters (keeping physical constants fixed to real values) which reproduced observed behavior. The simulation allows us the view that our instruments have not (yet), to see switching activity at the link-by-link level, and it is encouraging to see a distribution of (simulated) activity that reproduces the experimental data.

Chapter 2 contains more background information about complex systems, non-equilibrium thermodynamics, and other delightful topics. Complexity is difficult to write about, and even more difficult to study with proper scientific rigor. Working with ASNs has produced a continuous stream of frustratingly incomplete experiments, cut short by inopportune manifestations of the underlying nonlinear dynamics. But it has also led to some very interesting results, which have proved resistant to all attempts at unraveling. In the end, these devices do truly seem to be complex networks of nonlinear dynamic functional elements. The story of controlling complex systems and developing dynamic technology is just beginning: I hope that these early results might encourage more scientists to take the nonlinear risks and earn the resonant rewards of wrestling with complexity.

CHAPTER 2

Background

The role of attractors in computation—or in thinking, for that matter—raises a number of fascinating issues at the interface between dynamical systems theory and non-equilibrium physics on the one side, and computer and cognitive sciences on the other side. The results that will arise from this unexpected synthesis are likely to be far-reaching indeed.

— Ilya Prigogine

2.1   Complex Systems

When we think of the phrase *complex system* absent a particular frame of reference, any number of things can jump to mind: a fancy assemblage of gears, traders frantically shouting across a marketplace, an inscrutable logic puzzle, and so on. While these examples are all very different, we can still notice some common features that will serve as our generic point of departure to define complex systems [NPN89]: dynamic networks of interacting elements. The details of the interactions can be complicated, often including *nonlinear* effects such as resonance and memory. Our basic formalism (evidencing a dynamic bias) will be the temporal trajectory of this system: a system of equations describing the temporal evolution of the state variables $\{X_i\}$ that represent the networked elements, which proceeds according to system-specific functional relationships $\{F_i\}$ with the other state variables $\{X_j\}$.

$$\frac{dX_i}{dt} = F_i(X_j, \lambda) \tag{2.1}$$

We have also included a quantity λ, which we call a *control parameter*. As the obvious

outlier in Eq. 2.1, the control parameter is the essential feature delineating this formalism for complex systems, from systems of equations in general. A complex system exhibits different modes of behavior depending on the value of λ. These changes in behavior are commonly referred to as *phase transitions* because of their resemblance, mathematical and otherwise, to phenomena such as the change in magnetism at the Curie temperature. To summarize: changing control parameters will cause complex systems to undergo phase transitions between different modes of behavior. This is what makes them complex.

This is a rather specific perspective on complex systems, but it will hopefully prove a useful one. It at least explains why this work is ambitiously dedicated to "controlling" complex systems—shouldn't we simply try to understand them first? The idea is that understanding and control of complex systems converge at λ. The control parameter is a condensed statement of the key relationships within the network of elements being studied. It can be thought of as quantifying intuitive descriptions of a system, such as its distance from equilibrium. For example, consider the mechanical stresses, magma flow pressures, friction at material interfaces and so on that constitute the $\{X_i\}$ and $\{F_i\}$ of plate tectonics. Locally, microscopically, their world is a relatively simple one, with lots of reversible collision dynamics, some chemical transformations, but general maintaining temporal and other symmetries. It is changing λ, which enfolds all the specific inhomogeneities—the excess stress accumulating in particular regions due to differing rates of thermal expansion caused by spatial fluctuations in the flow of thermal energy from the sun, perhaps—that can suddenly alter even the local mode of behavior by triggering an earthquake. Suddenly, symmetries are broken, and tiny molecules miles apart all translate several feet in the same direction. This reconfiguration leads to λ changing back across the critical value associated with the earthquake phase transition, and the earth resumes its usual near-equilibrium mode of behavior. Obviously, it is no simple matter to calculate λ for such a large system, or even establish its functional form; but it does a good formal job of describing how systems become complex.

We have now introduced the concept of *symmetry breaking*, which is a regular occurrence in complex systems. The most well-known example of symmetry breaking comes from Rayleigh-Bénard convection cells [Kos93]: as a temperature gradient forms between the

(cooler) top and (warmer) bottom of a cup of tea, the molecules between begin to deviate from their usual, random Brownian motion due to the spatial variation in T, leading to a corresponding gradient in the density of the liquid. The density of the warmer, lower layers decreases due to the increased thermal motion of the fluid, increasing the density of the cooler, upper layers. Gravity opposes this arrangement, dragging the denser fluid downwards to restore spatial homogeneity. This competition between the temperature-related density gradient and the force of gravity is captured in the dimensionless Raleigh number, Ra.

$$Ra_L = \frac{g\beta}{\nu\alpha}(T_B - T_T)L^3 \tag{2.2}$$

where L is the height of the cup, T_B and T_T the temperatures at bottom and top, g is the acceleration due to gravity and the remaining terms represent properties of the fluid.

In this system, Ra functions as λ. When the tea has cooled to form a critical temperature gradient between top and bottom, the system undergoes a dynamic phase transition at λ_c marked by the spontaneous formation of Bénard convection cells, columnar structures defined by the flow of warmer fluid up one side and cooler fluid down the other. This flow can proceed in either a clockwise or counter-clockwise direction—which brings us back to *symmetry breaking* and brings in the associated notion of *bifurcation* [And66]. At λ_c, which can be reliably calculated using Eq. 2.2, the symmetry (i.e. spatial uniformity) of Brownian motion is broken and replaced by ordered patterns of convective flow. This process is repeatable over cycles of heating and cooling, and in that sense it is predictable. However, the direction of flow that will begin in some microscopic volume of the fluid as the system undergoes the symmetry breaking transition is not predictable, nor consistent between trials. On the other hand, once the direction of flow of one cell is known, the nature of convective flow throughout the system can be determined due to the regular alternation of flow direction in adjacent Bénard cells. Poised at λ_c, the system "makes a choice" between clockwise and counterclockwise, and the rest of the pattern forms predictably afterwards. This "choice" represents an instance of bifurcation.

Bifurcations occur at critical interactions between chance and constraint, between normal fluctuations and irreversible changes. As the cup of tea approaches λ_c, the constraint

10

dictates that the phase transition will occur, yet chance determines the details of how. Tea molecules colliding and solvating and generally fluctuating around the mean established by state variables suddenly plunge over an energetic cliff; somehow, that final fluctuation transcends the random and some molecule makes an as-if "meaningful decision" that triggers the self-organization towards coherent motion for 10^{20} molecules more. This nearly mystical interaction of scales is actually a regular feature of complex systems, associated with the idea of *criticality* [Ma00] and the emergence of long-range spatiotemporal correlations, which we will return to discuss later.

We have now developed a more precise picture of the different *modes of behavior* a complex system can transition between. There is another useful tool for understanding the dynamics of these different modes, and the general classes according to which similarities can be found between physically distinct systems, known as Lyapunov stability analysis [Mos73]. This analysis considers how a system will evolve in time when subjected to a perturbation.

$$X(t) = X_s + x(t) \tag{2.3}$$

where $X(t)$ = time evolution of system, X_s = initial or "reference" state, and $x(t)$ = perturbation/fluctuations representing internal dynamics

There are different classes of stability. In the case that a small initial perturbation has a persistent small effect, the system is referred to as *stable in the sense of Lyapunov*, or equivalently that it exhibits *orbital stability*. This is the case of a frictionless pendulum: given a small push, it retains a small oscillation. The meaning of orbital stability comes from considering the phase portrait of the system, representing the time evolution of state variables, on which the trajectory of such a system would proceed around a closed loop. When we add friction, the effect of the small push wears down over time, and $X(t)$ converges back to X_s, the equilibrium rest state, which now constitutes an *attractor* for the *asymptotically stable* region around X_s. Trajectories passing near X_s will spiral towards it. These classes can be combined into *asymptotic orbital stability*, perhaps by adding a motor to the pendulum with friction. The motor drives the pendulum along an orbital trajectory, while friction dampens

11

the effect of perturbations and returns to the stable orbit. It is worth noting that asymptotic stability is essentially a feature of dissipative systems, which can have some (irreversible) mechanism for eliminating the effect of the perturbative energy input.

The most famous stability class is, in fact, *unstable*. Unstable systems can lead to chaos, where even a small perturbation will launch the system on a trajectory that takes it far from its initial conditions [Man77]. But even simple, conservative systems can be unstable: consider the physicist's famous frictionless ball situated in a landscape of hills and valleys. The state in which the ball is precisely balanced atop the tallest hill is unstable, as any nudge will send it rolling off indefinitely to the chosen side. This emphasizes the importance of the choice of X_s. *Local stability* applies when the mode of behavior depends on the magnitude of the perturbation. For example, consider a ball in a smooth bowl contained inside a rough (friction) sphere: the system will exhibit orbital stability in response to a small nudge, as the ball rolls along the sides of the bowl, but a sufficiently large shake will launch the ball out of the bowl, where it will asymptotically converge towards the point attractor at the bottom of the sphere. *Global stability* applies in the classic isolated thermodynamic system, where all roads lead to equilibrium. In this case, entropy is the force driving the convergence on the globally stable equilibrium state, which qualifies it as a *Lyapunov function*.

This is perhaps worth mentioning because of the situation in open and dissipative systems, which complex systems commonly are [Pri67]. Because they are not isolated, they can exchange entropy with the environment ($d_e S$), meaning that the total entropy variation (dS) of the system will not necessarily be positive.

$$\frac{dS}{dt} = \frac{d_i S}{dt} + \frac{d_e S}{dt} \tag{2.4}$$

The entropy production $\frac{d_i S}{dt}$ resulting from internal changes in the system is still governed by the second law, meaning that $d_i S \geqslant 0$, which is why entropy is a Lyapunov function guaranteeing the global stability of isolated systems. However, since the entropy flux $\frac{d_e S}{dt}$ can be positive or negative, this does not hold for non-isolated systems, meaning that they need not converge on equilibrium without even breaking the second law.

We now return to the connection between complex systems and *criticality*. The term is

used for some of the same historical reasons as *phase transition*: there is much in common between a crystal undergoing a second-order phase transition, and a complex system near a critical state [NM84]. In both cases, the *correlation length* of the system approaches the system size. That is, a microscopic change in one local corner of the crystal can cause a corresponding change on the opposite side, a macroscopic distance away. This has been famously studied with statistical mechanics to produce the Ising model and its family; but what is startling, is the apparent ubiquity of critical states in naturally occurring complex systems. While the theory of self-organized criticality (SOC) [Bak97] is not universally accepted as a technically useful (i.e. predictive) description of the physical processes underlying the observation of critical exponents in natural systems, it is at least an interesting, intuitive point of departure for investigating complex systems at a conceptually high level.

SOC purports that any system, consisting of elements connected by nonlinear, threshold-governed dynamics, which is subjected to a slow, system-scale energetic driving force, followed by fast internal relaxation and local equilibration of threshold energies, will naturally organize towards a critical state. The fast relaxation of the slow driving energy serves to correlate the distribution of energy amongst adjacent thresholds, towards the (critical) point where added energy will quickly propagate across the entire system (often referred to as "avalanches" for various reasons) until some dissipative event is triggered such that the stimulation energy can be absorbed by the storage capacity freed by dissipation. As these cycles continue, the system continues to stay at or near the critical state, with equal flows of energy in and out, until some control parameter induces a phase transition (as when an epileptic fit changes neuron spiking patterns to an unstable, supercritical mode) that alters the dynamical structure [Chi10].

It has been proposed by Walter Freeman[KPB05] that the origins of *intelligence* are to be found in this dynamical regime; that the brain operates by utilizing regular transitions back and forth between critical and subcritical states at brain-wave frequencies. Incoming sensory stimulation pushes the neuronal network into a critical state during which it explores, alters and forms new features in an attractor landscape that influences the flow of electrical signals. During its periodic return to the subcritical, the system's trajectories localize around selected

attractors, forming a link between sensory activity and cognitive structures. This attractor landscape is viewed as our memories, the knowledge and wisdom built by experience, the echo left by countless instances of this process. The transition dynamics themselves constitute our thoughts, reflexes and intuitions, the selection principles that emphasize particular associations and thereby feed back into structuring the attractors.

While this simplified presentation of Freeman's interpretation of brain dynamics is sufficiently vague to be as irrefutable as it is unprovable, it serves to illustrate how the outstanding feature of complex systems—control parameter-mediated transitions between different modes of behavior—is closely linked to pattern formation, and offers a plausible mechanism for the operation of an adaptable, associative memory. Repeated dynamical phase transitions will tend to express connections between the different phases, creating patterns. Of course, patterns can be formed by simpler means, but complexity additionally enables these patterns to be adaptive, not restricted to a choice between the stable memory of periodic orbits or the ahistorical adaptability of chaos and relentlessly scale-free fractals. Complex systems can function as both, and ultimately emerge resembling neither.

2.2   Dynamic Technology

We now turn to the challenge of utilizing complexity. The human body, and especially the brain in it, is an inescapable example of the technological potential of complex systems. However, the historical trend in technological development is to increase control over structure and consistency of function; dynamical phase transitions, the hallmark of complexity, are generally limited to when things break. The power of the simplifying approach is clear upon consideration of the way that properties of the nanoscale have been harnessed to build modern solid-state electronic devices. A deep understanding of semiconductor materials and their interactions with dopants has allowed electrical engineers to create reliable functional components out of the famously slippery fabric of quantum mechanical interactions; the moving parts are ions and electrons, their spooky quantum natures corralled by materials, interfaces, and the controlled application of electric fields.

Designing dynamic technology requires a different perspective. The big picture includes both *dynamic* and more traditional components, combined to maximize the strengths of each: dynamic adaptability and traditional reliability. Of course, the actual function of traditional, "static" devices, such as electrochemical batteries, involves nonlinear dynamics, with battery voltage dependent on the (charge/discharge) history of the system. The point is that this dimension is effectively linearized by design, not utilized to technological effect. The dropping voltage of a battery can trip a switch to start drawing power from a second battery instead, as the first starts recharging, because the role of the battery system is to provide electric power at a designated voltage. To incorporate the battery as a dynamic component would be to use it as a sensor, to use the information about its instantaneous voltage, perhaps in concert with other observations of changes in its electrode structure, electrolyte composition, and so on, to perform some useful function. (Which is, incidentally, one valid description of the neuromorphic technology developed in this work).

It serves to mention that dynamic technology does not necessarily have to be complex. A famous example [Van95] is the Watt governor. Designed by James Watt (adapted from windmill technology) to stabilize the power output of steam engines to feed the factories of the industrial revolution, the "Watt centrifugal governor" (1827) uses a feedback mechanism to establish an inverse relationship between engine speed and throttle opening in order to maintain a desired steady-state setpoint. A spindle is connected by gears to the engine's main flywheel, causing it to spin at a rate directly proportional to engine speed. Balls on hinges are attached to this spindle, arranged such that the centrifugal force of the rotation causes the arms to climb as the angular velocity increases. These arms are in turn linked to the throttle, with the net effect of producing a nearly instantaneous control response to fluctuations in engine performance (caused by changing loads, boiler pressure, etc) so as to maintain smooth power delivery suitable for efficiently operating factory machinery.

While not particularly complex—especially in the sense of not exhibiting any distinct modes of dynamic behavior (spinning vs. resting or accelerating vs. decelerating being trivial cases: there may be obvious differences in the time-evolution of these states, but the forces mediating interactions between components of the system remain unchanged)—the function

performed by the Watt governor is fundamentally dynamic. Its function is predicated on feedback, a design principle shared by most dynamic technologies. Interconnections between subsystems within the device generate time-varying signals, both as inputs and outputs, which are linked back to the sources of the temporal fluctuations in such a manner as to dampen and eliminate them. This leads to the curious result that, taken as a whole, the governed steam engine becomes a less dynamic system; a successful dynamic governor design ensures this! It is an important and recurring hierarchical feature of network-based systems, that a description of their characteristic properties and behaviors might be accurate at one size scale and not another. This "simple" example underscores the most technologically interesting property of dynamical systems: their capacity to respond to changes in their environment, akin to what we might intuitively call *information processing*. Of course, any sensor needs to have this property as well; but as in the battery example, a good sensor design will restrict the dynamics in order to maximize consistency. Our goal is a technology that directly correlates dynamic richness with device performance.

The notion of *information* has found its way throughout the intellectual world, from the nanoscale intricacies of quantum computing, to traditional philosophical inquiries along epistemic and ontological lines. Perhaps the most famous collision of *information* with more established disciplines was Claude Shannon's co-opting of thermodynamic entropy to define a quantified measure that could serve as the basis for the nascent field of information theory [Sha48]. There is a relatively intuitive connection that can be made between the statistical formulation of entropy and a naive idea of information in a signal: since the default state of a signal would be that of maximum entropy, i.e. the most probable state (meaningful discussion of entropy should aim to avoid its commonly conflated counterpart, "randomness"), any regular deviations in statistical features of a signal from their most probable states, represent the presence of information. Someone or something has imposed a persistent change on the signal, which can be decoded and interpreted as a meaningful message. Entropy, in this light, is the physical manifestation of probability as a force, guiding systems towards their most probable state. Information is that which resists it.

The technological promise of dynamic devices lies in their implicit capacity to near-

instantly synthesize many information-rich signals into higher dimensional representations, potentially producing "smart" emergent behaviors. Traditional computers, especially as they become increasingly parallelized, can also deal with multiple simultaneous information streams; however, they process them as digitized abstractions, using semiconductor device physics to implement logical operations. A dynamic information processor uses its own device physics to directly convert all the incoming signals to a processed output. The Watt governor is limited to only one input signal (flywheel rotation), which it transforms into an output with two degrees of freedom (open or close throttle). In this so-called Information Age, our input/output ambitions have increased dramatically. We now envision brain-like dynamical systems capable of synthesizing many simultaneous streams of information—from video feeds, stock tickers, weather stations, heart monitors—and make "intelligent" decisions in lieu of a human operator (who is subject to fatigue, mood swings, and other seriously nonlinear effects) to control power grids, or temporarily shut down satellites to avoid damage from incoming high energy radiation.

Many approaches have been tried, and more continue to be developed towards producing this kind of dynamic information technology. Most efforts are still limited to simulation, modeling dynamic systems with equations to be numerically computed in traditional digital fashion. The neural network (NN) approach to machine learning is the most famous of these. Inspired by the biological model of signal-integrating, decision-making neurons connected by an assortment of dynamic, nonlinear synaptic junctions, simulated NNs are basically (abstracted) complex systems, and the form of the equations governing their interactions will determine the shape of their attractor landscapes and dynamical phase transitions. The simplest NNs have feedforward architectures, which are easily computed but (because) they are not complex. They perform some function, a deterministic mapping of input to output, which might be dynamically changed according to some algorithm, but they are not true dynamical systems [LJ09]. Recurrent NNs are in fact dynamical systems, in which activity can persist even in the absence of input signals. However, the richness of their dynamics tends to overwhelm the algorithms charged with training the recurrent NN to do useful work. One stream of research effort has focused on finding good ways to restrict the dynamics

without losing their benefits, as with the symmetrical synaptic weights in Hopfield networks [Hop82]. These were the first recurrent NNs to demonstrate stable memory, though at the cost of allowing only point attractors. This cost is too high for those who, like Freeman, are principally interested only in biologically plausible models, since their goal is not simply to produce better information processors, but to gain insight into how our brains work.

CHAPTER 3

Morphological Transitions from Dendrites to Nanowires in the Electroless Deposition of Silver

A morphological transition from dendrites to nanowires in the electroless deposition of silver by galvanic displacement of copper seeds is investigated as a function of seed size. The transition to dendritic growth is interpreted as arising from local reaction anisotropies interacting with the global solute concentration distribution. Reactions were performed on substrates bearing lithographically patterned grids of copper posts with sizes ranging from 1-50μm. When copper seed size exceeds 10μm, the deposition reaction consumes silver cations at a sufficient rate to create ripple-like Mullins-Sekerka instabilities in their distribution. The resulting concave growth fronts produce branched, dendritic structures. For copper posts smaller than 3.5μm, cation consumption is balanced by diffusion and the growth front's advance towards the bulk, leading to networks of nanowires formed as the local reaction anisotropy favors growth by stacking along Ag (111) planes.

3.1 Introduction

Morphological transitions in non-equilibrium growth processes arise from interactions between microscopic interfacial dynamics and macroscopic driving forces [Lan80, BGM88]. Such transitions occur when variation of a process parameter alters the expression of local anisotropy in the global growth mechanism [CH93]. Determining which parameters are responsible presents a challenge, as intuition derived from classical thermodynamics may become misleading far from equilibrium [FKH94]. Reliable selection of morphology requires parameters that control the interplay of temporal and spatial scales, functioning as non-

19

equilibrium analogues to thermodynamic state variables [BG90]. Experimental investigations can identify these control parameters for specific growth processes and enable their use in directing the morphology of self-assembling structures.

Electroless deposition (ELD), a general term encompassing processes also referred to as galvanic displacement or cementation, involves the reduction of metal ions in solution without the application of an external bias voltage. The technique is primarily used for depositing metal coatings, and differs from simple homogenous redox reactions in that deposition occurs at a specific interface and not in the bulk of the solution [Ohn91]. The utility of ELD as a fabrication strategy arises from its capacity to combine surface patterning with chemical self-assembly, gaining the flexibility of solution-phase synthesis while retaining the control of top-down design processes. This work focuses on the ELD of silver from copper seeds in silver nitrate solution, according to the reaction:

$$Cu^0_{(s)} + 2\,Ag^+_{(aq)} \longrightarrow 2\,Ag^0_{(s)} + Cu^{2+}_{(aq)} \tag{3.1}$$
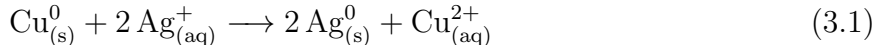
Controlled synthesis of silver nanostructures is of particular interest, as bulk silver has the highest electrical and thermal conductivity of all metals [RM07]. Extensive studies of silver nanostructures have also demonstrated strong antimicrobial characteristics [RYG09] as well as size/shape-dependent surface plasmonic effects, with particular implications for sensing and optical spectroscopies [XH05, WXM06, NE97]. The wiring of interconnects has become the most important factor in electronic chip design and performance [HMH01], motivating the development of biologically-inspired, self-assembled complex nanowire network architectures [TGL11] and devices [SAS12]. Higher dimensional, dendritic silver nanostructures have additional advantages in surface enhancement for catalysis [RM07], detection [WXM06], and as electrodes for electrochemical devices such as batteries, which harness the efficiency of branching geometries to optimize transport processes [PZW07].

We present a study on the morphology of ELD silver structures where the size of the copper seeds used to grow them under non-equilibrium conditions serves as a control parameter. Lithographically patterned Cu posts with edge lengths ranging from 1-50μm and heights of

20

200-790nm were reacted with 50mM silver nitrate solutions. This concentration was selected to investigate diffusion-limited deposition mechanisms [SDG86, KA95]. ELD occurred simultaneously at all Cu-solution interfaces upon immersing the substrate in $AgNO_3$, keeping all reaction parameters (temperature, concentration, reaction time) identical except for the dimensions of the Cu seeds (Figure 3.1).

3.2   Results and Discussion

Deposit morphology was observed to depend on seed size, with edge dimensions on the order of 1μm producing extended wires (Figure 3.2a), while above 10μm the deposits have a branched, dendritic structure (Figure 3.2b). This emergent length scale can be used to bridge the gap between top-down and bottom-up fabrication techniques in directing the self-assembly of functional nanostructured devices [ASM12].

Morphological transitions in non-equilibrium growth processes such as diffusion-limited ELD result from changes in the nature of the solid-solution interface at the growth front [GBC86]. The pure diffusion-limited aggregation (DLA) model of Witten and Sander has proven a powerful tool for understanding a range of fractal growth phenomena [WS81]. In to the DLA model, solid growth occurs as random walkers (in our case, Ag^+ cations) diffuse into contact with the solid and attach (e.g. are reduced to Ag metal), becoming part of the growing aggregate [MSH84]. Good agreement has been seen between DLA model predictions and Ag structures grown using diffusion-limited ELD from Cu at seed sizes larger than a millimeter [KA95, KAM94]. However, there is no size scale inherent in the DLA model, which approximates an idealized case of a solution approaching zero density [MSU05], and it is therefore unable to predict a morphological transition based on the size of the aggregate interacting with the solute distribution as a whole.

Size scales can be introduced by turning to mean-field models of diffusion-limited growth [RLT96]. They begin by defining a field controlling the growth process; in our case, the concentration distribution of diffusing Ag^+ cations, which has a maximum value of the bulk concentration and is zero at the solid-solution interface. Growth is most likely to
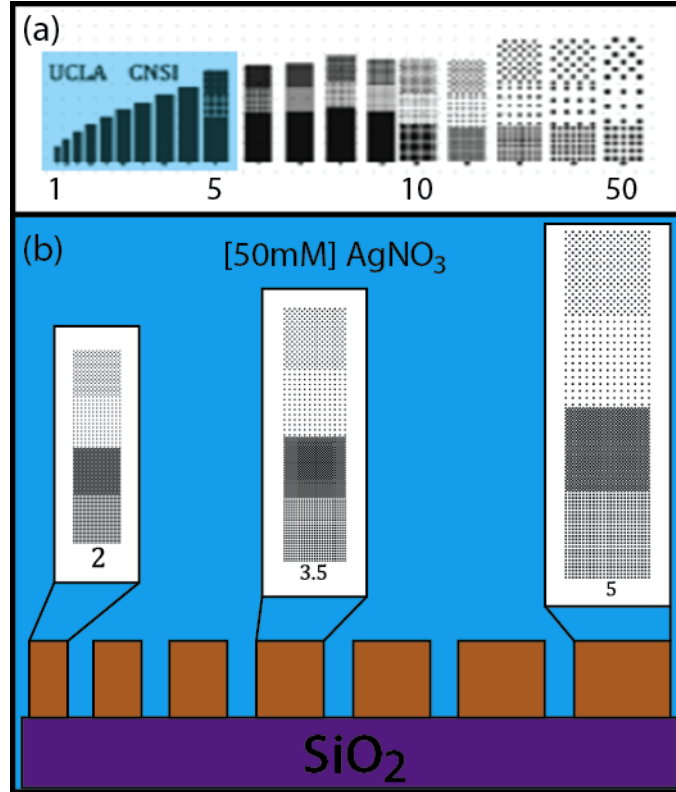
Figure 3.1: Experimental schematic. (a) Representation of the lithographic mask used for patterning Cu seeds of various size and pitch. Two distinct patterns, square and chessboard, are deposited onto SiO_2 substrates for each seed size with pitch equal to and double that of the respective seed edge length (1-50 microns). (b) Schematic of a SiO_2 substrate with Cu seeds immersed in a 50mM $AgNO_3$ solution, where individual blocks represent a grid of given size. ELD reactions occur simultaneously under identical reaction conditions (temperature, concentration, time) with the exception of Cu seed size. Post heights ranging from 200-790nm were used.

occur at protruding tips, as they extend furthest towards the bulk concentration. However, the interaction between the consumption of ions and the restoring forces resulting from concentration gradients at the interface is known to lead to instabilities in the distribution of ions around the growth front. The formation of such instabilities was analyzed by Mullins and Sekerka, who determined conditions for the propagation of perturbations at growth fronts [MS64], which have been used to explain the non-equilibrium formation of dendritic patterns [SB93]. We investigate these conditions experimentally, by simultaneously performing silver ELD reactions identical except for the size of the copper seeds.

Experiments were performed using microscale copper posts lithographically patterned on thermally oxidized (500nm SiO_2) silicon. Electron beam lithography was used to prepare $1\mu m^2$ Cu seeds, while UV lithography was used to deposit Cu grids with edges dimensions ranging from 2-50μm and thicknesses of 200-790nm. Microfluidic wells were fabricated around the Cu to facilitate the ELD reaction with aqueous $AgNO_3$. A thick layer of SU-8 (approximately 500μm) was deposited by spin coating, then UV exposed and baked at 95°C before developing in propylene glycol methyl ether acetate and a final hard baking at 130°C under nitrogen. Silver nitrate (99.98%, Fischer) was dissolved in 18.2MΩ deionized water to prepare 50mM solutions. Samples were characterized using optical and scanning electron microscopy.

Small Cu posts ($< 3.5\mu$m, Figure 3.4) were observed to exclusively grow nanowires when reacted with 50mM $AgNO_3$. At larger seed dimensions, branched structures were produced. The transition from wires to dendrites occurred for edge lengths near 10μm (see typical images shown in Figure 3.4). Extended wires were not observed at edge lengths greater than 15μm. No morphological dependence on the height of the posts was noted over the range examined.

In order to investigate the possible influence of the substrate on the morphological transition, we reacted Cu microspheres (99.995%, Alfa-Aesar, average diameters of 1 and 10μm) in stirred 50mM $AgNO_3$ solutions. These solution-grown Ag deposits were compared to structures produced from identical Cu seeds initially drop cast onto a supporting substrate. Optical images of each preparation showed no appreciable variation in structural morphol-
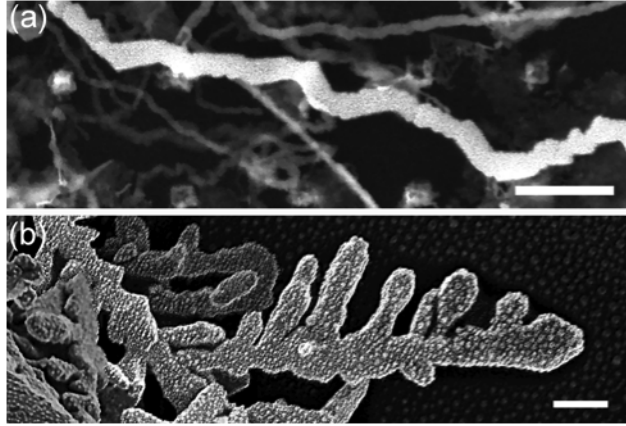
Figure 3.2: Branching of Ag structures increasing with the decreasing strength of anisotropic forces. Preferential orientations for crystal growth lead to the formation of nanowires (a) until the growth front is sufficiently large to interact with the concentration field and produce branched dendrites (b). Scale bars = 1μm.
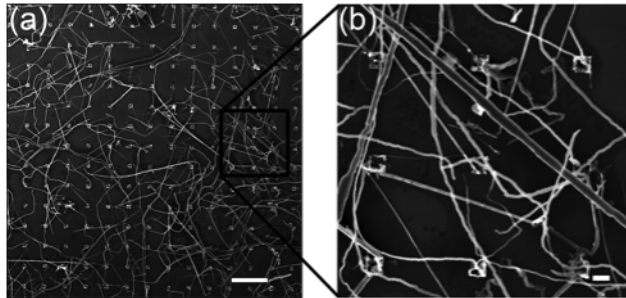
Figure 3.3: SEM images of Ag nanowires formed by ELD from lithographic Cu grids (1x1μm, 300nm thickness, 5μm pitch). The interpenetration of simultaneously grown wires highlights the predominance of local forces in the reaction at this seed size. Structures do not branch but may thicken. Scale bars: (a) 10μm, (b) 1μm.

ogy for a given seed size. However, comparison of XRD spectra for the deposits evoked distinctions, as collected using a Panalytical X'Pert Pro X-ray powder diffractometer using Cu Kα radiation (Figure 3.5).

Diffraction peaks near 38° and 44° were assigned to the (111) and (200) planes of fcc silver, respectively, according to standard values (Joint Committee on Powder Diffraction Standards file 04-0783). The shoulders on the (111) peaks are attributed to an Ag-Cu solid solution. Ag and Cu do not typically form alloys, despite both metals having fcc structures with a size mismatch satisfying the Hume-Rothery criterion for the formation of solid solutions ($< 15\%$), but they have been observed in non-equilibrium deposition processes such as sputtering [GBB08]. While the ELD mechanism is driven by simultaneous reduction and oxidation half-reactions at the metal-solution interfaces, the potential is transferred from the dissolving Cu seed to the Ag plating growth front through the metal-metal interface inside the deposit. The resultant local electric field is of sufficient strength to form an Ag-Cu solid solution at this interface.

The influence of size and substrate was taken from the XRD spectra by comparing the ratios of (111) and (200) peak intensities. This ratio gives a metric for the relative strength of anisotropic forces in the crystal growth process, where higher ratios are correlated to the preferential stacking of (111) planes associated with wire growth [CKM04]. In aqueous solution, the (111) and (100) facets of fcc Ag are the most stable, with water molecules interacting more strongly with the (100) surface, making (111) the preferred growth orientation [YCY11]. The observed trend in Figure 3.5 indicates that both smaller size and restricted volume (surface-based) growth serve to increase the anisotropy, with (111):(200) ratios increasing above the 10:4 standard for fcc silver crystals. This indicates that slower [Ag$^+$] depletion rates are associated with increased expression of oriented growth.

Given these observations, we find the transition between growth modes to be a feature of the non-equilibrium nature of the ELD process. Recent investigation into the effect of the size of Cu microspheres in a similar Cu/Ag$^+$ ELD reaction attributed the observed morphological transitions from plates to belts and branched structures to changes in the electrochemical potential as a function of the concentration of reactants, calculated using the

25
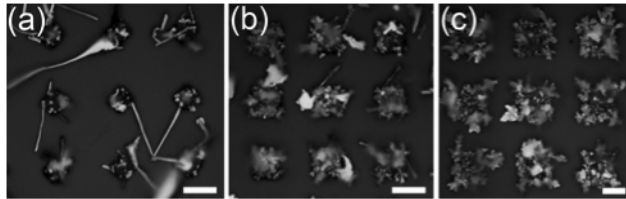
Figure 3.4: Optical micrographs illustrating the transition from wire to dendrite growth as a function of Cu seed size. At 7μm (a) wires predominate, with branched structures appearing as (b) seed size is increased to 9μm. (c) Wires were not observed for deposits from 15μm seeds. Scale bars $= 10\mu$m.
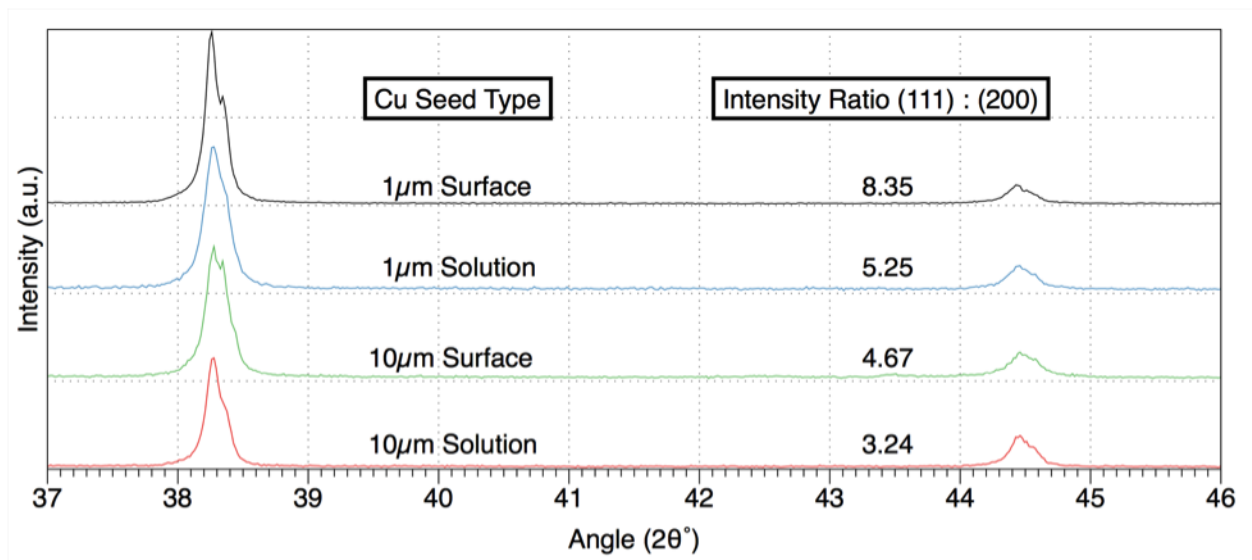
Figure 3.5: Comparing X-ray diffractograms of Ag structures grown from 1 and 10μm Cu microspheres in solution and on a glass surface shows that both seed size and surface proximity influence the preference for the (111) orientation associated with crystal growth anisotropy.

Nernst equation [LS11]. However, the Nernst equation is derived to estimate the reactivity of an electrode-solution interface at equilibrium, and is not applicable to the ELD process that occurs far from it. We propose that the formation of dendrites does not occur due to the reaction potential increasing with seed size, but rather because of Mullins-Sekerka (MS) instabilities appearing when the rate of depletion of reactants in the vicinity of the growth front critically outpaces restoring forces. Past this critical point, the growth mode changes because of non-equilibrium patterns in the solute concentration distribution caused by MS instabilities.

At a growing solid-liquid interface, the presence of a perturbation in the concentration field that is not stabilized by damping influences will propagate to form ripples in the distribution of solution-phase components. This tendency for an initially infinitesimal perturbation in a concentration distribution to increase and spread is the essence of the MS instability analysis. Above the emergent size scale ($\sim 10\mu$m Cu seeds for the reaction conditions used in this experiment), the consumption of Ag^+ at the growth front is sufficiently rapid to form MS instabilities, which create variations in the concentration distribution (Figure 3.6). Local regions of high $[Ag^+]$ reach sufficient chemical potential to nucleate branches, which can in turn form new MS instabilities. As the principal growth front advances at a constant velocity v, the instability-related branches grow at a rate proportional to $v^{\frac{1}{2}}$, creating a dendritic structure with a preferred axis of orientation through otherwise self-similar branches [KAM94].

Below the transitional Cu seed edge length, local forces sufficiently dampen the perturbations caused by the consumption of Ag^+ at the growth front, and no large-scale disruptions of the concentration field occur. The tip of the growing deposit moves smoothly towards higher concentration areas, such that local crystal growth anisotropy dominates the process and produces wires preferentially oriented along the (111) surface. The advancing growth front functions similarly to a directed drift term in diffusion-driven aggregation models, which predict needle-like growth when the flow of reactants towards the interface is sufficient to dampen instability [Nag89].

The localized nature of the wire growth mechanism is illustrated by the formation of in-
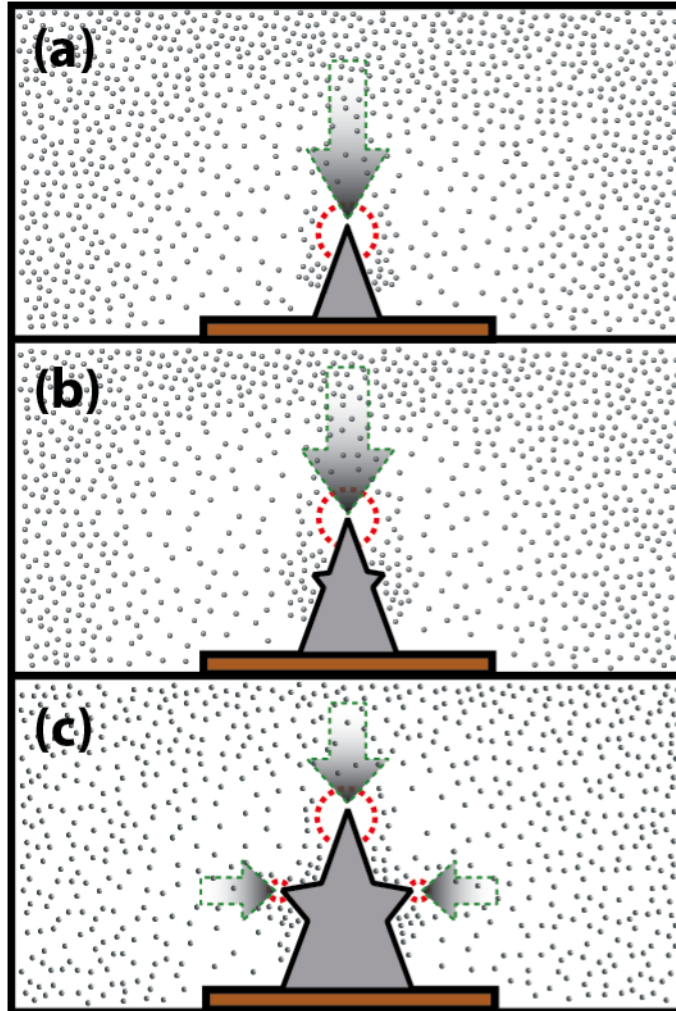
Figure 3.6: Dendritic growth due to Mullins-Sekerka instabilities. (a) For growth fronts of sufficient size, the consumption of Ag^+ outpaces the rate of replenishment, creating an instability in the concentration distribution. Diffusion gradients (represented as green arrows) are largest between the bulk and depleted regions, but the MS instability perturbs the flux of incoming cations to create a concave growth front. (b) The concave growth front leads to regions of increased Ag^+ concentration near the surface of the growing deposit with sufficient electrochemical potential to nucleate new growth sites. (c) As the branches grow, additional MS instabilities form, repeating the process and leading to the self-similar dendritic morphology.

terpenetrating wire networks (Figure 3.3). Since there is no disruption of the concentration field, each growth process is effectively independent, so the wires can grow past each other. Conversely, during dendritic growth, MS instabilities alter the distribution of available Ag^+ at a more global scale. As dendritic growth fronts approach, the depletion effects compound, and growth halts before deposits come into contact (Figure 3.4c). These observations support the notion that the transition in deposition morphology is associated with a change in the scope of the growth front's interaction with the solute concentration distribution. The specific magnitude of the critical parameters for inducing the transition are sensitive to many factors, from the bulk concentration of silver cations to the presence of hydroxide and nitrate anions, which have been found to promote nanowire formation in other Ag reduction processes [CBM03, KH12]. While the observed $\sim 10 \mu$m transition length is particular to our choice of reaction parameters, this investigation is of general interest because of the mechanistic insight gained by experimentally isolating a single parameter—the seed size—and observing its influence on the emergence of global non-equilibrium patterns from local anisotropy.

In conclusion, we have developed a flexible ELD technique using lithographically patterned copper seeds reacted with silver nitrate solutions to controllably produce either wires or dendrites by utilizing an emergent length scale in the non-equilibrium deposition process. We propose that at seed sizes on the order of 1μm, the process is controlled by local crystal growth anisotropy and produces wires, while above 10μm the growth front depletes reactive solute species at a rate sufficient to create MS instabilities in the concentration field and forms dendritic deposits. This combination of patterning and self-assembly is an effective means for constructing biomorphic electroionic devices [SAS12], and is a useful blueprint for connecting bottom-up and top-down methodologies to efficiently produce complex nanotechnology.

CHAPTER 4

Neuromorphic Atomic Switch Networks

Efforts to emulate the formidable information processing capabilities of the brain through neuromorphic engineering have been bolstered by recent progress in the fabrication of non-linear, nanoscale circuit elements that exhibit synapse-like operational characteristics. However, conventional fabrication techniques are unable to efficiently generate structures with the highly complex interconnectivity found in biological neuronal networks. Here we demonstrate the physical realization of a self-assembled neuromorphic device which implements basic concepts of systems neuroscience through a hardware-based platform comprised of over a billion interconnected atomic-switch inorganic synapses embedded in a complex network of silver nanowires. Observations of network activation and passive harmonic generation demonstrate a collective response to input stimulus in agreement with recent theoretical predictions. Further, emergent behaviors unique to the complex network of atomic switches and akin to brain function are observed, namely spatially distributed memory, recurrent dynamics and the activation of feedforward subnetworks. These devices display the functional characteristics required for implementing unconventional, biologically and neurally inspired computational methodologies in a synthetic experimental system.

4.1 Introduction

The human brain is the most powerful information processor known to man. Although the activity of individual neurons occurs orders of magnitude slower (ms) than the clock speeds of modern microprocessors (ns), the human brain can greatly outperform CMOS computers in a variety of tasks such as image recognition, especially in extracting semantic content from

limited or distorted information, when images are presented at drastically reduced resolutions [TFM96, TFF08, SWB07, Ull07]. These capabilities are thought to be the result of both serial and parallel interactions across a hierarchy of brain regions in a complex, recurrent network, where connections between neurons often lead to feedback loops [Abe91, DM07, BS09]. Recent research in systems neuroscience has developed models to explain this combination of rapid and complex processing which view the brain as a large network containing many recurrent loops with both excitatory and inhibitory connections, within which feedforward sub-networks are embedded for fast signal propagation [DM07, Gol09, TFS08].

In the brain, these excitatory/inhibitory connections between neurons, known as synapses, are nonlinear electroionic junctions whose conductivity changes in response to electrical and chemical signals. The relative timing of signals arriving from either side of the synaptic terminals, as well as larger-scale spatiotemporal patterns of network activity during these events, strongly influence the resultant change in synaptic strength, or plasticity [AN00, TFM96], a property postulated as the mechanistic basis for memory and learning [Heb49]. Recently, nanoscale electroionic circuit elements known as atomic switches [THN05] have been shown to exhibit input-dependent memory behaviors similar to short-term plasticity and long-term potentiation in neuronal synapses, where the time constant for conductance decay to the high resistance OFF state depends on the strength and timing of applied voltage pulses [HOT10]. This tendency to equilibrate produces short- and long-term memory behaviors that enable atomic switches to function as "inorganic synapses" [OHT11].

We present a detailed analysis regarding the consequences of coupling many atomic switches together in a highly interconnected, recurrent structure to create an operational neuromorphic device that self-assembles into a functional state. The motivation for building complex network-based computing devices extends beyond an interest in understanding and emulating brain function. Alongside efforts to reduce the dimensions of circuit elements while increasing their integration, the wiring of interconnects has become the limiting factor in both design and performance of electronic devices [TH08]. Wire delays are significantly slower than transistor switching speeds, producing a situation where more logic gates can be fabricated on a chip than are able to communicate in one processor cycle [HMH01].

31

This communication bottleneck can be addressed theoretically through the use of different network topologies, varying the number and type of interconnections. Complex nanowire networks are relatively simple to fabricate using self-assembly and would therefore be ideal wiring architectures, provided that they are useful.

Previously we reported an operational regime near the "edge of chaos" in similar network devices, as characterized by power law scaling of temporal metastability, avalanche dynamics and criticality [SAS12] reminiscent of electrical activity in biological neural systems [BP03, Chi10]. In such a state, the system is highly correlated and theoretically achieves maximum efficiency of information transfer while retaining a fading memory of prior states. These results indicate a potential capacity for efficient information processing, thereby surmounting problems associated with wire delays and interconnect structures. The distributed nature of the atomic switch array's dynamics makes it a candidate platform for efficient kernel design in the emerging field of "Reservoir Computation" (RC) [LJ09]. The fact that RC does not require subtle control of internal network dynamics and is therefore simpler to execute, makes it an appealing route to begin using neuromorphic devices to perform computational tasks. Complex network architectures generated through self-assembly of functional nanoscale elements, like those described here, offer the benefits of scalability and ease of fabrication combined with control of distributed nonlinear dynamics that may represent the architectural basis of a new computational paradigm.

4.2 Results

Atomic switch network devices were characterized using a range of potentiostatic inputs, including constant and ramped DC as well as sinusoidal AC signals. These complex atomic switch networks are shown to exhibit various nonlinear behaviors, depending on the magnitude and timing of both present and prior input signals. Behaviors include both weak (continuous I-V loop hysteresis) and strong (discrete threshold switching) memristance as well as nonlinear frequency response (higher harmonic generation) and persistent fluctuations in conductivity under constant bias (recurrent connectivity); results which were found

to agree with a recent theoretical study of current flow in memristor networks [OS11]. Operation of the device using pulsed voltage stimulation produced network-specific emergent behaviors, as spatially localized conductive channels akin to feedforward subnetworks were formed within the embedding recurrent network. While there are significant differences between these atomic switch networks and biological neural networks (NNs), we demonstrate the physical implementation of high-level NN features in an inorganic structure, including bottom-up self-assembly that is reminiscent of neuronal growth in the brain [SB98], nonlinear input-dependent conductance response which strongly resembles the function of biological synapses [BM09, Heb49], and emergent properties considered fundamental to brain function - recurrent dynamics which gives rise to large persistent, correlated network responses and the activation of feedforward subnetworks [Gol09, TFS08, GHS08, KRA10, MM09, RJ08].

4.2.1 Atomic switches, complex networks and neuromorphic hardware

Previous reports on the synapse-like properties of single atomic switches have demonstrated features similar to short-term plasticity and long-term potentiation, where applied bias voltage produced a junction conductance dependent on the history of stimulation (pulse frequency, length) [HOT10]. Individual atomic switches exhibit time-dependent nonlinear conductance due to several related mechanisms: (1) bias induced Ag^+ migration, (2) electrochemical redox reactions involving Ag^+/Ag^0 to produce metallic filaments, and (3) an associated non-equilibrium α/β-Ag_2S phase transition [XBW10], which all compete with thermodynamically driven stochastic renormalization to the equilibrium OFF state. Though atomic switches can be configured to operate in an essentially nonvolatile manner similar to memristors—two-terminal circuit elements whose resistance depends on the history of charge passed through them [SSS08]—their volatility indicates that they are more properly classified as "memristive systems" [Chu71, Chu11].

These mechanisms collectively produce the memristive switching and synaptic memory functions exhibited by a single atomic switch. Specifically, 'weak' memristance resulting from redistribution of Ag^+ dopant cations across the insulator leads to 'strong' memristance

characterized by abrupt switching through metallic filaments formed once the Ag^+ cations reach the cathode and are reduced to metallic silver [THN05]. TEM studies have shown that the metallic silver filaments formed during switching are surrounded by a sheath of β-Ag_2S, a conductive phase of silver sulfide normally unstable below 170°C [XBW10], possessing a body-centered cubic structure with sulfide anions forming channels in which silver cations are delocalized, highly mobile and dynamically correlated [AM59, GSC84]. This non-equilibrium phase transition is attributed to a relaxation of strain induced by lattice mismatch between Ag^0 and α-Ag_2S, the electrically insulating room temperature phase [WKT07]. In the absence of applied bias, thermodynamic pressures return the Ag_2S to its room-T α-phase, which drives the dissolution of the Ag^0 filaments and turns the atomic switch OFF at a rate dependent on the history of applied bias, producing the observed memory effects.

A great deal of effort has been put towards building biologically inspired computational hardware [DMM95, ILH11a, LMM03, Mea90, RJB96, TVH02, XRC09, MM88], though matching the complexity of the brain in a usable electronic device presents an exceedingly difficult engineering challenge. Fabrication requirements force design concessions, such as approximating the complex, recurrent connectivity between neurons by a simpler network geometry. The amenability of crossbar structures to conventional fabrication techniques has led to their use in neuromorphic hardware, with pre- and post-synaptic CMOS neurons connected by memristive elements at the crosspoints [JCE10]. This is an ideal hardware implementation of a 3-layer neural network model [Ros58], where input and output neurons are connected by a synaptic "hidden layer" of variable strength, and is also a promising platform for building dense, fast solid-state memory devices [CDL10]. However, the structural simplicity of the crossbar architecture is both a strength, enabling independent control of each synaptic element, and a weakness, since the well-defined grid lacks complex structures with the recurrent connections believed to be essential to brain function [DM07, KRA10]. While it is possible to program these features into a software model implemented on neuromorphic hardware, the physical existence of these complex structures may be essential to successfully generate the requisite spatiotemporal interactions between multiple signals simultaneously traveling through the network [BM09, Sea80].

4.2.2 Device fabrication and characterization

Based on the view that recurrent connectivity is essential to brain-like function, we have built, characterized and operated devices using massively interconnected (109 junctions/cm^2 according to analysis of SEM images), silver nanowire networks functionalized with interfacial Ag—Ag$_2$S—Ag atomic switches. These nanowire networks were prepared through self-assembly without pre-patterning of the network topology using the electroless deposition of Ag from Cu inside the SU-8 reaction well of an I/O device platform [SAS12, MVW12]. Specifically, spontaneous oxidization of metallic copper through reaction with dilute aqueous solutions of AgNO$_3$ produces a metallic silver structures with variable morphologies depending on the concentration of Ag$^+$ and distribution of Cu [KA95, LSZ09, WXM06]. Dendritic silver nanowires with minimum feature sizes <100nm seen in Figure 4.1b were produced by using lithographically patterned Cu posts shown in the inset of Figure 4.1a. Control over the size and distribution of Cu seeds increased device yield by ensuring the formation of conductive pathways between the Pt device I/O electrodes as seen in Figure 4.1b. Ag—Ag$_2$S—Ag interfaces were formed spontaneously within the network during gas phase sulfurization [KTH06]. Following optimization of fabrication protocols, a total of 96 networks were used for the device characterization described below.

Theoretical analysis of current flow in memristor networks during bias voltage sweeps indicated the possibility of a phase transition in device behavior from 'weak' to 'strong' memristive regimes [OS11]. Initial voltage sweeps of these network devices (Figure 4.2a and 4.S1) typically demonstrated smooth, pinched hysteresis loops characteristic of weakly memristive systems followed by an abrupt, nearly discontinuous jump to a distinct, high conductance ON state occurs at an activation bias voltage (V_a). This behavior represents activation of the network and is shown as an illustrative example of a network device undergoing a behavioral phase transition similar to the bias-driven forming step required to activate single resistive switches. Following network activation, devices subjected to repeated bias sweeping generally exhibit robust, strong memristive behavior, typified by hard switching (inset). Robust switching over 10,000 cycles was demonstrated at an operational threshold
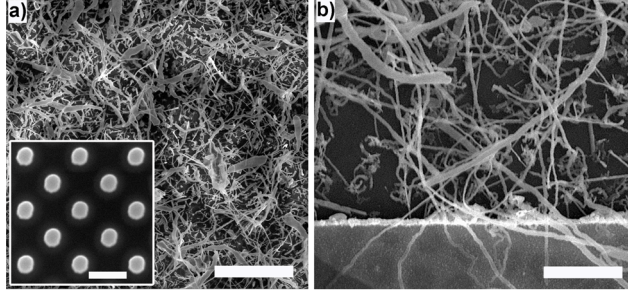
Figure 4.1: Device Fabrication (a) SEM image of complex Ag networks (scale bar = 10 μm) produced by reaction of aqueous AgNO$_3$ (50 mM) with (inset) lithographically patterned Cu seed posts (scale bar = 1 μm). (b) High resolution image of the functionalized Ag network at the device electrode interface (Pt) showing wire widths ranging from 100nm to 3μm (average <1μm) and lengths extending from a few microns to almost a millimeter (scale bar = 700 nm).

voltage (V_t) of reduced magnitude (Figure 4.S2) as compared to the formation bias voltage, a general phenomenon in resistive switches [WA07]. While the specific magnitude of V_a and V_t differ significantly between devices due to inherent variability in the solution-phase methods used to fabricate them, the qualitative transition from weak to strong memristive behavior was observed regularly, consistent with theoretical predictions [OS11].

Similar to the electroforming step usually required to activate single atomic switches and memristors [WA07], the observed transition from weak to strong memristive behavior is assigned to two related mechanisms. In poorly conducting regions comprised mainly of Ag$_2$S, anodic silver dissolves into and travels across the electrically insulating sulfide as Ag$^+$, decreasing resistance and producing a weakly memristive effect. In regions of higher Ag$^+$ dopant concentrations, mobile cations reach the cathode and are reduced to Ag^0, creating metallic filaments across the insulator that cause an abrupt change to an ON state with a sharp increase in conductance at V_t associated with the electrochemical process of filament formation. At the network level, the bias-induced creation of additional memristive junctions and filament formation across existing ones combine to produce the theoretically predicted transition of network I-V behavior to a strongly memristive phase (schematically illustrated
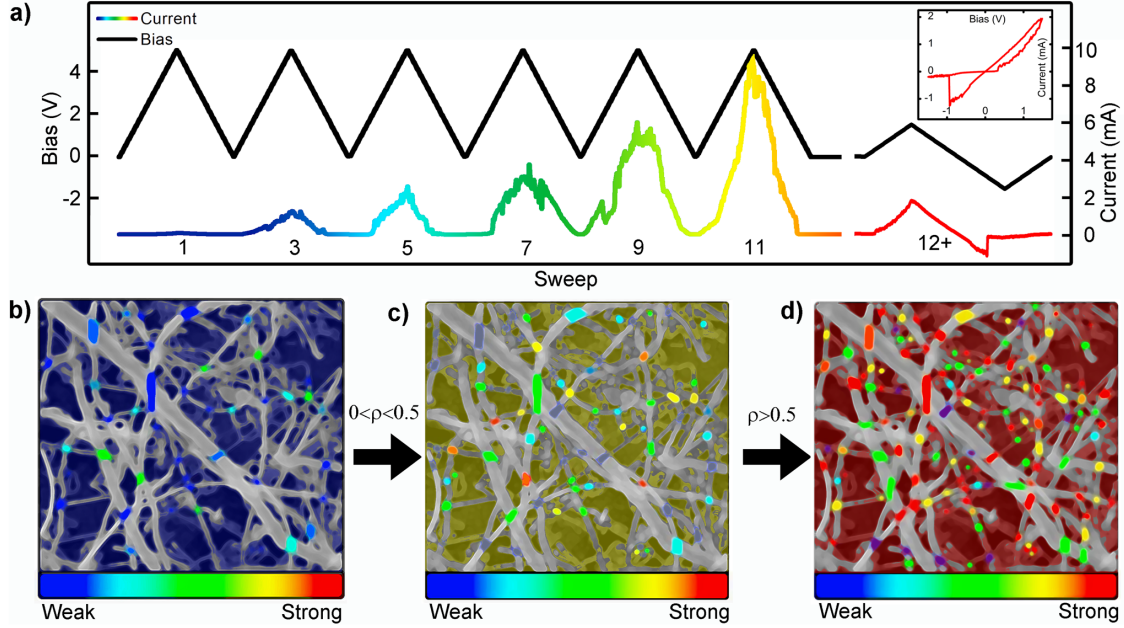
Figure 4.2: Network Activation - memristive behavior. (a) Representative example of initial bias sweeps (0-5V sweep at 1 V/s) applied to a pristine device which steadily activate higher percentages of atomic switches, resulting in increased current. After 11 sweeps, the device resistance decreases from $\sim 10M\Omega$ to $\sim 500\Omega$. Subsequent ± 1.5 V bipolar sweeps result in repeatable pinched hysteresis behavior (inset: $R_{OFF} = 25k\Omega$, $R_{ON} = 800\Omega$), and bistable switching. (b-d) Schematic representation of the mechanism producing the I-V characteristics shown in (a). The network initially consists of weakly memristive junctions and ohmic contacts (b). Continued application of unipolar bias voltage (c) drives the dissolution of silver into silver sulfide, increasing the number of memristive elements, while cation migration across extant memristive junctions leads to filament formation and the onset of hard switching behavior. (d) After the proportion of strong memristors exceeds the percolation threshold ($\rho > 0.5$), the network functions reliably in the hard switching regime.

in Figure 4.2b-d) as the proportion of switching elements in the network exceeds the percolation threshold (50%) [OS11]. Having undergone this transition, the continuously swept network operates as a hard switching memristor shown in Figure 4.2a (inset). All further data presented was acquired from devices following activation.

4.2.3 Network-specific properties

While weak and strong memristive behavior can be exhibited by single resistive switches, the most interesting features of this complex atomic switch device are its network-specific properties. In order to confirm that the entire network was involved in processing the input signals, devices were imaged using an IR camera with 20mK sensitivity to track Joule heating from current flow during slow bias sweeps. The IR images revealed power dissipation occurring across the network, indicating that the phase change in network I-V behavior was not attributable to the formation of a single maximum conductivity pathway of switches arranged in series between the active electrodes [SAS12]. The distribution of activity indicates that the observed I-V characteristics are due to the sum of parallel current flow, meaning that network structure and connectivity are actively influencing device function.

As recent theoretical models predict passive generation of second harmonics in both singular memristors and in random networks, the distribution of switch function throughout the network was examined through analysis of the device?s frequency response [OS11, CPD12]. Simulation of current flow in memristor networks indicate that 2nd harmonic generation will occur under an applied sinusoidal voltage in networks whose percentage of hard switching junctions exceeds the percolation threshold [OS11]. Further, the relative magnitude of higher harmonics is predicted to increase with the relative number of hard switching junctions. Following activation, device response to a 10 Hz sinusoidal voltage signal varying in strength from 250 mV to 4 V shows a large increase in higher frequency components after functionalization (Figure 4.3b). The proportion of higher harmonics generated increases with signal amplitude (Figure 4.3c), with the largest increase occurring between 250 and 500 mV. A larger degree of higher harmonic generation is consistent with an increased number of memristive junctions operating in the hard switching regime above V_t (~ 0.5 V). Both the distributed power dissipation [SAS12] and harmonic generation are characteristic of activity distributed throughout the network.

Having characterized atomic switch operation in an interconnected complex network, we examined the device for emergent behaviors specific to its brain-like recurrent structure.
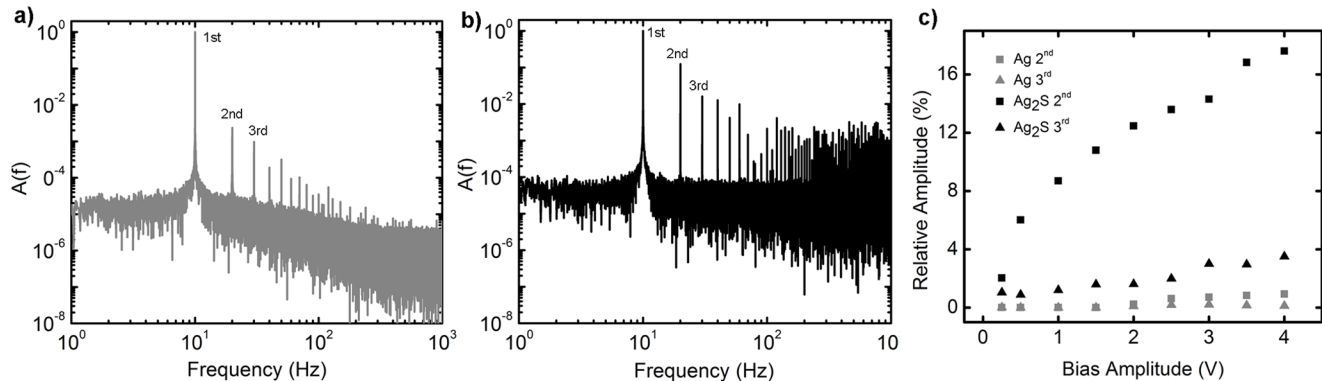
Figure 4.3: Frequency Response — distributed conductance (a) Amplitude spectrum from a Fourier transform of a control device's response to a 2 V, 10 Hz sinusoidal input signal compared to (b) that of a functionalized device which shows enhanced overtones of the input signal with respect to (a). (c) Plot of 2nd and 3rd harmonic generation in current response as a function of bias voltage in both functional (black) and control (gray) networks. Harmonic magnitudes are represented as percentage of the fundamental for a 10 Hz sinusoidal input signal.

Structurally, the atomic switch network is recurrent in the sense that there exist pathways such that electrical signals produced at one junction may lead to (delayed) feedback at the same junction. Here we present experimental evidence of spatially distributed and correlated network dynamics, which are attributed to such recurrent connectivity. These recurrent dynamics are presented as an emergent property of the atomic switch network.

Applying a constant 1V DC bias (Figure 4.4a) produced persistent, bidirectional fluctuations—both increases and decreases—in network conductivity of large magnitudes ($\sim$20-150%) over a range of time scales (seconds-hours). In the absence of recurrent structures within the network, the filamentary mechanism of an atomic switch implies that conductivity would increase monotonically under constant DC bias. The applied voltage leads to the thickening of filaments until the potential drop across the junctions is insufficient to reduce more silver cations [THN05]. However, large bidirectional fluctuations (ΔI greater than 100% on the scale of hours) in the current response persisted for several days under constant applied voltage, demonstrating that the complex network connectivity inherently resists localized

39

positive feedback that would lead to the serial formation of a single, dominant high conductivity pathway between electrodes. Rather, recurrent loops in the network create complex couplings between switches, resulting in network dynamics that do not converge to a steady state even under constant bias. A single switch turning ON does not simply lead to an increased potential drop across the next junction in a serial chain, but redistributes voltage across many recurrent connections that can ultimately produce a net decrease in network conductivity. This behavior represents a network-scale analog of defect-defect interactions that have been observed to produce current fluctuations in metal nanobridges [RB91]. The nanoscale switch filaments couple these interactions with electrochemical redox processes, leading to significant changes in the conductivity state of the entire network.

These fluctuations are of a magnitude significantly greater than what can be considered noise. An internal control experiment compared Fourier transformed current responses (Figure 4.4b) of the devices to constant voltage before and after functionalization. The formation of atomic switch junctions expands the degree of correlation in current fluctuations, producing 1/f-like behavior across the entire sampled range, far exceeding that of control devices (unsulfurized silver network, grey line in Figure 4.4b), which flattens to white noise and some high energy, high frequency fluctuations attributed to arcing between neighboring wires. Functionalization with atomic switch elements increases the influence of past events on the present state of the network, in accordance with their memristive characteristics [HOT10, OHT11, Kes82]. This results in an expanded degree of correlation in the measured frequency response. Similar 1/f spectra have been observed along with current fluctuations in other resistive switching systems, exhibiting relative resistance changes $\frac{\Delta R}{R}$ ranging from < 0.002 for metallic filaments to an experimental and theoretical maximum of 0.5 in the semiconducting high resistance OFF state [INC10]. The network device of Figure 4.4 is operating in an intermediate state with an average resistance of $172k\Omega$ (compared to $R_{OFF} > 10M\Omega$) and fluctuations of $\frac{\Delta R}{R} \sim 1$. In order to produce relative resistance changes of such high magnitude, switching events within the network must be correlated. While stochastic processes may be involved in the correlation of these fluctuations [Kes82, CT03], their magnitude and persistence is an emergent feature of recurrent connectivity in the device

40
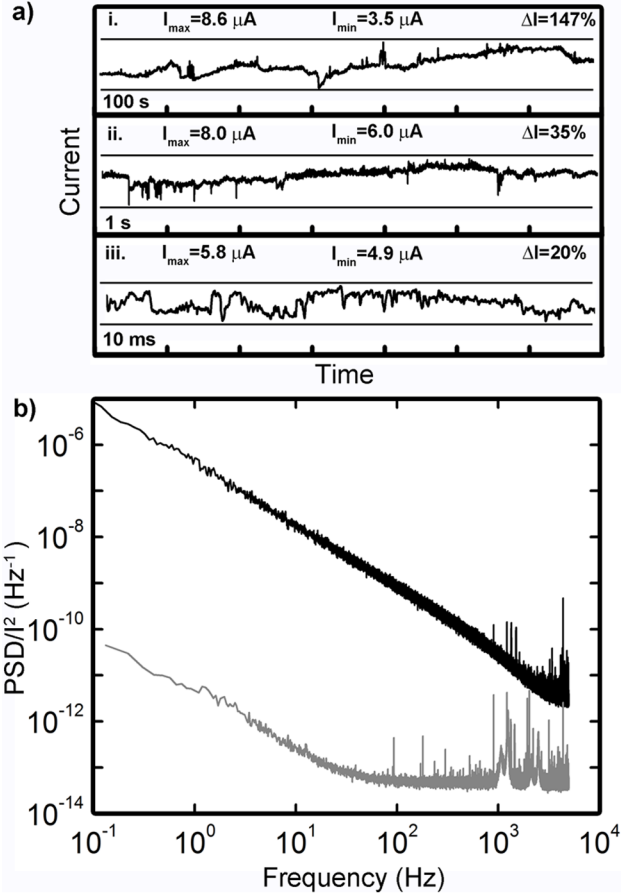
Figure 4.4: DC Response — recurrent dynamics (a) Time traces of current response to 1 V DC bias show large current increases and decreases at all time scales around a mean of 5.81 μA (172 kΩ); shorter time traces (ii-iii) are subsets of (i). Representative device parameters: $R_{OFF} > 10M\Omega, R_{ON} < 20k\Omega, V_T = 3$ V during activation (b) Fourier transforms of DC bias response for Ag control (grey) and functionalized Ag—Ag$_2$S (black) networks. The power spectrum of the functionalized network displays $1/f^\beta$ power law scaling ($\beta = 1.34$).

architecture that has not been observed in simpler atomic switch geometries.

Inside the generally recurrent structure of the brain's neural network, there is evidence for the existence of feedforward subnetworks utilized for the fast propagation of certain signals [GHS08]. In this device, persistent fluctuations in current under constant DC bias are produced by the recurrent network architecture, creating operational dynamics that resist the feedfoward activation of serial chains of switches. However, by altering the form of the

input signal, we were able to independently operate conductance channels between different pairs of electrodes within the same device.

The application of a single, large voltage pulse ($\pm$3V, 1s) selectively switched connections between electrode pairs ON and OFF (Figure 4.5a) with a R_{ON}/R_{OFF} ratio greater than 30. In the example shown, the conductive paths between the two channels overlap spatially, yet are switched independently, indicating that local sub-regions of the network can transition to distinct operational modes despite being embedded within a highly interconnected, largely metallic structure. This is analogous to the presence of feedforward subnetworks within the recurrent architecture of the cortex. Single pulses of sufficient magnitude overwhelm the recurrent dynamics and induce feedforward activation of local sub-regions along a path connecting the involved pair of electrodes without significantly altering the conductivity of other spatially intertwined channels within the same nanowire network.

The degree to which pulse-mode channel creation influences overall network connectivity can be visualized in electrode resistance cross-correlation matrices (Figure 4.5b). In this case, net electrode resistance is calculated from the pair-wise resistances to be a representative measure of the overall connectivity of a given electrode to the network. The correlation strength (denoted by color) represents the degree to which a pair of net electrode resistances fluctuate in unison, interpreted as a measure of the number of shared network sub-regions connected to both electrodes (Supporting Information). Correlation strength increases strongly between electrodes connected by an ON channel, and decreases again when the channel is switched OFF, with a varying degree of influence on electrodes not directly involved in the switching. This implies that spatially central regions of the network can be selectively associated with particular pairs of electrodes without globally increasing the network connectivity. However, when conductive channels exist between all four electrodes, the overall magnitude of correlation in the network is correspondingly large, as fluctuations are spread evenly throughout the increasingly metallic network. This simple example of the interaction between local and global operational characteristics is a promising indicator of the possibility for the creation of a brain-like hierarchy of distinct functional regions within a single network where the functional connectivity of the network itself is both dynamic and
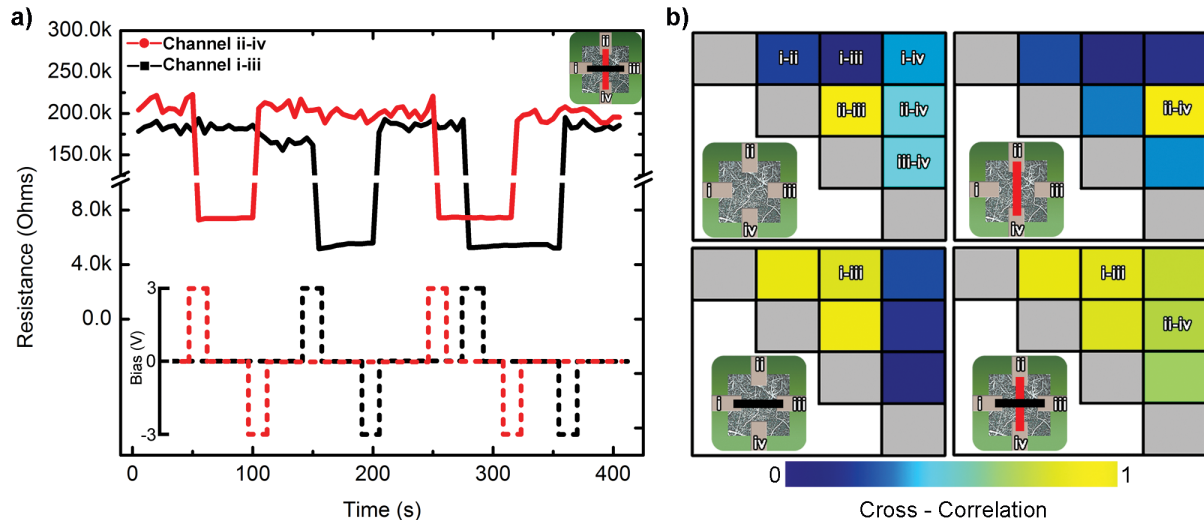
Figure 4.5: Distributed Memory Storage from Network-scale Switching (a) The device operates as a 2-bit non-volatile memory device. The resistance states across two channels (i-iii and ii-iv) are monitored. ON/OFF switching of each channel is induced using super-threshold pulses (3V, 1s in duration); the threshold voltages for each channel are ~1.5 V. The resistances are measured every 5s with a sub-threshold 200mV, 100ms pulses. (b) Although the device operates with a four state output (both channels ON, 1 ON/1 OFF, etc), the network's internal configurations show diverse correlated patterns, from no correlation (blue) to total correlation (yellow). The figure shows correlation coefficients of channel resistances for all 6 pairwise electrode combinations. The correlation coefficients are calculated during each of the 4 network switching configurations; the black and red bars (insets) show the channels that are ON in the switching state.

self-organized [BWP11].

4.3 Discussion

Using a simple, two-step fabrication procedure combining top-down and bottom-up fabrication techniques, we have created functional neuromorphic devices based on a self-assembled, complex network architecture. We describe these atomic switch networks as neuromorphic not only in that the massively interconnected, dendritic features observed in biological neu-

ral networks inspired the device architecture, but also due to several important network scale properties reported here. The devices demonstrate weak and strong memristive behaviors, as well as higher harmonic generation, confirming theoretical predictions on current flow through memristor networks. Previously unreported emergent behaviors specific to the complex architecture were observed as persistent bidirectional fluctuations of the current in response to constant applied voltage and the pulse-based feedforward switching ON and OFF of localized conductance channels within the highly interconnected network. Despite lacking the brain's rich assortment of neurotransmitter systems, with distinct excitatory and inhibitory neurons, the complex network of atomic switches produces multiple behaviors from a single basic unit through a capacity for localizing function in subnetworks inside a structure correlated by the nonlinear memory response of individual atomic switches. This diversity of function indicates the device's potential as a universal approximator of dynamical systems [FN93], with possible applications in physically implementing unconventional computational strategies [LJ09] and as an inorganic experimental platform for the investigation of systems neuroscientific theories of biological brain function.

4.4 Materials and Methods

4.4.1 Substrate fabrication

Electrodes were patterned on the surface of a Si wafer (525μm thickness; p-type; 100mm diameter; 500nm thermal oxide) by photolithography. A Cr/Pt (15/150nm) bilayer was deposited using e-beam evaporation. Subsequently, microfluidic reaction wells were patterned from a thick layer of SU-8 (approx. 500 μm) deposited by spin coating. The resist was UV exposed with a dose of 1200 mJ/cm^2 followed by a post-exposure bake beginning at 65°C and ramping up to 95°C before cooling to room temperature at 1°C/min. The SU-8 was developed by immersion in PGMEA (Propylene Glycol Methyl Ether Acetate). Fully developed wafers were rinsed with isopropanol and hard baked at 130°C on a hotplate in N_2 atmosphere to increase SU-8 resistance to high temperatures.

4.4.2 Network synthesis and functionalization

Electroless deposition of Ag from Cu was performed by pipetting aqueous $AgNO_3$ (Fischer, 99.98%) at concentrations ranging from 0.1-100 mM into microfluidic cells containing Cu seed posts, leading to a spontaneous reaction between Ag^+ and Cu. Optimal conditions were achieved with Cu posts ranging from 0.25-4 μm in diameter at pitches of 0.5-4 μm reacted with 50mM $AgNO_3$, sulfurized at 130°C for 10 minutes under N_2 flow at atmospheric pressure. The silver networks self-assembled during this processes, and were then functionalized by reaction with sulfur (Sigma-Aldrich, 99.5%) in a Pyrex tube. The sulfur was melted in an evaporation boat at 130°C and delivered to the substrate by N_2 flow.

4.4.3 Measurement apparatus

Electrical characterization of the devices was conducted using four Pt electrodes positioned around the edges of the Ag network. Current-voltage spectroscopy was conducted using a bipotentiostat (Pine Instruments model AFCBP1) in conjunction with a DAQ module (National Instruments USB 6259) at a sample rate of 10 kHz. Measurements were performed in a two-electrode configuration. Multi-channel resistance measurements were obtained using a multiplexed (National Instruments PXI 1073) SMU (National Instruments PXI 4130). The entire I/O system was housed in a Faraday cage and mounted on a vibration isolation table (TMC). Devices were characterized after each stage of the fabrication cycle. Subsequent data analyses were carried out using MATLAB 2010b (MathWorks) and Origin 8.1 (OriginLab Corporation).

4.4.4 Network resistance correlations

The full dataset used in Figure 4.5b contained resistance data from all 6 combinations of the 4 electrodes in a device (for clarity, only 2 combinations are shown in Figure 4.5a). The network resistance of each electrode was calculated as the parallel resistances to the other 3 electrodes. The dataset was parsed into the appropriate subsets (A on and B off, etc.) and the MATLAB function corrcoef() was used to calculate the correlation coefficients for the

different configurations.

4.5   Supporting Information
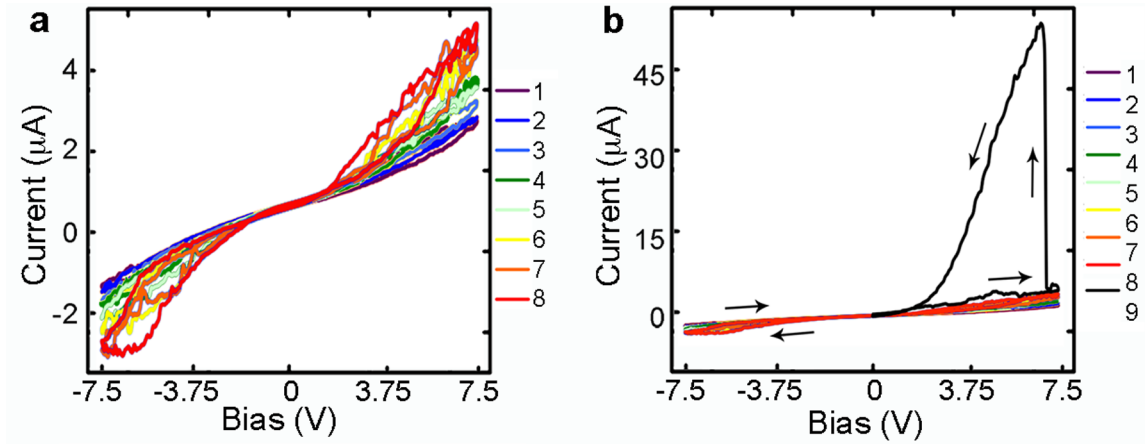
Figure 4.6: (a) Initial bias sweeps ($\pm 7.5V\,at\,1V/s$) demonstrate weakly memristive behavior with increasing hysteresis magnitude (70% increase in maximum ON/OFF, from 1.12 to 1.92 after 8 sweeps). (b) Bias sweeps from (a) rescaled to include the hard switching (ON/OFF ratio of 14.3, 650% increase from maximum weak ON/OFF) phase transition event at $V_a \approx 7.5V$.
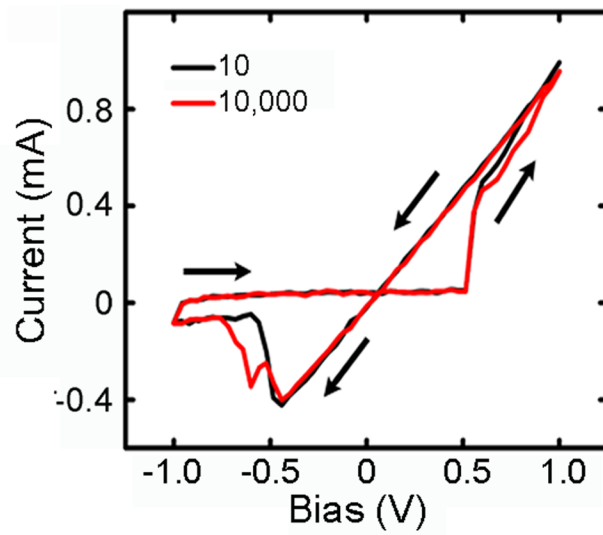
Figure 4.7: Operation of a device following the phase transition (activation) exhibiting typical, robust pinched hysteresis/switching. Shown device parameters: sweep rate = $103V/s(1kHz)$, $R_{ON} = 1k\omega$, $R_{OFF} > 20k\omega$, $V_t = 0.5V$.

CHAPTER 5

A Theoretical and Experimental Study of Neuromorphic Atomic Switch Networks for Reservoir Computing

Atomic switch networks (ASN) have been shown to generate network level dynamics that resemble those observed in biological neural networks. To facilitate understanding and control of these behaviors, we developed a numerical model based on the synapse-like properties of individual atomic switches and the random nature of the network wiring. We validate the model against various experimental results highlighting possibility to functionalize the network plasticity and the differences between an atomic switch in isolation and its behaviors in a network. The effects of changing connectivity density on the nonlinear dynamics are examined as characterized by higher harmonic generation (HHG) in response to AC inputs. To demonstrate their utility for computation, we subjected the simulated network to training within the framework of Reservoir Computing (RC) and show initial evidence of the ASN acting as a reservoir which may be optimized for specific tasks by adjusting the input gain. The work presented represents steps in a unified approach of experimentation and theory of complex systems to make ASNs a uniquely scalable platform for neuromorphic computing.

5.1   Introduction

Synapses play an essential role in cognitive function. Brain activity is characterized by spatio-temporal varying electrical signals travelling through a vast interconnected recurrent network of neurons, where the synapses mediate signaling. Until recently, research has tended

to focus on an approach which promulgates that advances beyond complementary metal-oxide semiconductors ("beyond-CMOS") computation [nan11] may be achieved by fabricating electronic elements which recreate the fundamental behaviors of neurons and synapses [Mea90, MD91]. Accordingly, new generations of synthetic synapses have been demonstrated or modeled which display short- and long-term potentiation/depression (STP, LTP and LTD respectively), spike timing dependent plasticity, and other neuroscientific phenomena [ILH11b, JKZ13]. These devices have been incorporated into hybrid-CMOS/molecular CMOS [JKZ13, LS05] circuitry with the aim to recreate synaptic spiking patterns typically realized with crossbar array geometries for optimized memory storage [BLS09, XRC09, ZAD10, CJK11, KRL11, SKJ11, CYS12, KGW11, KJY12]. The architecture of the arrays is designed to address each functional element individually and sequentially in a programmed fashion, essentially precluding the elements to interact within a network. However, actual complex systems exploit the non-trivial effects of interconnectivity [Sim62, Str01] that allow individual units to function in synchrony over multiple spatial and temporal scales resulting in self-organized patterns of activity [BP03, LHG07, MM09, Chi10, SYY11]. Consequentially, emergent phenomena are distributed throughout the entire system and cannot be associated with any particular node or local group [Jen98, SCK04, BM09]. In the brain, modification of these intricate networks is believed to form the basis of memory, motor pathways, and cognition [Heb49, FBH03, CMS04, KPB05].

Through a combination of top-down and bottom-up fabrication techniques, highly interconnected wire networks containing synaptic functional units have been fabricated and studied [ASM12, SAS12]. These atomic switch networks (ASN), composed of more than 109 individual inorganic synapses/cm^2 [HOT10, OHT11, YTL12], i.e. atomic switches [THN05], represent a unique class of physical devices capable of exhibiting synapse-like properties in neurally-inspired architectures. Interfacing functionalized networks with multielectrode arrays offers the ability to harness intrinsic system dynamics through input and read out of real-time electrical signals at various spatiotemporal scales toward practical implementation of neuromorphic computation [ASM12, SAS12]. ASNs retain the adaptive plasticity and memory of their component atomic switches while exhibiting emergent properties such as

criticality and spontaneous switching between discrete metastable resistance states.

Most attempts to mimic the brain's function use simulated neural networks. Recurrent neural networks consist of nodes, each with an adjustable connective weight, and allow signals to propagate forwards and backwards through the network [HT85]. Such structure allows information to be integrated at different time points, enabling online training. The main drawback of recurrent networks remains the difficulty of adjusting individual connective weights, which results in an inability to efficiently differentiate inputs or adapt to increasing noise levels in the environment [Jae02]. The computational degrees of freedom are also too vast to permit convergence in a reasonable time.

Recently, Reservoir Computing (RC) was developed to overcome these issues, while retaining biologically relevant features such as feedforward and recurrent structures [Jae01, MNM02, SVV07, VSd07, LJ09, BSL10]. RC is achieved through a two-step process. First, time varying input data is introduced to a fixed weight recurrent network or "reservoir", in which the nonlinear action of nodes produces higher dimensional representations of the input data. This transformation permits the second step, where the new representations are read out through a feedforward network or "linear readout". Information that was not initially linearly separable can then be processed through simple linear regression techniques in the feedforward layer. Consequently, RC can perform complicated classifications in real time, and enables generalization of learned tasks. Currently, RC is the most effective technique available for certain tasks and has been realized in a variety of physical implementations as proof-of-concept [FS03, SMS04, PDS12].

Atomic switch networks (ASNs) were proposed as well-suited to RC, because they contain a physically recurrent network of nonlinear elements which are amenable to serve as a reservoir while also exhibiting feedforward properties useful for the output layer [SAS12]. Atomic switch networks also possess a readily scalable architecture, multiple spatio-temporal outputs, and synaptic non-linear elements displaying critical dynamics. Consequently, ASNs are potential embodiments for enabling neuromorphic computational theories and represent physical neuromorphic devices that have a direct connection with neuroscience.

Understanding and harnessing the rich dynamics found in complex networks comprised of coupled nonlinear elements is challenging. In particular, practical engineering goals are based on stimulus-response relationships governed by internal system reorganization with minimal fine-tuning at the microscopic level. Here we present a numerical model of ASNs which illustrates key aspects of the spatial and temporal dynamics of the system, and investigates their utility in the context of RC. Our simulation was built from the physical ASN devices: the design and implementation was based on the well-documented physics of single synaptic switches, and the connectivity was modeled on the known network architectures determined from SEM images. The goal of the simulation was to deepen our understanding of network function, optimize network design and explore the applicability of device architectures for neuromorphic computational tasks.

First, we validated the accuracy of the simulation by reproducing data from the devices such as controlled interconnect plasticity and emergent behavior despite the simulation's much smaller network size. Second, we show that fluctuations in a simulated isolated single link are distinctly different from those of an identical link within the network. This highlights the role of the network where synaptic elements behave differently as a result of interconnectivity. The simulation was also found to show emergent properties that are impossible to measure in a single device. Third, we show that higher harmonic generation reported experimentally [ASM12] and theoretically predicted [CPD12, OS11], can be modeled and utilized for reservoir computing. We finally discuss the potential impact of ASNs as a unique physical embodiment that is capable of integrating neuromorphic architecture, dynamics, and computation.

5.2 Methods

5.2.1 Network devices

The ASNs were grown using self-assembly of a rhizomic-dendritic network of highly inter-connected silver (Ag) nanowires which were sulfurized to provide distributed nanojunctions

comprised of inorganic synthetic synapses. ASNs were interfaced to input-output electrodes fabricated using conventional micro-lithographic processing to create a functional device [ASM12, SAS12] (Figure 5.1a). Electrodes were fabricated by electron beam evaporation following photolithography on the surface of a p-type Si wafer (boron doped, 0-100 Ωcm^{-1}) insulated by a 500 nm thick thermal oxide layer. Deposition of 4 to 16 Cr/Pt (15/150 nm) electrodes with diameters of 10 to 50 μm at pitches between 50 and 500 μm was followed by spin-coating and patterning of an insulating layer of SU-8 deep UV resist, which served to expose only point contact regions of the electrodes. Micron diameter cylindrical copper seeds were then deposited at areal densities between $1*10^6$ and $2.5*10^7$ seed sites/cm^2 for the electroless deposition (also referred to as galvanic displacement or cementation) of Ag from Cu on the SU-8 layer. Electroless deposition was performed under diffusion-limited conditions using 50 mM aqueous solutions of $AgNO_3$ [KAM94]. This spontaneous electrochemical reaction produced complex networks of metallic silver nanowires shown in Figure 5.1b. Previous studies have shown that the geometry and spacing of pre-patterned Cu posts provides control over the global qualities of the network generating structures ranging from extended nanowires to dendrites and fractals [SB93, AMS13]. The pitch of the Cu posts was found to determine the relative density of the network (Figure 5.1c, d) while seed size was used to control the presence of long-range connections. Typically, smaller Cu seeds ($< 3.5\mu$m) produce many long wires and larger seeds ($> 3.5\mu$m) produce spatially confined dendritic or fractal structures.

The self-assembled silver networks intrinsically contain crossbar-like junctions resulting from the three-dimensional nature of the solution deposition process. Upon exposure to sulfur gas [KTH06] (10^{-1} torr at 130°C for 3 min), the Ag nanowire junctions are functionalized to form thin Ag—Ag_2S—Ag metal-insulator-metal interfaces which, in the presence of postprocessing activation with external bias potential, are transformed into "atomic switches". Electrical characterization of the devices was conducted through current-voltage (I-V) spectroscopy using a bipotentiostat (Pine Instruments model AFCBP1) in conjunction with either a data acquisition module (National Instruments USB 6259) or a multiplexed (National Instruments PXI 1073) source-measurement unit (National Instruments PXI 4130).
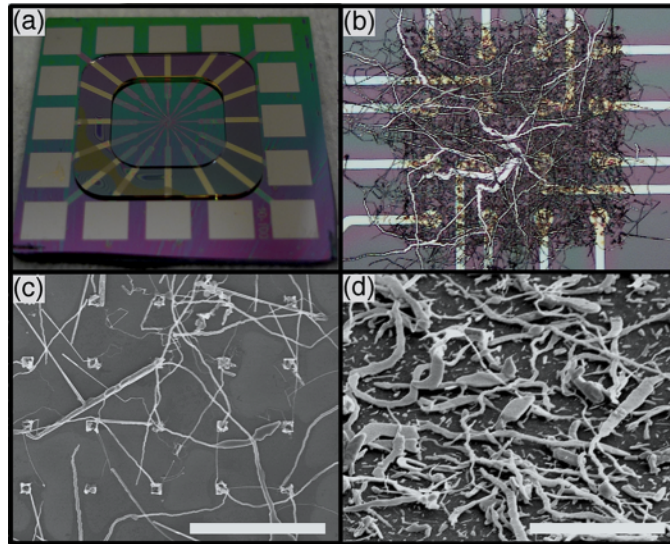
Figure 5.1: a) Atomic switch network devices were fabricated on a SiO_2 substrate with 16 Pt electrodes and an insulating SU-8 layer. Devices are approximately 4 cm^2. b) Resultant Ag wires vary in size (< 100 nm to > 1 mm) and create self-assembled networks with complex interconnections (109 cm^{-2}). Electrodes shown have 10 μm diameter and 50 μm pitch, and range up to 50 μm diameter with 500 μm pitch. c-d) The density of interconnections can be changed by altering the size/pitch of the Cu posts shown c) 1 μm/5 μm d) 1 μm/1 μm. Scale bars = 10 μm.

The maximum bandwidth of the measurement systems is 1 MHz and 10 kHz enabling 2 Ms and 20 ks per second with 16-bit resolution. Subsequent data analyses were carried out using MATLAB 2010b (MathWorks) and Origin 8.1 (OriginLab Corporation).

5.2.2 Network model and simulation

Simulation efforts employed previously reported physical properties of atomic switches composed of an Ag—Ag$_2$S—Ag interface, shown schematically in Figure 5.2, that exhibit both volatile and non-volatile memory properties as well as multi-state switching [HOT10, OHT11, THN05]. Atomic switches are known to operate through two mechanisms: (i) formation/dissolution of conductive filaments, and (ii) a phase transition between monoclinic acanthite (α) and body centered cubic argentite (β) Ag$_2$S. Application of a bias voltage across the junction induces the formation of nanoscale conducting channels across the Ag$_2$S interface through a bias-catalyzed phase transition, converting the surrounding α-Ag$_2$S matrix to a conductive and β-Ag$_2$S phase which exhibits high ionic mobility as illustrated by TEM-electron diffraction studies [XBW10]. In the absence of continued applied bias, the conductive channels eventually return to their stoichiometric, thermodynamically favored equilibrium state, which reverts the atomic switch to its initial high resistance. This transition gives rise to a weakly memristive behavior prior to the formation of Ag filaments across the interface.

Continued application of bias voltage results in a concurrent increase in current through the device, which then further drives migration of silver cations toward the cathode. At the cathode mobile silver cations are subsequently reduced to Ag^0, forming a highly conductive Ag nanofilamentary wire. The completion of this filament results in a strong transition to an ON state with a dramatic increase in conductivity [XBW10]. Removal of the applied bias results in filament dissolution as the device again returns its thermodynamic equilibrium state. The completion and dissolution of this filament characterizes strongly memristive behavior. Continuous application of a bias voltage serves to increase filament thickness as additional silver cations are reduced, causing thickening of the metallic filament. This
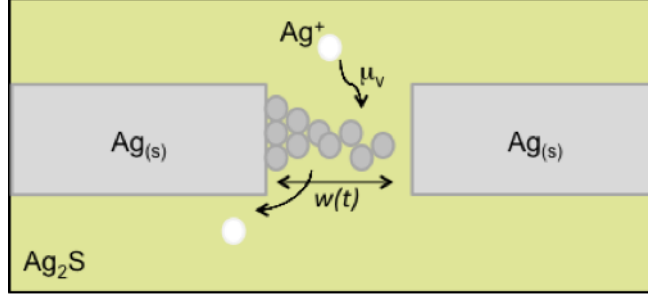
Figure 5.2: Atomic switches are comprised of a Ag—Ag$_2$S—Ag junction. Applied electrical bias causes Ag cation migration to the cathode where it is reduced, forming a stable metallic filament, resulting in resistance change. This migration is modeled by the filament length $w(t)$, Ag cation mobility μ_v, and additional stochastic terms.

dynamic process has been shown to alter the dissolution time constant, and can be externally controlled by changing the input bias pattern (e.g. pulse frequency). Such changes in volatility can be interpreted as long-term or short-term potentiation (LTP and STP) [HOT10, OHT11].

Using a similar construction, a recent report simulated a nearest neighbor grid of resistors and memristors [OS11]. Here, the memristive equations were augmented with new terms that reflect the known properties intrinsic to Ag—Ag$_2$S—Ag atomic switches as well as network effects. The state variable of the memristive elements was chosen to be the length of the Ag filament, represented as $w(t) \in [0, w_0]$, where the junctions' gap sizes, w_0, were randomized with a mean of 5 nm according to known values [HOT10, OHT11, THN05]. The voltage across each atomic switch junction is given by:

$$V(t) = [R_{on}\frac{w(t)}{w_0} + R_{off}(1 - \frac{w(t)}{w_0})] I(t) \tag{5.1}$$

where R_{on} and R_{off} represent the resistance values for the ON/OFF states and $I(t)$ the current across the atomic switch junction. The rate of change in filament length was modeled according to:

$$\frac{dw(t)}{dt} = [\mu_v \frac{R_{on}}{w_0} I(t)]\Omega - \tau[w(t) - w_0] + \eta(t) \tag{5.2}$$

where μ_v signifies the ionic mobility [Chu71, SSS08]. The window function, given by:

$$\Omega = [\frac{w(t)(w_0 - w(t))}{w_0^2}] \tag{5.3}$$

was included in (2) to incorporate the behavior of elements with state variables at the extreme limits due to ionic drift [OS11, SSS08]. The term $[\mu_v \frac{R_{on}}{w_0} I(t)]\Omega$ provided the dependence of filament growth rate on the electronic flux, while $\tau[w(t) - w_0]$ operated as a dissolution term that served to return the filament length to its original value w_0 due to the thermodynamic stability of the high resistance state. Although the dissolution rate constant τ has not been extensively investigated in the network setting, a numerical survey over three orders of magnitude ($1 to 1000s^{-1}$) determined the value that best reproduced the prior experimental results for the size of the simulated network. Lastly, a stochastic term $\eta(t)$ accounted for fluctuations in the density of available silver ions and the stochastic nature of the filament formation/dissolution process in physical ASNs. This term, defined by:

$$\eta(t) = \alpha(t)\Delta w(t) \tag{5.4}$$

governed the growth rate of filament sizes, where $w(t)$ represented the change in filament length at time t reflecting the amount of electric flux through the switch junction. Here, the random variable $\eta(t)$ introduced a noise factor to the term $\eta(t)$ that was distributed across the network following a random distribution centered at zero with a standard deviation σ_a. The probability distributions for both w_0 and α were examined using simulated network sizes ranging from 3x3 to 10x10 arrays with varying degrees of connectivity densities.

Finally, the connectivity in the simulation was modeled after the known interconnectivity of ASNs [SAS12]. Physical networks are grown from copper seeds spatially distributed on the substrate, which serve as nucleation sites for the electroless deposition of silver metal under diffusion-limited conditions [AMS13]. This directed self-assembly process generates

networks with a large distribution of wire lengths, characterized by SEM in the range of 100 nm to over 1 mm. The network contains elements of a nearest neighbor network, since the wires are likely to connect to those grown from nearby copper seeds (Figure 5.1c-d). They also exhibit characteristics of a random network as long wires extend across the entire network, connecting distant nodes, and also connecting many nodes at once (Figure 5.1b).

Connectivity in the simulation was created by starting with a square lattice of nodes mimicking the copper posts in the hardware design. Links connecting nearest neighbors as well as distant nodes were then assigned randomly with the total number of connections ranging from N=50 to 400. The simulation results reported here represent the typical network response observed with connections reassigned for each run. Finally, the values of the physical parameters such as ionic mobility, R_{ON}/R_{OFF} ratio, and average gap size were chosen according to experimental literature values as schematically illustrated in Figure 5.2 [HOT10, OHT11, THN05], leaving the only the network size and wiring density as free parameters. Table 5.1 summarizes the range of the values of the parameters explored to produce the results in this report.

w_0 (nm)	$\mu_v(m^2 s^{-1} V^{-1})$	R_{ON}/R_{OFF}	τ (s^{-1})	α	N
Avg: 5	0.5×10^{-12}	Avg: 10^{-1} to 10^{-3}	1 to 10^3	Avg: 0	50 to 400
σ: 0-40%		σ: 0-40%		σ: 0-30%	
				of Δw(t)	

Table 5.1: Parameters used in the simulation were tested over ranges that are physically relevant to the Atomic Switch Network system: total gap width w_0; ionic mobility μ_v of Ag$^+$ in Ag$_2$S; R_{ON}/R_{OFF} is the ratio of resistances at w = 0 and w = w_0; τ is the filament dissolution time constant; α modulates the level of noise in the w(t) term with each time step; and N is the total number of connections.

Network simulations were executed in MATLAB through a graphical user interface (GUI) that provides control over these parameters in addition to the locations and numbers of sources/drains, structure of input waveforms, and magnitude of input signals. The GUI also

provides direct monitoring of simulated I-V statistics as well as the current, power dissipation and conductivity of each link within the simulated network.

5.3   Results & Discussion

Various studies were carried out under conditions similar to the physical implementations in order to compare the numerical model's results with prior ASN device experiments [SAS12]. Results from these simulations are examined in the context of network complexity on the basis of the underlying device physics and their associated emergent properties. The simulation was then used to explore the parameter space of ASNs, establishing a systematic approach to optimize network performance in the context of given training schemes and computational tasks.

5.3.1   Device activation

Robust, hysteretic switching in ASN devices requires device activation by a symmetric triangle wave ramp applied across the network. As net flux through the network increased, connections became increasingly polarized and conductive, resulting different behavioral regimes (insets of Figure 5.3a-c). A lack of completed metal filaments characterizes the initial state in Figure 5.3a (inset) as the "soft switching" regime. Continued sweeping causes the formation of a continuously conductive path across the network, with intermediate connections operating in a higher conductance state. This transition is observed as a dramatic change in conductance, shown in the inset of Figure 5.3b, where network response changes from soft to "hard switching" as the fraction of strongly memristive elements increases past the percolation threshold [SAS12]. Continuous sweeping of the applied bias is known to encourage thickening and stabilization of as-formed nanofilaments [HOT10, OHT11, THN05], producing behavior that is robust to fluctuations in silver ion deposition/dissolution (Figure 5.3c inset). As a result, there is an increased likelihood for an element in the network to operate in the strongly memristive regime.

To reproduce this activation process, the simulation included the effects of filament sta-

bility on network response by tuning the distribution of noise factor $\alpha(t)$ while holding input bias amplitude and frequency constant. A high noise level ($\sigma_\alpha > 7$) was found to inhibit stable transitions, or $w(t)$ from crossing the interfacial barrier in the window function, which enforced the soft switching state (Figure 5.3a). Lowering σ_α enables $w(t)$ to increase past the barrier without interruption, inducing the transition from soft to hard switching at the network level (Figure 5.3b-c). Consequently, the noise level serves as a control parameter for the number of strongly memristive elements and the soft/hard switching behavior, supporting the conjecture on the mechanism behind the different switching behaviors.

Selecting the appropriate strength of the stochastic term enabled the ASN simulation to agree qualitatively with the experimental memristive behavior. While simulation and experiment show a quantitative difference in the hard switching regime (Figure 5.3c and inset), specifically in the rate of change between the high and low resistance states, stronger agreement with respect to R_{ON}/R_{OFF} ratio and the rate of resistance state change (Figure 5.6b) was observed in a more densely connected simulated network. To elucidate the underlying dynamics of the activation process, internal conductance maps of a sparse network reveal the conductive pathways responsible for maximum current flow when operating in the soft switching, transitional, and hard switching states. A single, dominant pathway emerged at the transitional state and was destroyed in the subsequent input bias sweeps that drove the network into the hard switching state. Further examination of functional connectivity over the entire activation process enabled identification of equivalent regions of network conductance for the transitional and hard switching states. In particular, the network followed different trajectories to achieve values of maximum conductance, whereby network conductance was increasingly distributed in nature for the hard switching case.

In the results described below, both w_0 and $\alpha(t)$ were sampled from Gaussian distributions. Parameters of the distribution of w_0 were selected to reproduce the experimental I-V curves by matching the bias voltage used in the simulation to our experiment.
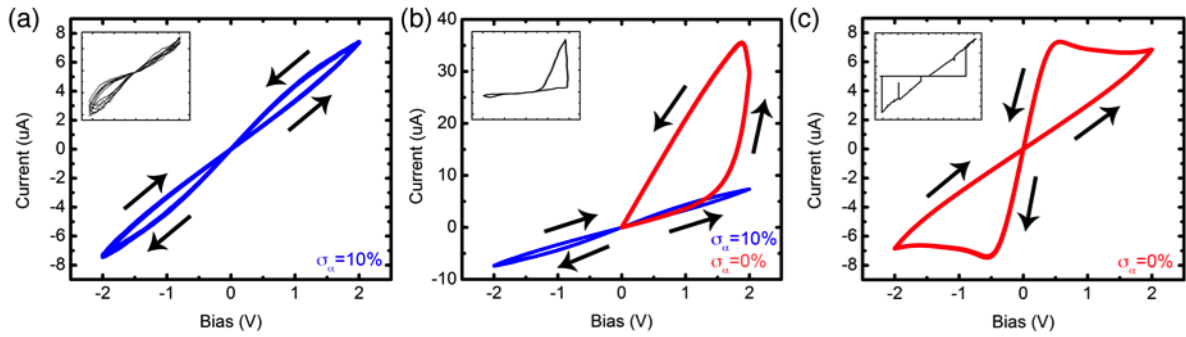
Figure 5.3: Simulation of device activation using a 10x10 network with N=126, average $R_{on}/R_{off} = 10^{-2}$ and $\tau = 10s^{-1}$ under a triangle wave input bias of $\pm 2V$ at 10 Hz demonstrating a) an initial soft switching ($\sigma_\alpha = 10\%$) repeated indefinitely until b) a transition in behavior from soft (blue, $\sigma_\alpha = 10\%$) to hard (red, $\sigma_\alpha = 0\%$) switching. c) Hard switching persists indefinitely with $\sigma_\alpha = 10\%$. This behavior was ubiquitous across all configurations with discrepancies in the bias amplitude/frequency. Experimental device activation curves shown as insets for comparison.

5.3.2 Recurrent structure

Physically implemented ASNs are observed to exhibit non-equilibrium dynamics under applied DC bias [SAS12]. These network fluctuations are attributed to two primary mechanisms: (i) external bias causes silver ion migration toward the cathode where they are reduced to form metallic filaments, in opposition to the stochastic, thermodynamically driven return to equilibrium and (ii) fluctuations in local resistance within the highly recurrent network can trigger cascading resistance changes elsewhere in the system. The behavior can be likened to neuronal avalanches observed in multielectrode array studies of neuronal cultures [BP03, SAS12]. In a single isolated link (Figure 5.4a), the stochastic term $\eta(t)$ results in the generation of white noise in the current output. In contrast, when embedded within a recurrent network single links displayed $1/f^\gamma$ power law scaling. This clear difference in characteristics shows the role of connectivity in a network. Each link in the network receives voltage inputs from many locations in the system and integrates which in turn modifies the link's instantaneous resistance. This behavior facilitates the emergence of spatially correlated structures in local network activity. The recurrent structure also enables the integration of signals originating at different points in time, giving rise to non-trivial correlations in the temporal domain as indicated by $1/f^\gamma$ power law scaling with $0 < \gamma < 2$ in the power spectral density (Figure 5.4). The current passing across the ASN in both simulation and physical measurements also displays $1/f^\gamma$ in the power spectrum (Figure 5.4b) [Kes82]. Although challenging to characterize in physical devices, the simulation data provides insight to both spatial correlation and phase synchrony for experiment.
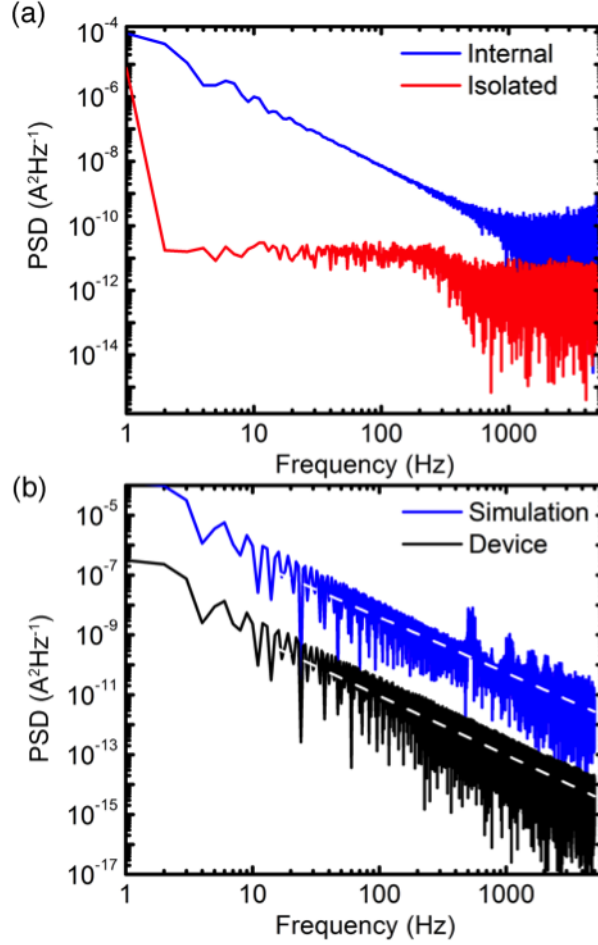
Figure 5.4: Comparisons of the power spectrum of a simulated 10x10 network N=332, average $R_{on}/R_{off} = 10^{-2}, \tau = 10s^{-1}, \sigma_\alpha = 2.5\%$ (blue) with a) a simulation of a single isolated atomic switch with identical parameters. The isolated atomic switch (red) shows a power spectrum dominated by white noise in contrast with a single element in network (blue) show $1/f^\gamma$ power law scaling, and b) that of a network device (black) that shows $1/f^\gamma$ power law scaling with $\gamma = 1.87$ (simulation) and 1.78 (device).

5.3.3   Feedforward subassemblies

Network plasticity was investigated as a mechanism for the formation of feedforward pathways within ASNs, although they have an inherently recurrent architecture. Previous studies on physical ASNs have demonstrated their functionality as a two-bit memory storage device with spatially controlled, independent switching channels using pulsed electrical stimulation [SAS12]. This experimental result, which used macroscopic electrodes in contact with a large area of the network to apply bias voltage stimulation, was also successfully simulated as illustrated in Figure 5.5. To comply with the experimental setup, a 10x10 network simulation was partitioned such that in each corner, a 4x4 block of nodes served the same purpose as a physical device electrode. A channel was defined by selection of one block as the source and another as the drain for application of an input bias voltage, with 4 blocks allowing for 6 possible channels. As shown in Figure 5.5, suprathreshold training pulses applied across 2 channels altered their respective conductances independently, even though the pathways were physically overlapping. By monitoring simulated connectivity maps of the other 4 conductance channels during this process, dynamical reconfigurations of the network connectivity were observed. Thus, nonvolatile memory write/rewrite steps occur concurrently with nontrivial changes elsewhere in the network. Different write/rewrite pulse combinations can store information while simultaneously allowing the network to evolve through new configurations. Investigations of structures and stability of feedforward subassemblies may be conducted by carrying out random or targeted deletion of links belonging to a given channel in relation to the strength and duration of the external pulses that induced its formation. Scaling the network size increases the number of distinguishable network states, allowing for increased memory storage and diversity of nonlinear interactions.
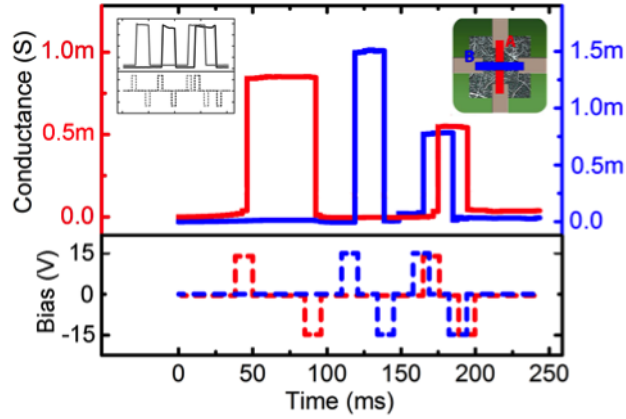
Figure 5.5: Spatially overlapping channels A and B can be modified independently by write/rewrite pulses, emulating the 2-bit switching functionality of actual device behavior (inset). This simulated 10x10 network (N=219, average $R_{on}/R_{off} = 10^{-3}$, $\sigma_\alpha = 2.5\%$) was partitioned with 4 separate 4x4 blocks to serve as electrodes. Spatially defined ON/OFF switching was induced by applying write/rewrite voltage pulses (15 V, 10 ms duration) across the channels specified in the figure. Measurements of conductance across all 6 possible channels were conducted with 1 V read pulses of negligible period.

64

5.3.4 Nonlinear network dynamics

Resistive switches have recently attracted attention for higher harmonic generation (HHG), presented in both single switches and networks [CPD12, OS11]. Experimental atomic switch networks show HHG to be a function of applied input bias amplitude [SAS12]. Here, numerical simulation was employed to explore HHG by stimulating a network with a sinusoidal input (10Hz) while varying the input amplitude and network connection density (connectivity). For each simulated network of a given connectivity, the HHG analysis was performed on data collected over 10 cycles of the input signal. The network was then reset to the same initial state for the next level of input amplitude. A sharp rise in the ratio of higher harmonic amplitudes to the fundamental at a threshold voltage was found in both experiment and simulation (Figure 5.6a).

The network I-V response curves at increasing levels of input bias amplitude (Figure 5.6b) illustrate the onset of nonlinearity as characterized by HHG in Figure 5.6a-c. As the voltage increased past the threshold magnitude, the switching behavior moved progressively toward the hard switching regime. The threshold voltage decreased with increased density of connections as shown in Figure 5.6c. An increase in connectivity provides more recurrent substructures in the network and can be related to the nonlinearity in the integration of electrical responses within the system. The decrease in the magnitude of the threshold voltage can be attributed to an enhanced nonlinearity in the network dynamics where even at lower bias voltage levels, the system tends to reside outside of a linear regime. These changes in the behavior of HHG suggest a way toward quantitative characterization of functional connectivity within ASNs based on their dynamics. As illustrated in Figure 5.1 and described elsewhere [AMS13], fabrication conditions for ASNs allow substantial control over the size, morphology and density of interconnects. Simulations may therefore be used to optimize physical networks for specific applications.
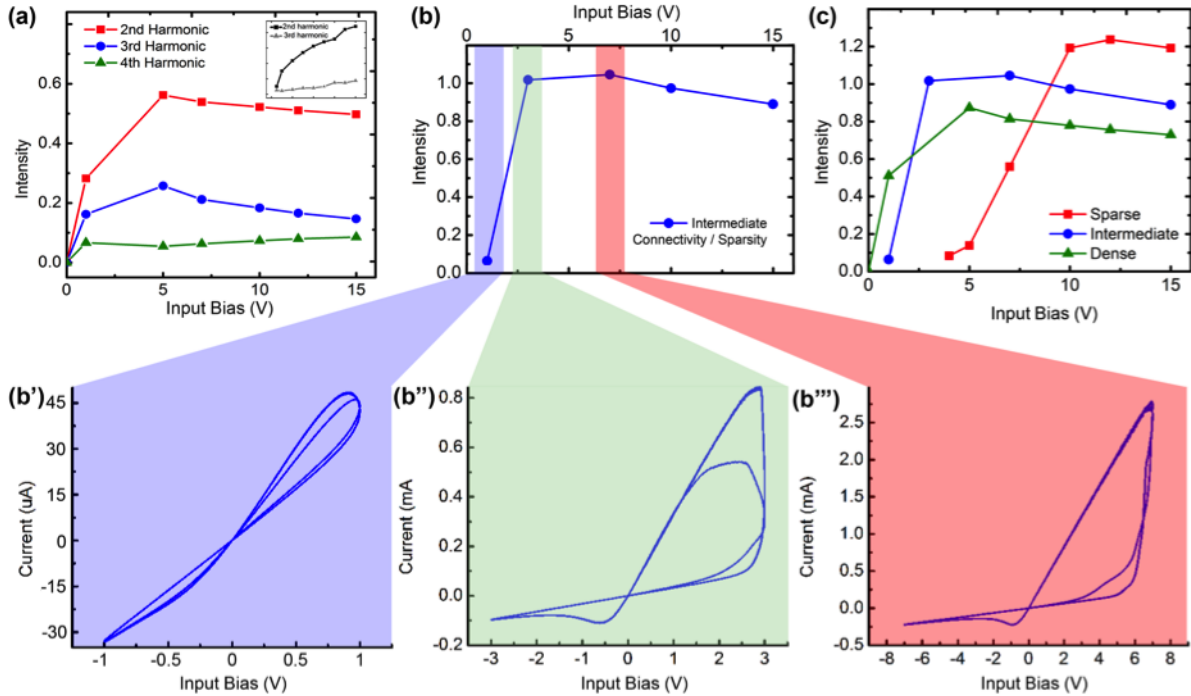
Figure 5.6: Higher harmonic generation can be influenced by network connectivity and input amplitude. Harmonic overtones of several simulated 10x10 networks with average $R_{on}/R_{off} = 10^{-2}$, $\sigma_\alpha = 2.5\%$, and $\tau = 10s^{-1}$. a) The first 3 harmonic overtones of a network with N=332 showed a threshold voltage for higher harmonic generation. Experimental device curves shown as an inset for comparison. b) Harmonic generation as a function of input bias amplitude for a network of intermediate connectivity (N=229). The network I-V characteristics tend towards hard switching behavior and increased higher harmonic generation as a function of input bias amplitude. c) The sum of the first 3 harmonic overtones of several simulated of networks with N=(126, 229, 332) indicated a shift toward lower threshold voltages with increasing connectivity ascribed to an increasingly complex network.

5.3.5 Reservoir computing

Higher harmonic generation is potentially of great usefulness in a modern computational paradigm utilizing recurrent complex networks, called reservoir computing (RC). The amplitude and frequency characteristics of produced higher harmonics may be used to quantitatively evaluate the efficiency of a reservoir in different dynamical regimes by accounting for the accessible degrees of freedom in higher dimensional representation space. Using voltage time traces as outputs, it is shown here that the ASN can effectively serve as a nonlinear reservoir capable of performing the waveform generation task (Figure 5.7) considered as a prerequisite to perform reservoir computing [Jae02].

Maximizing the number of output signals is advantageous in the context of RC training. Each network node was therefore chosen to serve as an output electrode. By subjecting the network to a sinusoidal input at one corner electrode in the form of an input bias voltage, multiple waveforms including triangle, square and frequency doubling sinusoidal waveforms were constructed through superposition of voltage outputs at each electrode in the simulation. The generated waveform r_q $(q = 1, 2, 3)$ was then a weighted sum of the voltage outputs from the electrodes with the weights W_q^i calculated by linear regression:

$$r_q = \sum_{i=1}^{m} W_q^i V_i, \ q = 1, 2, 3 \ (5)$$

where V_i are the output electrode voltages. Reservoir performance was assessed by the quality of waveform generation and compared across networks with different parameters by calculating the mean square error (MSE), which quantifies the differences between the target and the generated waveforms:

$$MSE = \frac{\sum_{n=1}^{p} (y_{target}(t_n) - \sum_{i=1}^{m} W^i V_i(t_n)^2)}{P} \ (6)$$

where y is the target waveform. W^i represent the weight coefficients to be trained with maximum number of outputs $(m = 16)$ at discrete time indices (t_n) over a total length (P) from $n = 1$ to 9000. To see whether the diverse dynamical regimes of ASN may affect the efficiency of RC training, the input gain was varied to access the different characteristics generated of the higher harmonics. The weights were calculated independently using the output responses from the network at each input voltage amplitude. As the magnitude of the applied
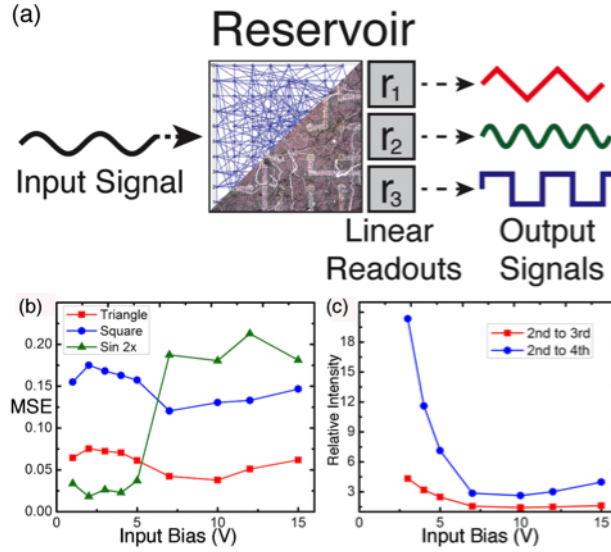
Figure 5.7: a) Schematic of network simulation used in the waveform generation RC task, with specific electrodes chosen as inputs/outputs (16 output electrodes). RC was implemented using a 10x10 network (N=126, $\sigma_\alpha = 2.5\%$) with a 5 V, 10 Hz sinusoidal input signal and tasked to produce 10 Hz triangle/square and 20 Hz sinusoidal waveforms. b) Mean-squared error (MSE) for each task with respect to driving amplitude showed minimal error in triangle/square waveform generation task at 10 V, corresponding to the onset of higher harmonic generation (see red curve of Figure 5.6b). Performance in the 20 Hz sinusoidal waveform generation task decreased when c) the relative amplitude of the average 2nd harmonic intensities of the readouts becomes increasingly diminutive. These results correspond to a strong dependence on the 2nd harmonic for 20 Hz sine generation and the need for HHG in triangle/square generation as expected by Fourier analysis.

input voltage was increased, an abrupt onset of HHG (Section 3.4) was observed to influence the associated error for the waveform generation tasks. Specifically, the ratio of the second to higher harmonics (calculated with unweighted average of network outputs) dropped rapidly with increasing voltage ($\approx 8V$) as seen in Figure 5.7c. This bias-dependent reduction in second harmonic amplitude was found to correlate directly with the critical voltage where MSE increased dramatically in the task of generating a sine wave exhibiting frequency doubling of the input signal. As the 2nd harmonic becomes less pronounced compared to the higher harmonics it becomes more difficult to isolate in a linear combination of the output signals through linear regression. In contrast, an increased ratio of higher harmonics to the second harmonics resulted in better performance for the generation of waveforms containing higher harmonic components such as square and triangular waveform. While HHG is not a universal parameter designed to indicate increased computational performances, it does faithfully explain computational performances on specific RC tasks.

The results clearly demonstrate that an ASN can be used as a pattern-generating kernel in RC where it can be optimized by adjusting input gain and network connectivity. Training ASNs to carry out more complex tasks requiring multiple, simultaneous inputs/outputs as well as real-time feedback are currently under investigation [SVV07].

5.4   Conclusions & Outlook

Numerical modeling of atomic switch networks is essential for understanding the experimentally observed emergent phenomena, and the microscopic degrees of freedom for synaptic elements. A valid numerical simulation offers a controllable, convenient platform from which to study specific aspects of the device functionality, and permits identification of control parameters for network level behaviors as well as system optimization. By extracting the relevant dynamical components of the network, our model can be expanded to understand the functionalities of ASNs with respect to a larger theoretical framework.

The simulation, incorporating network stochasticity and filament dissolution into its state equation, shows ASNs as devices capable of forming feedforward subassemblies that utilize

69

network plasticity. Simulation results also reveal the networks' nonlinear integration of local electrical responses. Specifically, individual atomic switch elements show changes in their power spectral density when embedded in a network, while HHG emerges in the ASN with external bias and connectivity as control parameters.

Our simulation results support the feasibility of utilizing nonlinear dynamics without needing to control or "train" the connections in the reservoir, and have indicated how to best optimize physical device parameters to maximize RC efficiency for a given task. Future efforts will focus on implementing benchmark tasks in RC in both simulation and hardware to quantitatively assess the kernel quality and generalization rank [SVV07] in relation to the changing parameters as compared to other software and hardware reservoirs. Note that the plasticity intrinsic to the ASN makes it a dynamical reservoir, which show improved function for some RC tasks [LPT09]. The dynamics of these devices during the training period may be further characterized by calculating the Lyapunov exponent and used to elicit the connections to increased computational power at the edge of chaos [Lan90].

The results presented here also demonstrate the value of using synaptic elements within a biologically inspired connective architecture. Substantial efforts have been undertaken to characterize and comprehend the dynamical hierarchy of a functioning complex system such as the brain [KPB05, Fri08, MLF09, GS10]. The existence of a readily scalable, physical device exhibiting many of the same dynamics as biological neural assemblies underscores its potential as a tool to study complexity. The greatest potential of ASNs lies not only in the versatility of hardware design but also in their scalability. A strategy which scales up the hierarchical dimension, combined with insights obtained by actual learning and task performance through RC could generate valuable new computational devices.

CHAPTER 6

Emergent Criticality in Complex Turing B-Type Atomic Switch Networks

Recent advances in the neuromorphic operation of atomic switches as individual synapse-like devices demonstrate the ability to process information with both short-term and long-term memorization in a single two terminal junction. Here it is shown that atomic switches can be self-assembled within a highly interconnected network of silver nanowires similar in structure to Turing's "B-Type unorganized machine", originally proposed as a randomly connected network of NAND logic gates. In these experimental embodiments, complex networks of coupled atomic switches exhibit emergent criticality similar in nature to previously reported electrical activity of biological brains and neuron assemblies. Rapid fluctuations in electrical conductance display metastability and power law scaling of temporal correlation lengths that are attributed to dynamic reorganization of the interconnected electroionic network resulting from induced non-equilibrium thermodynamic instabilities. These collective properties indicate a potential utility for real-time, multi-input processing of distributed sensory data through reservoir computation. We propose these highly coupled, nonlinear electronic networks as an implementable hardware-based platform toward the creation of physically intelligent machines.

6.1   Introduction

Modern state-of-the-art computers are the product of over half a century spent refining implementations of Turing's automatic machine (TAM)[Tur50] using Von Neumann's computational architecture[Neu88]. The TAM is the principal theoretical framework for computation

using sequential logical operations on single-purpose hardware consisting of an infinite tape of symbols, a read/write head, and a control mechanism that acts based on a transition table or instruction sheet. Von Neumann's introduction of the concept of memory into the computer architecture provided a blueprint for the physical realization of multi-functional TAM machines that utilize multiple stored programs via two main functional units - processors and memory. This flexible control mechanism made the TAM truly universal in its capacity to complete any algorithmically defined task.

The von Neumann architecture has the principle advantage of clarity from the engineering perspective. Reduction in the physical size and increased areal density of electronic components directly scales up performance in terms of increased bytes of storage and processor cycles per second. The extension of this trend toward biologically inspired or artificially intelligent computation has resulted in attempts to simulate every neuron in the mammalian cortex and to outperform human experts in games of strategy[AES09, CHH02]. These achievements, while impressive, are not readily scalable due to the basic constraints of the CMOS architecture, its associated methods of fabrication, and the limits of its operational mechanism [HBT11]. Further, the requisite passage of program instructions and data between processor and memory has evolved as a speed-limiting step known as the "von Neumann bottleneck" (vNB)[Bac78] (Figure 6.1a), which results in idle processor cycles and power dissipation as information is simply being transferred, not processed. In combination, these factors generate a computational architecture that consumes orders of magnitude more space and energy than intelligent biological systems.

While current state of the art approaches to computation represent tremendous progress in performance and efficiency versus their historical counterparts, computer scientists have drawn inspiration from biology in an effort to develop computational strategies that are able to match the capabilities of biological neural networks (BNN). Remarkably, such concepts were proposed over sixty years ago as Turing's "B-Type unorganized machine"[Tur92] (TBTu), and have been subsequently popularized by Rosenblatt's perceptron, recurrent neural networks, and reservoir computing [Ros58, Hop82, AHS85, BM95, MNM02, BN04, VSd07, LJ09]. These bio-inspired designs are generally associated with the notion of "connection-
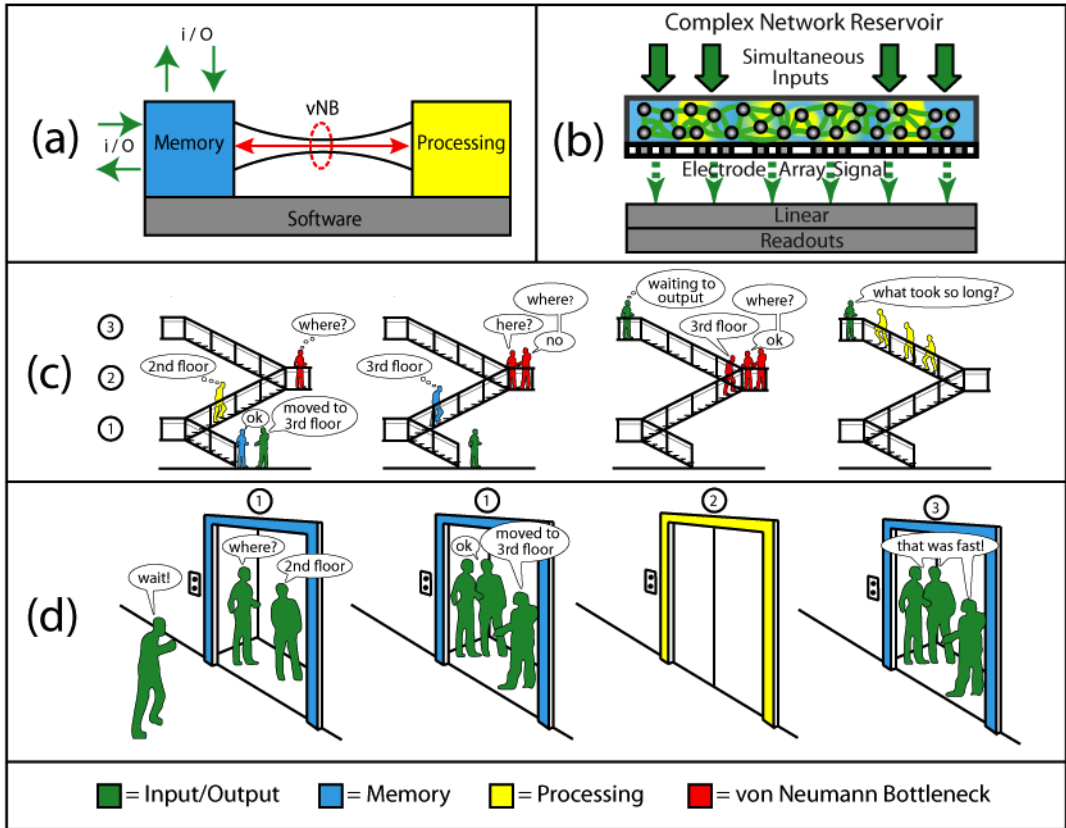
Figure 6.1: Comparison of computation using Turing automatic machines (TAM) and Turing B-Type unorganized machines (TBTu)/Complex Network Reservoirs (CNR). (a): Conventional TAM computation suffers from the intrinsic von Neumann bottleneck (vNB), as instructions and data must be shuttled back and forth between memory and processor cores. (b): TBTu/CNR computation transforms simultaneous input streams into a higher dimensional forms/patters that are converted to intelligible outputs by a linear classifier, which can be readily trained to detect various categories of CNR behavior. (c) As calculations proceed sequentially in TAM (yellow figures), new input is delivered to memory (blue and green figures, respectively). Earlier processes are unable to produce desired output due to outdated instructions and must idle in the vNB (red figures). Upon the arrival of new instructions from memory, calculations can resume and proceed towards the output (green figure on third floor). (d) In TBTu/CNR computation, inputs combine simultaneously to fill the waiting elevator. This process is more time consuming (it is a slow elevator!), but upon arriving at the third floor (output), they have undergone a complex transformation, having spent time interacting to create a new state of the system.

ism". Connectionist theories are based on complex networks composed of simple units, which, as a whole, produce emergent behavior not found or associated with any particular unit [Jen98]. What constitutes a "complex system" is difficult to define precisely. However, extensive studies of complex, real-world networks have revealed the importance of both structural topology and internal dynamics. Various models of connectivity and interaction have been shown to accurately describe phenomena ranging from relationships between corporate directors to the backbone of the Internet[Str01].

To date, artificial realization of connectionist architectures has been limited by the capacity to fabricate robust interconnects between electronic components in a cost-efficient manner, especially in designs utilizing unconventional topologies. Recent advances in nanoscale science and technology have enabled the direct self-assembly and integration of functional circuit elements within the wiring scheme of nanoscale devices with the unique architectures[RJB96, JGA00, TVH02, LMM03, ASM12]. Here, we utilize these concepts to construct a densely interconnected network of synapse-like circuit elements, atomic switches, using bottom up self-assembly. We find that this system demonstrates synaptic properties as well as some of the emergent behaviors commonly observed in biological neural networks[BP03, LHG07, MMK10, Wer07, HB05]. These complex atomic switch networks provide as a promising new direction for the development of functional TBTu-inspired neuromorphic computing devices, with specific implications toward physically implementable reservoir computation.

6.2 Computational Models

Building upon decades of inspired research based in the TAM/von Neumann computational paradigm, modern processors routinely include multiple cores and large memory caches to maximize efficiency by parallelizing computations and reducing memory access times. In addition to physical limitations on component size and the vNB, leakage currents through gate dielectrics, programming challenges in parallel processing, and intolerance to faulty elements have begun to impact operational performance. These obstacles provide strong motivation to develop and implement alternative computational strategies. To this end, numerous theories

and proposals have been put forth toward biologically inspired, neuromorphic computing devices[Mea90].

Biological neural networks utilize self-configuring, hardware-based architectures capable of dynamic topological alteration and function without the need for pre-programming or an underlying software algorithm. These intrinsically nonlinear, complex systems demonstrate extraordinarily efficient transmission of information and emergent behaviors commonly associated with intelligence such as associative memory, learning, and predictive capacity in non-deterministic environments. Once such theoretical construct, the TBTu, was conceived of as a randomly interconnected network of nothing more than modifiable NAND logic gates. Since NAND gates may be combined to perform any other logic function, Turing hypothesized that a sufficiently large network could serve as a usable computer, capable of any TAM operation[Tur50]. Moreover, he showed that its connections and operations could be trained over time to alter its behavior, in a similar fashion to that of a biological brain.

This concept has been applied in the fields of cognitive modeling and artificial intelligence to form the basis of contemporary research into artificial neural networks (ANN). These ANNs are typically implemented as software running on conventional TAM systems, mimicking information processing in natural systems. The earliest ANNs, commonly known as the "perceptron", utilized a feed-forward design in which artificial neurons are connected by modifiable synaptic weights and can "learn" to map input-output relationships according to any (mathematical) function[Ros58]. The development of recurrent neural networks (RNN) enabled the inclusion of adaptive capacities through feedback strategies[Hop82]. The existence of cyclical connections makes the RNN a dynamical system, capable of sustaining internal activity in the absence of additional signals, not merely mapping input to output. However, basic RNN training strategies still involve the direct modification of internal synaptic weights implemented abstractly using algorithms inspired by biological neural networks. In addition, ANNs are generally designed and optimized to perform specific computational tasks, occasionally utilizing purpose-built hardware for increased functionality. This enhanced performance comes at the expense of flexibility, adaptability, and the capacity to synthesize multiple time-varying input signals or to operate in a non-deterministic fashion

— all hallmarks of biological neural systems.

Reservoir computation (RC) is a promising extension of RNNs towards more accurately modeling biological neural networks that has been successfully implemented in various engineering applications[MNM02, BN04, VSd07, LJ09]. Instead of tracking and modifying individual synaptic weights, the complex network of artificial neurons is treated as a reservoir, which is dynamically modified by the input, while retaining some (fading) memory of previous input signals as well. The complex network reservoir (CNR) acts to map these lower-dimensional input signals into a higher-dimensional space, represented by patterns in the state of the system and contains temporal information through integration of the input history. Poised between simply periodic and wildly unpredictable oscillations, the CNR is thereby allowed to operate at the edge of chaos[Lan90].

This approach overcomes the challenge of training individual synaptic weights inside RNNs by not explicitly modifying them at all. Instead, a separate readout/output function is trained to examine the response of the reservoir, interpreting the spatiotemporal patterns formed by the collective effect of the input signals and transforming this higher-dimensional information into the desired output. Through appropriate training, RC methods are capable of simulating any Turing-type computational machine. Since the reservoir functions autonomously, a variety of readout functions can be used simultaneously, thereby allowing the system to carry out multiple computational tasks on the same input stream in real-time[MNM02, BN04].

While simulation and modeling efforts using traditional computational architectures remain the general, near-term focus of reservoir approaches, calls for the development of hardware-based CNR systems continue to form the basis for inquiry into a new paradigm of computational methods. Achieving these goals requires the development of physical systems whose properties mimic those of artificial, simulated reservoirs as well as a means to harness the power of information rich output patterns they generate. We propose that the former can be achieved by applying the concept of Turing's connectionist networks to the fabrication of complex device architectures comprised of highly interconnected, nonlinear electronic elements. The latter requirement necessitates a near-infinite set of internal sys-

tem states capable of receiving/storing information from all parallel input streams as well as the ability to combine complex, dynamic signals into a single, higher-dimensional output. This type of behavior principally describes that of a system operating in a critical state, a property commonly associated with complex networks of nonlinear elements, where the divergence of the system correlation length in both space and time provides all these requisite characteristics[Jen98, Bak97].

6.3   Complex Device Architectures

The structure and activity of the biological brain is intrinsically complex, comprised of billions of neurons interacting recurrently through trillions of synaptic interfaces by utilizing a range of signaling chemicals to produce excitatory and inhibitory changes in electroionic conductivity. This dynamic, evolving system produces emergent phenomena with which we are intimately familiar such as consciousness, intelligence, learning, and prediction. The realization of hardware-based neuromorphic networks requires the ability to fabricate highly interconnected, complex wiring architectures with integrated circuit elements whose nonlinear properties emulate those of biological neurons and synapses. Fabrication of micro- and nanoscale devices with complex architectures, especially those with some degree of random structural topology, is difficult using solely lithographic methods due to challenges in forming robust intra- and inter-device connections in a cost-efficient manner. However, combining directed and self-assembly of nanoscale building blocks into functional device components offers a promising route to creating intricate patterns of nanoscale components. To create operable devices based on nanoscale architectures, two basic issues must be addressed: which materials to use and how to pattern them into networks that have some degree of randomness without negatively affecting their functional characteristics.

Simple metals continue to be the material of choice for wires and interconnects in the fabrication of electronic devices. The power-law relationship known as Rent's Rule formalized the trend between the number of connections in integrated circuit designs and the number of internal components, such as logic gates, and how these are strongly related to both logical
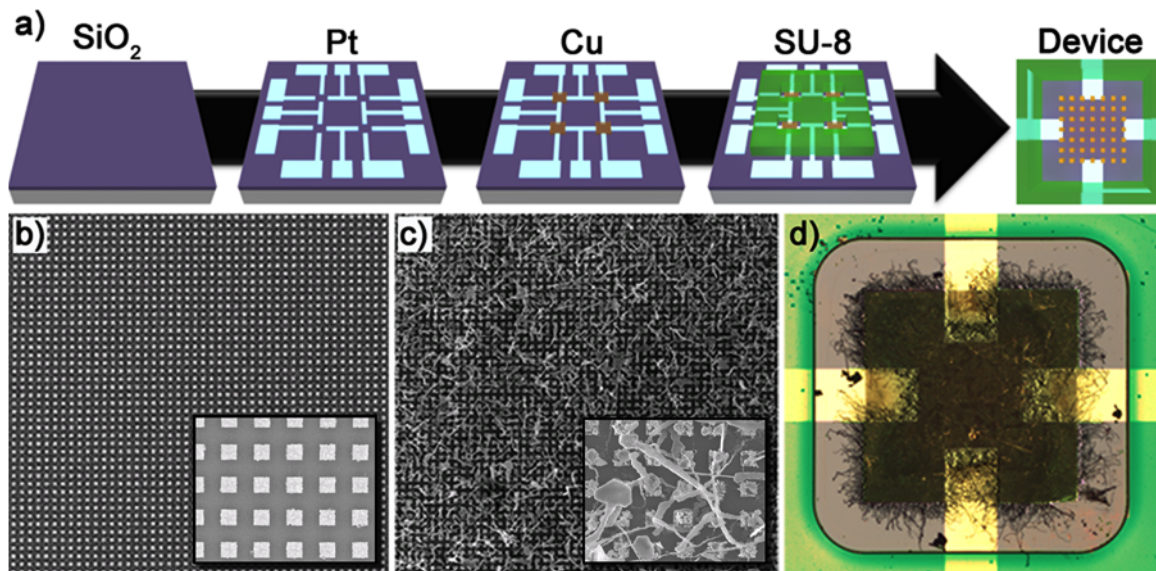
Figure 6.2: Fabrication scheme for complex, electronic networks. (a) Schematic of the substrate/device microfabrication through various lithographic techniques. (b) Cu seed posts (1 μm^2, 1μm pitch, 300 nm height) deposited onto the substrate by electron beam lithography react with $AgNO_3$ within a reaction well formed from SU-8 epoxy photoresist, (c) resulting in electroless deposition of complex Ag nanowire networks. (d) The network extends throughout the device well and is electrically probed via macroscopic Pt electrodes.

capacity and complexity of the interconnect architecture. This relationship infers that the limits on synthetic complex architectures lies in the cost of fabrication, with specific focus on interconnect and wiring strategies[LR71, CS00]. Research has shown that biological neural systems also obey this relationship[BGM10]. Whereas biological networks realize a balance of cost and complexity through structural self-similarity and hierarchical modularity, ANN implementations based on TAM/von Neumann architectures remain at the mercy of this "cost of wiring". While motivating the creation of bio-inspired devices, Rent's Rule further underscores the fact that new methods, differing not only in scale but also in kind, must be developed to meet these challenges.

Solution phase electrochemistry offers an intriguing approach to the unconventional fabrication of complex metallic structures. In particular, the electroless deposition of various metals through the spontaneous reduction of soluble metal cations is a mature technology that has been employed extensively in macroscopic plating applications and the manufacture of printed circuit boards (PCBs). In contrast to plating applications, dendritic (fractal) growth processes have been studied extensively for various reasons[WS81, KA95, MSU97]. Unwanted, spontaneous growth of dendritic metal protrusions through insulating layers has posed an engineering challenge as the resulting electrical shorts lead to device failures. In a more positive light, interest in these intricate structures generated insightful mechanistic models, such as diffusion-limited aggregation (DLA), that were tested and confirmed through comparison of simulated structures to physically produced metallic silver fractals by reducing controlled concentrations of Ag^+ using seed metals such as copper and zinc.

Here, the electroless deposition process has been extended to produce devices with complex architectures possessing both regular and random features by combining top-down directed patterning of seed materials at the microscale with bottom-up self-assembly of functional nanomaterials. Lithographic patterns of metallic copper were reacted with dilute solutions of silver cations to create complex networks of metallic silver nanostructures (Figure 6.2). Optimization of this process enabled the controlled production of structures ranging from extended nanowires to dense fractals, similar to biological neural assemblies such as axons and dendrites[AMS13]. Spontaneous generation of nanogaps between these

79

as-prepared metallic nanostructures has been attributed to ionic depletion in the interfacial regions, due to the DLA growth mechanism. In addition, the formation of nanowire crossbar-like junctions resulted from the three-dimensional nature of the solution deposition process. By combining this wiring approach with compatible materials that demonstrate synaptic properties, we have generated a complex network of randomly distributed, highly interconnected inorganic synapses.

6.4 Synthetic Synapses

Performing distributed, real-time computation of complex information requires suitable electronic device elements capable of mimicking salient aspects of biological synapse function at the relevant physical scales. Recent research has developed a vast catalogue of nonlinear, solid-state electronic elements for use in integrated circuits and solid-state memory. A class of these, known as resistive switches, has received substantial attention as a synapse-like element for use in next generation neuromorphic computers. Resistive switches (RS) are two-terminal circuit elements that are distinguished from simple resistors by nonlinearities in the relationship between current and voltage across their terminals[WA07]. These nonlinearities can take various functional forms, from a smooth dependence on the time integral of current passed through the device, to discontinuous jumps at some threshold value, or combinations thereof. The resultant nonlinear dynamics can produce behaviors typically associated with biological neural networks, including long-term potentiation, long-term depression, spike timing dependent plasticity, and associativity[HOT10, PD10, LZL10, OHT11]. The basic RS is a nanoscale device composed of a metal-insulator-metal (MIM) junction that can be fabricated using a variety of materials.

An exciting subset of electroionic RS known as atomic switches exhibit common RS characteristics including pinched I-V hysteresis and large ON/OFF switching ratios as well as more exotic behaviors such as multistate switching in quantized increments of conductance[THN05]. The distinguishing feature of the atomic switch is its operational mechanism: atomic switches utilize metal filament formation/annihilation and concurrent bias-catalyzed phase transition

within a solid-state electrolyte metal-insulator-metal (MIM) interface. One prevalent atomic switch configuration employs MIM interfaces of silver and silver sulfide (Ag_2S). This chalcogenide undergoes a temperature-dependent and bias-catalyzed transition from the monoclinic, semiconducting α-Ag_2S phase (acanthite, $2.5 * 10^{-3}\Omega^{-1}cm^{-1}$) to a body-centered cubic, metallic β-Ag_2S phase (argentite, $1.6 * 10^{3}\Omega^{-1}cm^{-1}$)[XBW10]. The argentite phase has a remarkably high diffusion coefficient for silver, approximately equal to that of gaseous silver atoms at an equivalent temperature and density. Under applied external bias, this formulation operates via redox coupled ion migration of silver ions within the metallic argentite phase. While some RS are strictly non-volatile, the Ag-Ag_2S atomic switch exhibits nonlinear, time-dependent conductance that has lead to the observation of a number of fascinating synapse-like properties including short- (volatile) and long- (non-volatile) term memory[HOT10, OHT11]. Robust operation of these devices at rates up to 1 MHz over 105 cycles further enhances their potential applicability as a synthetic synaptic element.

To date, atomic switches have been primarily fabricated through advanced lithographic methods in regular, crossbar-type architectures that are promising candidates for nanoscale memory applications when operated in isolated, single device configurations. However, their operational characteristics are less well understood when connected in series, parallel, or directly coupled through their ionically conductive active layer, as would be required to implement computation in the TBTu/CNR paradigm. Inspired by the exciting synaptic properties of the Ag—Ag_2S—Ag atomic switch configuration and its and material compatibility with our scheme for fabricating complex nanowire networks, we have characterized the properties of interconnected atomic switches as a means to examine their potential applicability as physical implementations of TBTu/CNR-based computation.

6.5 Critical Atomic Switch Networks

Complex networks of coupled nonlinear elements commonly manifest non-trivial spatiotemporal evolution through dynamic system reconfigurations[BMA06, DGM08] which enable enhanced maintenance of system correlations and more effective signal propagation[Str01].

Such behaviors can be attributed to a system governed by critical dynamics and are crucial to the proposed implementation of hardware-based TBTu/CNR-inspired machines. As such, we have fabricated and examined the operational characteristics of an electronic device comprised of a highly interconnected network of interfacial atomic switches wired through electroless self-assembly. Formation of the complex atomic switch network entailed conversion of as-prepared metallic nanogap and crossbar-like interfaces into metal-insulator-metal (MIM) junctions (Ag—Ag_2S—Ag) through gas phase sulfurization. Due to the nature of the electroless deposition process and resulting random network topology, a thorough survey of sulfurization conditions was carried out to optimize the fabrication protocol.

Progressing from isolated, individual synthetic synapses to an assemblage of electro-ionically coupled units introduces an extensive set of collective interactions potentially capable of producing emergent behaviors. Spatially distributed atomic switch junctions are expected to interact through local variations in ionic concentration and electrochemical potential that depend on the combined electrical resistance of the entire network as well as the configuration, or state, of all other electro-ionically interconnected switches. Furthermore, given that atomic switch synapses exhibit a conductance decay time constant dependent on their operational history[OHT11], one can expect their dynamical behaviors to be additionally complex.

To examine these properties, atomic switch networks were investigated by I-V spectroscopy. In common with isolated crossbar-type devices, as-fabricated atomic switch networks required an initial forming step whereby a sustained, high ($\approx$ 6V) bias would bring about a large but temporary drop in resistance. While parameters of the forming step varied from device to device, this requisite step indicates the successful preparation of MIM interfaces within the network. After forming, slow voltage sweeps (1 V/s) resulted in pinched hysteresis curves (Figure 6.3a) with an ON/OFF ratio of 103, further validating the formation of a functional atomic switch network with behavior analogous to that of a two-terminal RS device. Repeatable switching was observed over 104 cycles, and was successfully operated up to a 1 kHz switching rate. Extended periods of device interrogation under no applied bias resulted in a return to the OFF state, as expected from the operational mechanism
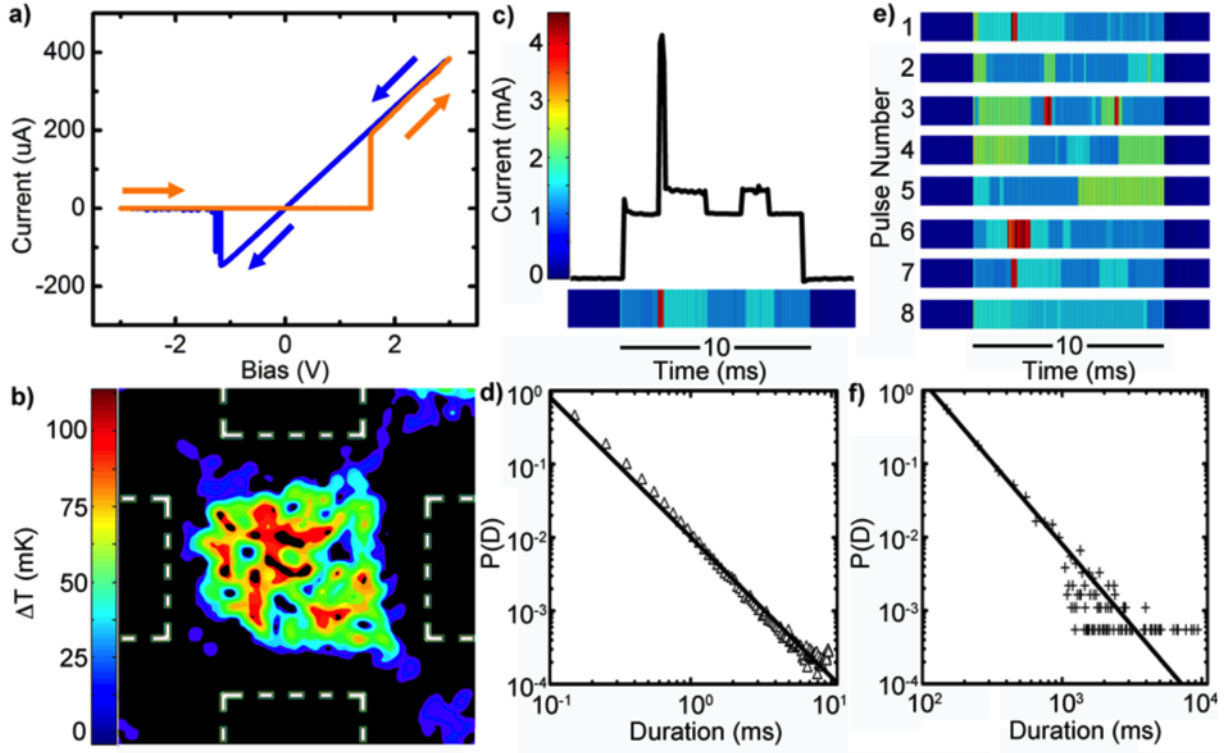
Figure 6.3: Electrical characteristics of complex nanoelectroionic networks. (a) Experimental I-V curve demonstrating pinched hysteresis; $R_{ON}=8$ kΩ, $R_{OFF}>10$ MΩ. (b) Ultrasensitive IR image of a distributed device conductance under external bias at 300K; electrodes are outlined in white. (c,e) Representative experimental network current response to a 2V pulse showing switching between discrete, metastable conductance states. (d,f) Temporal correlation of metastable states observed during pulsed stimulation demonstrated power law scaling for probability, P(D), of metastable state duration. Power law scaling existed for residence time both (d) within a single 10 ms pulse and (f) over 2.5 s during extended periods of pulsed stimulation.

of this particular Ag—Ag$_2$S—Ag configuration. Un-sulfurized control devices comprised of a purely metallic network demonstrated ohmic I-V characteristics at intermediate voltages (±3V) followed by irreversible breakdown (melting) at high bias.

To rule out the possibility that network activity was simply the result of conductance localization along a dominant pathway, creating in essence a single large, serial atomic switch, the device was characterized using ultra-sensitive IR imaging (Figure 6.3b). These results revealed thermal emission at room temperature from Joule heating throughout the network, indicating distributed and dynamic power dissipation during operation. Further, the application of spatially-defined voltage stimulation enabled controlled activation/deactivation of specific regions within the network (data not shown). Finally, enhanced overtones in the device current response were observed[ASM12] as predicted by recently reported modeling of random resistive switching networks stimulated with a sinusoidal voltage[OS11]. These results collectively indicate the successful formation of an interconnected network of nonlinear elements, in this case atomic switches.

Emergent behavior was observed during pulsed voltage stimulation, in analogy to methods employed in neuroscience to probe cortical cultures. Under typical conditions (2 V, 10 ms pulses, 10% duty cycle), the current response fluctuated over a wide range of metastable conductance states associated with discrete network configurations (Figure 6.3c-f), as classified by residence times in a given state ranging from milliseconds (within a single stimulation pulse) to several seconds (across hundreds of pulses). Specifically, temporal metastability was designated for all conductance states whose persistence time exceeded that of the measurement bandwidth (10 kHz). Observation of both increased and decreased conductivity during stimulation can be attributed to internal network dynamics, as conductance of isolated atomic switches only increases in response to sequences of identical stimulation pulses[HOT10, OHT11, THN05].

Previously unreported current fluctuations of this kind are ascribed to dynamic redistribution of network connectivity caused by actions of both individual switches as well as electroionic coupling throughout the shared active layer. Specifically, formation of a conducting filament results in localized depletion of silver cations within the solid electrolyte

and thereby inhibits the formation of filaments at nearby MIM interfaces. Due to the high diffusion constant of Ag^+ in the β-Ag_2S, this non-stoichiometric region may extend relatively large distances and induce weak electroionic coupling even between distant switches. Furthermore, concurrent formation and annihilation of conductive filaments will redistribute current flow, thereby modifying local electrical potentials across the network. These local variations sum to produce the observed fluctuations in global network conductance. While direct mechanistic confirmation of the observed conductance fluctuations would be useful, the inferred mechanism proposed here provides a rationale for future optimization of the network architecture.

Critical dynamics are of ultimate importance for applications of TBTu/CNR-based computation. Indicators of criticality typically include power-law scaling of 1/f fluctuations and temporal metastability. Analysis of the power spectral density of network conductivity in the activated state revealed 1/f power law scaling over five orders of magnitude with $\alpha \approx 1.4$ (data not shown). Electroionic coupling within the atomic switch network generated metastable conductance states, which were analyzed for temporal correlations. Comparing the probability of state duration with its likelihood indicated a power law distribution with $\alpha \approx 1.8$ (Figure 6.3c-f), indicating a diverging temporal correlation length. Observations of both spatially distributed electroionic activity within the network and the long-term persistence of metastable state residence times alongside short-term, rapid fluctuations between many available conductance states are strong indicators of critical system dynamics during intermittent pulse operation. These metastable conductance states represent unique configurations of the network and infer behavior similar to those of spatiotemporal states associated with neural dynamics and those required by reservoir computation models.

6.6 Outlook and Perspectives

The value of exploring new paradigms in computation cannot be overstated, as the challenges of moving "beyond CMOS" undoubtedly provide inspiration and motivation for the next generation of scientists and engineers. Likewise, elucidating the fundamental nature

of intelligence remains a question for the ages in fields spanning all of human endeavor. Drawing on a historical perspective of seminal developments in computer science, complex systems theory and neuroscience, we have set out to propose a hardware-based approach to neuromorphic computation that aims to harness the power of highly coupled, nonlinear systems. We feel that the perspectives and results described herein represent a potentially important link between the requirements for real-time, multi-sensory computation and on-going advances in neuroscience through a readily addressable physical system with collective behaviors analogous to those currently observed in biological neural networks.

Research into applications of artificial neural networks toward biologically inspired computation has been greatly facilitated by modern developments in neuroscience. Recent findings have shown biological neural networks to operate in a persistent critical state, a feature commonly associated with the critical point of a second-order phase transition and power law scaling of internal system dynamics[KSC09, Chi10]. Under such circumstances, the system correlation length diverges in both space and time, whereby the influence of past events decays slowly and physically distinct points within the system are coupled regardless of the magnitude of separation. Spatiotemporal correlations of this type have been shown to maximize memory, transmission of information, and adaptability within complex networks, such that each part of the system is communicating with every other part of the brain, for every time of its history. A class of critical systems emerge from coupled networks of nonlinear elements governed by threshold dynamics that relax quickly compared to a slower external driving force, an arrangement that allows these systems to settle into a range of correlated metastable states. This model is more than superficially reminiscent of our current understanding of neural dynamics, and has been employed in recent forms of advanced neural network research including, but not limited, to reservoir methods such as liquid state machines and echo state networks.

To our knowledge, the self-assembled atomic switch network described here represents a unique implementation of a purpose-built electronic device composed of coupled nonlinear elements that clearly demonstrates critical dynamics. We propose that such a system provides a robust, flexible, and scalable experimental platform for controlled examinations

86

of criticality and its potential applicability in the fields of neuroscience and neuromorphic computation. Further, the inherent properties of single atomic switches and emergent behaviors observed in these complex atomic switch networks indicate a capacity for memory and learning via temporally correlated, metastable critical states[AH10]. Such an approach has potential utility for real-time, reservoir computation of multi-domain data systems such as those used in autonomous locomotion, proximity sensing and global positioning as well as a wide variety of sensing applications. Technological trends toward the growth of multi-domain and distributed sensing systems represent the seminal challenge for new forms of emerging computation in the centenary of Turing's birth.

CHAPTER 7

Conclusions

Determining control parameters for complex systems will be an increasingly important task for scientists working in the 3rd millennium. Previous trends in experimental tool development have encouraged focusing on the small, probing into single molecules and beyond, which has produced an enormous amount of interesting discoveries and technologies. The perspective of nanotechnology is now encouraging the development of techniques to build up from the bottom, designing materials and devices with mesoscale structures, fabricated by leveraging molecular properties to achieve some degree of self-assembly. We are now learning that, at a practical level, the basic laws governing such physical concepts as fundamental as transport and chemical transformation can be essentially system-dependent, and differ according to emergent size scales. This is especially true for dissipative non-equilibrium systems, which are a major source of the natural pattern formation mechanisms that nanotechnology aims to harness.

Now is the time to reckon with nonlinearity. It has been several decades since the rise of fractals, chaos, and the associated mathematics that seemed poised to extend our modeling capacity beyond the infinite cylinders and periodic boundary conditions that were necessary approximations for obtaining analytical solutions. Yet linearization remains the preferred approach to dealing with complexity, as it allows access to the complete library of computer math algorithms, maximizing computational performance. However, such simplification, while completely valid in many realistic contexts, has the basic consequence of flattening the attractor landscape and smoothing out the chaotic trajectories inherent to nonlinear interactions. By eliminating the possibility of "unexpected" resonant couplings between otherwise weakly linked parameters, the linearized model loses its capacity to capture complexity and

provide insight about unexpected behaviors and unforeseen dynamical phase transitions.

True, this is a difficult task. The demonstration of stable memory in threshold neural networks by Hopfield in 1982 represented a milestone for bio-inspired computing with a dynamical system. But this actual, tangible achievement required enforcing symmetry in connection strengths, strongly constraining the system dynamics, allowing only point attractors. New techniques are being developed to extract information from signals in increasingly nonspecific ways, trying to determine patterns and structures inside data without necessarily inputting a model to fit against. Cellular automata have been effectively employed in such tasks, developing the concept of *intrinsic computation* to be measured in terms of generic elements (memory, information production/transfer, logical operations, etc) which can be used to assess the computational power of dynamical systems, albeit largely restricted to off-line analysis of collected time series.

There will always be tradeoffs. But the dynamic form of available computing resources— for example, the recent rise of GPU utility for numerical simulations—means that there is no "slow-but-steady" incremental road to improving algorithmic performance, as the limiting constraints themselves are also changing. The tools of inquiry increasingly resemble the system of interest, which is a good sign to those who believe in the inherently hierarchical nature of complexity and ubiquity of self-organization towards critical interfaces. It is up to an emerging class of complex systems scientists to develop intuitions regarding the nature of control parameters, in both their theoretical and physical forms. It is simple enough to write down the formalism that functionally defines a control parameter; it is another business entirely to establish their functional form given all the parameters at work in a real complex system. This is the basic challenge facing researchers willing to take on complexity, embracing its essentially elusive and surprising character. Their payoff will be a profound advancement of understanding—the next quantum leap, as it were—along with the technology developed from this understanding, which will usefully control complex dynamical systems, that in turn will enable researches to open new fields of inquiry not yet visible from current perspectives.

As far as the current state of dynamic technology: seen through the lens of working with ASNs, the principle challenge is to obtain many reliable, simultaneous measurements of the

complex components. Time multiplexing is unsatisfactory, as it undermines the essential advantage of using complex dynamic components. However, interference between measurements, distinguishing between *external* stimulus signals (and their ghosts) and the *internal* dynamics of system response, and establishing criteria for characterizing the *initial state* of complex systems with inherent history dependence, to provide stable reference points that can be used to make meaningful comparisons between and aggregations of data from different experiments, are all significant challenges that underscore the famous difficulties in distinguishing observer from observed in a quantum universe. Some problems, it seems, manage to propagate quite easily through any hierarchy of size scales, be they extended in spatial or informational dimensions.

ASNs in particular must be understood in tandem with the measurement systems they interface with. Being itself a collection of wires hosting electronic flows mediated by time-dependent resistances, (mem-)capacitances, etc., coupling at electrode interfaces to more wires leading to semiconductor-based elements such as amplifiers, ADCs, and so on, it seems necessary to consider the entire ensemble as drawn on a single (complex) circuit diagram. This is not necessarily true for all dynamic technology development: for example, using non-linear optics to generate the complex dynamics could reduce the cross-coupling measurement issues to the points where the optical system is sampled and transduced for processing (assuming that this device still requires interfacing with conventional experimental hardware). ASN-based devices as we have built them truly are a single electronic system, where the simultaneous voltage measurements of distinct spatial regions within the network are approximately independent due to the high impedance of the electrode connections. But the switching activity in the network can produce effective impedance changes of many orders of magnitude, which can approach a small but significant percentage of the electrode resistance, and further development of the technology should account for these observer-observed type of effects in the measurement electronics as well as the ASN. Of course, from an RC perspective, this may amount to nothing more than expanding the reservoir, as the quantities of interest are the digitized time-series outputs, with the additional crosstalk coming out as just more high-dimensional dynamical richness for the linear classifiers to work on.

For now, this close connection between ASNs and more static computing devices should be viewed as a strength. It is a basic and confounding tenet of complex systems research that it is practically (and sometimes theoretically) impossible to reproduce experimental initial conditions, modify one parameter, and collect another data point. The systems have a history, and the parameters are usually multi-dimensional. From this perspective, there is a happy simplicity to restricting the signals of interest to electrical ones. The study of complexity is fundamentally interdisciplinary, and sticking with one physical medium for the device allows electrochemists and electrical engineers to bring their distinct-yet-connected intuitive understandings of electrical signals together, which is exactly the sort of synthesis that constitutes progress towards controlling complex systems and developing dynamic technology.

References

[Abe91]   Moshe Abeles. *Corticonics: Neural circuits of the cerebral cortex.* Cambridge University Press, 1991.

[AES09]   Rajagopal Ananthanarayanan, Steven K Esser, Horst D Simon, and Dharmendra S Modha. "The cat is out of the bag: cortical simulations with 109 neurons, 1013 synapses." In *High Performance Computing Networking, Storage and Analysis, Proceedings of the Conference on*, pp. 1–12. IEEE, 2009.

[AH10]   Lucilla de Arcangelis and Hans J Herrmann. "Learning as a phenomenon occurring in a critical state." *Proceedings of the National Academy of Sciences*, **107**(9):3977–3981, 2010.

[AHS85]   David H Ackley, Geoffrey E Hinton, and Terrence J Sejnowski. "A learning algorithm for Boltzmann machines." *Cognitive science*, **9**(1):147–169, 1985.

[AM59]   Roy L Allen and Walter J Moore. "Diffusion of Silver in Silver Sulfide." *The Journal of Physical Chemistry*, **63**(2):223–226, 1959.

[AMS13]   Audrius V Avizienis, Cristina Martin-Olmos, Henry O Sillin, Masakazu Aono, James K Gimzewski, and Adam Z Stieg. "Morphological Transitions from Dendrites to Nanowires in the Electroless Deposition of Silver." *Crystal Growth & Design*, **13**(2):465–469, 2013.

[AN00]   Larry F Abbott and Sacha B Nelson. "Synaptic plasticity: taming the beast." *Nature neuroscience*, **3**:1178–1183, 2000.

[And66]   Aleksandr Aleksandrovič Andronov. *Theory of Oscillators.*, volume 4. DoverPublications. com, 1966.

[ASM12]   Audrius V Avizienis, Henry O Sillin, Cristina Martin-Olmos, Hsien Hang Shieh, Masakazu Aono, Adam Z Stieg, and James K Gimzewski. "Neuromorphic atomic switch networks." *PloS one*, **7**(8):e42772, 2012.

[Bac78]   John Backus. "Can programming be liberated from the von Neumann style?: a functional style and its algebra of programs." *Communications of the ACM*, **21**(8):613–641, 1978.

[Bak97]   Per Bak. *How nature works.* Oxford university press Oxford, 1997.

[BG90]   Eshel Ben-Jacob and Peter Garik. "The formation of patterns in non-equilibrium growth." *Nature*, **343**:523–530, 1990.

[BGM88]   E. Ben-Jacob, P. Garik, T. Mueller, and D. Grier. "Characterization of morphology transitions in diffusion-controlled systems." *Phys. Rev. A*, **38**:1370–1380, Aug 1988.

[BGM10]   Danielle S Bassett, Daniel L Greenfield, Andreas Meyer-Lindenberg, Daniel R
          Weinberger, Simon W Moore, and Edward T Bullmore. "Efficient physical em-
          bedding of topologically complex information processing networks in brains and
          computer circuits." *PLoS computational biology*, **6**(4):e1000748, 2010.

[BLS09]   Julien Borghetti, Zhiyong Li, Joseph Straznicky, Xuema Li, Douglas AA Ohlberg,
          Wei Wu, Duncan R Stewart, and R Stanley Williams. "A hybrid nanomem-
          ristor/transistor logic circuit capable of self-programming." *Proceedings of the
          National Academy of Sciences*, **106**(6):1699–1703, 2009.

[BM95]   Dean V Buonomano and Michael M Merzenich. "Temporal information trans-
          formed into a spatial code by a neural network with realistic properties." *Science*,
          pp. 1028–1028, 1995.

[BM09]   Dean V Buonomano and Wolfgang Maass. "State-dependent computations:
          spatiotemporal processing in cortical networks." *Nature Reviews Neuroscience*,
          10(2):113–125, 2009.

[BMA06]   Danielle S Bassett, Andreas Meyer-Lindenberg, Sophie Achard, Thomas Duke,
          and Edward Bullmore. "Adaptive reconfiguration of fractal small-world human
          brain functional networks." *Proceedings of the National Academy of Sciences*,
          103(51):19518–19523, 2006.

[BN04]   Nils Bertschinger and Thomas Natschläger. "Real-time computation at the edge
          of chaos in recurrent neural networks." *Neural computation*, **16**(7):1413–1436,
          2004.

[BP03]   John M Beggs and Dietmar Plenz. "Neuronal avalanches in neocortical circuits."
          The Journal of neuroscience, **23**(35):11167–11177, 2003.

[BS09]   Ed Bullmore and Olaf Sporns. "Complex brain networks: graph theoretical
          analysis of structural and functional systems." *Nature Reviews Neuroscience*,
          10(3):186–198, 2009.

[BSL10]   Lars Büsing, Benjamin Schrauwen, and Robert Legenstein. "Connectivity, dy-
          namics, and memory in reservoir computing with binary and analog neurons."
          Neural computation, **22**(5):1272–1311, 2010.

[BWP11]   Danielle S Bassett, Nicholas F Wymbs, Mason A Porter, Peter J Mucha, Jean M
          Carlson, and Scott T Grafton. "Dynamic reconfiguration of human brain net-
          works during learning." *Proceedings of the National Academy of Sciences*,
          108(18):7641–7646, 2011.

[CBM03]   KK Caswell, Christopher M Bender, and Catherine J Murphy. "Seedless, surfac-
          tantless wet chemical synthesis of silver nanowires." *Nano Letters*, **3**(5):667–669,
          2003.

[CDL10]   Andy Chung, Jamal Deen, Jeong-Soo Lee, and M Meyyappan. "Nanoscale mem-
          ory devices." *Nanotechnology*, **21**(41):412001, 2010.

[CH93]   M. C. Cross and P. C. Hohenberg. "Pattern formation outside of equilibrium." *Rev. Mod. Phys.*, **65**:851–1112, Jul 1993.

[CHH02]   Murray Campbell, A Joseph Hoane Jr, and Feng-hsiung Hsu. "Deep blue." *Artificial intelligence*, **134**(1):57–83, 2002.

[Chi10]   Dante R Chialvo. "Emergent complex neural dynamics." *Nature Physics*, **6**(10):744–750, 2010.

[Chu71]   Leon Chua. "Memristor-the missing circuit element." *Circuit Theory, IEEE Transactions on*, **18**(5):507–519, 1971.

[Chu11]   Leon Chua. "Resistance switching memories are memristors." *Applied Physics A*, **102**(4):765–783, 2011.

[CJK11]   Ting Chang, Sung-Hyun Jo, Kuk-Hwan Kim, Patrick Sheridan, Siddharth Gaba, and Wei Lu. "Synaptic behaviors and modeling of a metal oxide memristive device." *Applied Physics A*, **102**(4):857–863, 2011.

[CKM04]   RJ Chimentao, I Kirm, F Medina, X Rodriguez, Y Cesteros, P Salagre, and JE Sueiras. "Different morphologies of silver nanoparticles as catalysts for the selective oxidation of styrene in the gas phase." *Chemical communications*, (7):846–847, 2004.

[CMS04]   Dmitri B Chklovskii, BW Mel, and K Svoboda. "Cortical rewiring and information storage." *Nature*, **431**(7010):782–788, 2004.

[CPD12]   Guy Z Cohen, Yuriy V Pershin, and Massimiliano Di Ventra. "Second and higher harmonics generation with memristive systems." *Applied Physics Letters*, **100**(13):133109–133109, 2012.

[CS00]   Phillip Christie and Dirk Stroobandt. "The interpretation and application of Rent's rule." *Very Large Scale Integration (VLSI) Systems, IEEE Transactions on*, **8**(6):639–648, 2000.

[CT03]   S Coombes and Y Timofeeva. "Sparks and waves in a stochastic fire-diffuse-fire model of Ca^{2+} release." *Physical Review E*, **68**(2):021915, 2003.

[CYS12]   Jose M Cruz-Albrecht, Michael W Yung, and Narayan Srinivasa. "Energy-efficient neuron, synapse and STDP integrated circuits." *Biomedical Circuits and Systems, IEEE Transactions on*, **6**(3):246–256, 2012.

[DGM08]   Sergey N Dorogovtsev, Alexander V Goltsev, and José FF Mendes. "Critical phenomena in complex networks." *Reviews of Modern Physics*, **80**(4):1275, 2008.

[DM07]   Rodney J Douglas and Kevan AC Martin. "Recurrent neuronal circuits in the neocortex." *Current Biology*, **17**(13):R496–R500, 2007.

[DMM95]   Rodney Douglas, Misha Mahowald, and Carver Mead. "Neuromorphic analogue VLSI." *Annual review of neuroscience*, **18**:255–281, 1995.

[FBH03]   Walter J Freeman, Brian C Burke, and Mark D Holmes. "Aperiodic phase re-
          setting in scalp EEG of beta–gamma oscillations by state transitions at alpha–
          theta rates." *Human brain mapping*, **19**(4):248–272, 2003.

[FKH94]   V Fleury, JH Kaufman, and DB Hibbert. "Mechanism of a morphology transition
          in ramified electrochemical growth." *Nature*, **367**(6462):435–438, 1994.

[FN93]   Ken-ichi Funahashi and Yuichi Nakamura. "Approximation of dynamical systems
          by continuous time recurrent neural networks." *Neural networks*, **6**(6):801–806,
          1993.

[Fri08]   Karl Friston. "Hierarchical models in the brain." *PLoS Computational Biology*,
          4(11):e1000211, 2008.

[FS03]   Chrisantha Fernando and Sampsa Sojakka. "Pattern recognition in a bucket." In
          Advances in Artificial Life, pp. 588–597. Springer, 2003.

[GBB08]   Smita Gohil, Rajarshi Banerjee, Sangita Bose, and Pushan Ayyub. "Influence of
          synthesis conditions on the nanostructure of immiscible copper–silver alloy thin
          films." *Scripta Materialia*, **58**(10):842–845, 2008.

[GBC86]   D Grier, E Ben-Jacob, Roy Clarke, and L-M_ Sander. "Morphology and mi-
          crostructure in electrochemical deposition of zinc." *Physical review letters*,
          56(12):1264, 1986.

[GHS08]   Surya Ganguli, Dongsung Huh, and Haim Sompolinsky. "Memory traces
          in dynamical systems." *Proceedings of the National Academy of Sciences*,
          105(48):18970–18975, 2008.

[Gol09]   Mark S Goldman. "Memory without feedback in a neural network." *Neuron*,
          61(4):621–634, 2009.

[GS10]   Pablo M Gleiser and Victor I Spoormaker. "Modelling hierarchical structure in
          functional brain networks." *Philosophical Transactions of the Royal Society A:
          Mathematical, Physical and Engineering Sciences*, **368**(1933):5633–5644, 2010.

[GSC84]   BH Grier, SM Shapiro, and RJ Cava. "Inelastic neutron scattering measurements
          of the diffusion in β-Ag_ {2} S." *Physical Review B*, **29**(7):3810, 1984.

[HB05]   Clayton Haldeman and John M Beggs. "Critical branching captures activity in
          living neural networks and maximizes the number of metastable states." *Physical
          review letters*, **94**(5):058101, 2005.

[HBT11]   Atif Hashmi, Hugues Berry, Olivier Temam, and Mikko Lipasti. "Automatic
          abstraction and fault tolerance in cortical microachitectures." In *ACM SIGARCH
          Computer Architecture News*, volume 39, pp. 1–10. ACM, 2011.

[Heb49]   DO Hebb. "The organization of behavior: A neuropsychological theory.", 1949.

[HMH01]   Ron Ho, Kenneth W Mai, and Mark A Horowitz. "The future of wires." *Proceedings of the IEEE*, **89**(4):490–504, 2001.

[Hop82]   John J Hopfield. "Neural networks and physical systems with emergent collective computational abilities." *Proceedings of the national academy of sciences*, **79**(8):2554–2558, 1982.

[HOT10]   Tsuyoshi Hasegawa, Takeo Ohno, Kazuya Terabe, Tohru Tsuruoka, Tomonobu Nakayama, James K Gimzewski, and Masakazu Aono. "Learning Abilities Achieved by a Single Solid-State Atomic Switch." *Advanced Materials*, **22**(16):1831–1834, 2010.

[HT85]   John J Hopfield and David W Tank. "Neural computation of decisions in optimization problems." *Biological cybernetics*, **52**(3):141–152, 1985.

[ILH11a]   Giacomo Indiveri, Bernabe Linares-Barranco, Tara Julia Hamilton, André van Schaik, Ralph Etienne-Cummings, Tobi Delbruck, Shih-Chii Liu, Piotr Dudek, Philipp Häfliger, Sylvie Renaud, et al. "Frontiers: Neuromorphic Silicon Neuron Circuits." *Frontiers in Neuromorphic Engineering*, **5**, 2011.

[ILH11b]   Giacomo Indiveri, Bernabé Linares-Barranco, Tara Julia Hamilton, André Van Schaik, Ralph Etienne-Cummings, Tobi Delbruck, Shih-Chii Liu, Piotr Dudek, Philipp Häfliger, Sylvie Renaud, et al. "Neuromorphic silicon neuron circuits." *Frontiers in neuroscience*, **5**, 2011.

[INC10]   Daniele Ielmini, Federico Nardi, and Carlo Cagli. "Resistance-dependent amplitude of random telegraph-signal noise in resistive switching memories." *Applied Physics Letters*, **96**(5):053503–053503, 2010.

[Jae01]   Herbert Jaeger. "The" echo state" approach to analysing and training recurrent neural networks-with an erratum note'." *Bonn, Germany: German National Research Center for Information Technology GMD Technical Report*, **148**, 2001.

[Jae02]   Herbert Jaeger. *Tutorial on training recurrent neural networks, covering BPPT, RTRL, EKF and the" echo state network" approach.* GMD-Forschungszentrum Informationstechnik, 2002.

[JCE10]   Sung Hyun Jo, Ting Chang, Idongesit Ebong, Bhavitavya B Bhadviya, Pinaki Mazumder, and Wei Lu. "Nanoscale memristor device as synapse in neuromorphic systems." *Nano letters*, **10**(4):1297–1301, 2010.

[Jen98]   Henrik Jeldtoft Jensen. *Self-organized criticality: emergent complex behavior in physical and biological systems*, volume 10. Cambridge university press, 1998.

[JGA00]   Ch Joachim, JK Gimzewski, and A Aviram. "Electronics using hybrid-molecular and mono-molecular devices." *Nature*, **408**(6812):541–548, 2000.

[JKZ13]   Doo Seok Jeong, Inho Kim, Martin Ziegler, and Hermann Kohlstedt. "Towards artificial neurons and synapses: a materials point of view." *RSC Advances*, **3**(10):3169–3183, 2013.

[KA95]   Alexander Kuhn and Françoise Argoul. "Diffusion-limited kinetics in thin-gap electroless deposition." *Journal of Electroanalytical Chemistry*, **397**(1):93–104, 1995.

[KAM94]   A Kuhn, F Argoul, JF Muzy, and A Arneodo. "Structural analysis of electroless deposits in the diffusion-limited regime." *Physical review letters*, **73**(22):2998, 1994.

[Kes82]   Marvin S Keshner. "1/f noise." *Proceedings of the IEEE*, **70**(3):212–218, 1982.

[KGW11]   Kuk-Hwan Kim, Siddharth Gaba, Dana Wheeler, Jose M Cruz-Albrecht, Tahir Hussain, Narayan Srinivasa, and Wei Lu. "A functional hybrid memristor crossbar-array/CMOS system for data storage and neuromorphic applications." *Nano letters*, **12**(1):389–395, 2011.

[KH12]   Chien Lin Kuo and Kuo Chu Hwang. "Nitrate ion promoted formation of Ag nanowires in polyol processes: a new nanowire growth mechanism." *Langmuir*, **28**(8):3722–3729, 2012.

[KJY12]   Duygu Kuzum, Rakesh Gnana David Jeyasingh, Shimeng Yu, and H-SP Wong. "Low-Energy Robust Neuromorphic Computation Using Synaptic Devices." 2012.

[Kos93]   Ernst L Koschmieder. *Bénard cells and Taylor vortices*. Cambridge University Press, 1993.

[KPB05]   Robert Kozma, Marko Puljic, Paul Balister, Bela Bollobás, and Walter J Freeman. "Phase transitions in the neuropercolation model of neural populations with mixed local and non-local interactions." *Biological Cybernetics*, **92**(6):367–379, 2005.

[KRA10]   Arvind Kumar, Stefan Rotter, and Ad Aertsen. "Spiking activity propagation in neuronal networks: reconciling different perspectives on neural coding." *Nature Reviews Neuroscience*, **11**(9):615–627, 2010.

[KRL11]   Carsten Kügeler, Roland Rosezin, Eike Linn, Rainer Bruchhaus, and Rainer Waser. "Materials, technologies, and circuit concepts for nanocrossbar-based bipolar RRAM." *Applied Physics A*, **102**(4):791–809, 2011.

[KSC09]   Manfred G Kitzbichler, Marie L Smith, Søren R Christensen, and Ed Bullmore. "Broadband criticality of human brain network synchronization." *PLoS computational biology*, **5**(3):e1000314, 2009.

[KTH06]   Manisha Kundu, Kazuya Terabe, Tsuyoshi Hasegawa, and Masakazu Aono. "Effect of sulfurization conditions and post-deposition annealing treatment on structural and electrical properties of silver sulfide films." *Journal of applied physics*, **99**(10):103501–103501, 2006.

[Lan80]   J. S. Langer. "Instabilities and pattern formation in crystal growth." *Rev. Mod. Phys.*, **52**:1–28, Jan 1980.

[Lan90]   Chris G Langton. "Computation at the edge of chaos: phase transitions and emergent computation." *Physica D: Nonlinear Phenomena*, **42**(1):12–37, 1990.

[LHG07]   Anna Levina, J Michael Herrmann, and Theo Geisel. "Dynamical synapses causing self-organized criticality in neural networks." *Nature Physics*, **3**(12):857–860, 2007.

[LJ09]   Mantas LukošEvičIus and Herbert Jaeger. "Survey: Reservoir computing approaches to recurrent neural network training." *Computer Science Review*, **3**(3):127–149, 2009.

[LMM03]   Konstantin Likharev, Andreas Mayr, Ibrahim Muckra, and Özgür Türel. "Cross-Nets: High-Performance Neuromorphic Architectures for CMOL Circuits." *Annals of the New York Academy of Sciences*, **1006**(1):146–163, 2003.

[LPT09]   Andreea Lazar, Gordon Pipa, and Jochen Triesch. "SORN: a self-organizing recurrent neural network." *Frontiers in computational neuroscience*, **3**, 2009.

[LR71]   Bernard S Landman and Roy L Russo. "On a pin versus block relationship for partitions of logic graphs." *Computers, IEEE Transactions on*, **100**(12):1469–1479, 1971.

[LS05]   Konstantin K Likharev and Dmitri B Strukov. "CMOL: Devices, circuits, and architectures." In *Introducing Molecular Electronics*, pp. 447–477. Springer, 2005.

[LS11]   Ran Liu and Ayusman Sen. "Unified synthetic approach to silver nanostructures by galvanic displacement reaction on copper: from nanobelts to nanoshells." *Chemistry of Materials*, **24**(1):48–54, 2011.

[LSZ09]   Sa Lv, Hui Suo, Tieli Zhou, Chunxu Wang, Shengyu Jing, Qingbo Fu, Yanan Xu, and Chun Zhao. "Effect of synthesis route on the morphologies of silver nanostructures by galvanic displacement reaction." *Solid State Communications*, **149**(5):227–230, 2009.

[LZL10]   Qianxi Lai, Lei Zhang, Zhiyong Li, William F Stickle, R Stanley Williams, and Yong Chen. "Ionic/electronic hybrid materials integrated in a synaptic transistor with signal processing and learning functions." *Advanced Materials*, **22**(22):2448–2453, 2010.

[Ma00]   Shang-Keng Ma. *Modern theory of critical phenomena.* Number 46. Da Capo Press, 2000.

[Man77]   Benoit B Mandelbrot. *Fractals: form, chance, and dimension.* WH Freeman San Francisco, 1977.

[MD91]   Misha Mahowald and Rodney Douglas. "A silicon neuron." *Nature*, **354**(6354):515–518, 1991.

[Mea90]   Carver Mead. "Neuromorphic electronic systems." *Proceedings of the IEEE*, **78**(10):1629–1636, 1990.

[MLF09]   David Meunier, Renaud Lambiotte, Alex Fornito, Karen D Ersche, and Edward T Bullmore. "Hierarchical modularity in human brain functional networks." *Frontiers in neuroinformatics*, **3**, 2009.

[MM88]   Carver A Mead and Misha A Mahowald. "A silicon model of early visual processing." *Neural networks*, **1**(1):91–97, 1988.

[MM09]   Brendan K Murphy and Kenneth D Miller. "Balanced amplification: a new mechanism of selective amplification of neural activity patterns." *Neuron*, **61**(4):635–648, 2009.

[MMK10]   Daniel Millman, Stefan Mihalas, Alfredo Kirkwood, and Ernst Niebur. "Self-organized criticality occurs in non-conservative neuronal networks during/up/'states." *Nature physics*, **6**(10):801–805, 2010.

[MNM02]   Wolfgang Maass, Thomas Natschläger, and Henry Markram. "Real-time computing without stable states: A new framework for neural computation based on perturbations." *Neural computation*, **14**(11):2531–2560, 2002.

[Mos73]   Jürgen Moser. *Stable and Random Motions in Dynamical Systems: With Special Emphasis on Celestial Mechaniscs*, volume 1. Princeton University Press, 1973.

[MS64]   WILLIAM W Mullins and RF Sekerka. "Stability of a planar interface during solidification of a dilute binary alloy." *Journal of Applied Physics*, **35**(2):444–451, 1964.

[MSH84]   M Matsushita, M Sano, Y Hayakawa, H Honjo, and Y Sawada. "Fractal structures of zinc metal leaves grown by electrodeposition." *Physical review letters*, **53**(3):286, 1984.

[MSU97]   Satoru Miyashita, Yukio Saito, and Makio Uwaha. "Experimental evidence of dynamical scaling in a two-dimensional fractal growth." *Journal of the Physical Society of Japan*, **66**(4):929–932, 1997.

[MSU05]   Satoru Miyashita, Yukio Saito, and Makio Uwaha. "Fractal aggregation growth and the surrounding diffusion field." *Journal of crystal growth*, **283**(3):533–539, 2005.

[MVW12]   Cristina Martin-Olmos, L Guillermo Villanueva, Peter D van der Wal, Andreu Llobera, Nico F de Rooij, Jürgen Brugger, and Francesc Perez-Murano. "Conductivity of SU-8 Thin Films through Atomic Force Microscopy Nano-Patterning." *Advanced Functional Materials*, **22**(7):1482–1488, 2012.

[Nag89]   Takashi Nagatani. "Growth model with phase transition: Drift-diffusion-limited aggregation." *Physical Review A*, **39**(1):438, 1989.

[nan11]   "2011 International Technology Roadmap for Semiconductors: Emerging Research Devices." 2011.

[NE97]   Shuming Nie and Steven R Emory. "Probing single molecules and single nanoparticles by surface-enhanced Raman scattering." *science*, **275**(5303):1102–1106, 1997.

[Neu88]   John von Neumann. "The principles of large-scale computing machines." *IEEE Annals of the History of Computing*, **10**(4):243–256, 1988.

[NM84]   Grégoire Nicolis and M Malek Mansour. "Onset of spatial correlations in nonequilibrium systems: a master-equation description." *Physical Review A*, **29**(5):2845–2853, 1984.

[NPN89]   Gregoire Nicolis, Ilya Prigogine, and G Nocolis. "Exploring complexity." 1989.

[Ohn91]   Izumi Ohno. "Electrochemistry of electroless plating." *Materials Science and Engineering: A*, **146**(1):33–49, 1991.

[OHT11]   Takeo Ohno, Tsuyoshi Hasegawa, Tohru Tsuruoka, Kazuya Terabe, James K Gimzewski, and Masakazu Aono. "Short-term plasticity and long-term potentiation mimicked in single inorganic synapses." *Nature Materials*, **10**(8):591–595, 2011.

[OS11]   Ehsan Nedaaee Oskoee and Muhammad Sahimi. "Electric currents in networks of interconnected memristors." *Physical Review E*, **83**(3):031105, 2011.

[PD10]   Yuriy V Pershin and Massimiliano Di Ventra. "Experimental demonstration of associative memory with memristive neural networks." *Neural Networks*, **23**(7):881–886, 2010.

[PDS12]   Yvan Paquot, Francois Duport, Antoneo Smerieri, Joni Dambre, Benjamin Schrauwen, Marc Haelterman, and Serge Massar. "Optoelectronic reservoir computing." *Scientific reports*, **2**, 2012.

[Pri67]   Ilya Prigogine. "Introduction to thermodynamics of irreversible processes." *New York: Interscience, 1967, 3rd ed.*, **1**, 1967.

[PZW07]   Benjamin Y Park, Rabih Zaouk, Chunlei Wang, and Marc J Madou. "A case for fractal electrodes in electrochemical applications." *Journal of the Electrochemical Society*, **154**(2):P1–P5, 2007.

[RB91]   Kristen S Ralls and Robert A Buhrman. "Microscopic study of 1/f noise in metal nanobridges." *Physical Review B*, **44**(11):5800, 1991.

[RJ08]   Nathan C Rowland and Dieter Jaeger. "Responses to tactile stimulation in deep cerebellar nucleus neurons result from recurrent activation in multiple pathways." *Journal of neurophysiology*, **99**(2):704–717, 2008.

[RJB96]   VP Roychowdhury, DB Janes, S Bandyopadhyay, and Xiaodong Wang. "Collective computational activity in self-assembled arrays of quantum dots: a novel neuromorphic architecture for nanoelectronics." *Electron Devices, IEEE Transactions on*, **43**(10):1688–1699, 1996.

[RLT96]   Douglas Ridgway, Herbert Levine, and Yuhai Tu. "Front stability in mean-field models of diffusion-limited growth." *Physical Review E*, **53**(1):861, 1996.

[RM07]   Md Harunar Rashid and Tarun K Mandal. "Synthesis and catalytic application of nanostructured silver dendrites." *The Journal of Physical Chemistry C*, **111**(45):16750–16760, 2007.

[Ros58]   Frank Rosenblatt. "The perceptron: a probabilistic model for information storage and organization in the brain." *Psychological review*, **65**(6):386, 1958.

[RYG09]   Mahendra Rai, Alka Yadav, and Aniket Gade. "Silver nanoparticles as a new generation of antimicrobials." *Biotechnology advances*, **27**(1):76–83, 2009.

[SAS12]   Adam Z Stieg, Audrius V Avizienis, Henry O Sillin, Cristina Martin-Olmos, Masakazu Aono, and James K Gimzewski. "Emergent Criticality in Complex Turing B-Type Atomic Switch Networks." *Advanced Materials*, **24**(2):286–293, 2012.

[SB93]   Ofer Shochet and Eshel Ben-Jacob. "Coexistence of morphologies in diffusive patterning." *Physical Review E*, **48**(6):R4168, 1993.

[SB98]   Ronen Segev and Eshel Ben-Jacob. "Self-wiring of neural networks." *Physics Letters A*, **237**(4):307–313, 1998.

[SCK04]   Olaf Sporns, Dante R Chialvo, Marcus Kaiser, and Claus C Hilgetag. "Organization, development and function of complex brain networks." *Trends in cognitive sciences*, **8**(9):418–425, 2004.

[SDG86]   Yasuji Sawada, A Dougherty, and JP Gollub. "Dendritic and fractal patterns in electrolytic metal deposits." *Physical review letters*, **56**(12):1260, 1986.

[Sea80]   John R Searle et al. "Minds, brains, and programs." *Behavioral and brain sciences*, **3**(3):417–457, 1980.

[Sha48]   Claude E Shannon. "A Mathematical Theory of Communication." *Bell system technical journal*, **23**(3):656–715, 1948.

[Sim62]   Herbert A Simon. "The architecture of complexity." *Proceedings of the American philosophical society*, **106**(6):467–482, 1962.

[SKJ11]   Kyungah Seo, Insung Kim, Seungjae Jung, Minseok Jo, Sangsu Park, Jubong Park, Jungho Shin, Kuyyadi P Biju, Jaemin Kong, Kwanghee Lee, et al. "Analog memory and spike-timing-dependent plasticity characteristics of a nanoscale titanium oxide bilayer resistive switching device." *Nanotechnology*, **22**(25):254023, 2011.

[SMS04]   Felix Schürmann, Karlheinz Meier, and Johannes Schemmel. "Edge of chaos computation in mixed-mode vlsi-a hard liquid." In *Advances in Neural Information Processing Systems*, pp. 1201–1208, 2004.

[SSS08]   Dmitri B Strukov, Gregory S Snider, Duncan R Stewart, and R Stanley Williams. "The missing memristor found." *Nature*, **453**(7191):80–83, 2008.

[Str01]   Steven H Strogatz. "Exploring complex networks." *Nature*, **410**(6825):268–276, 2001.

[SVV07]   Benjamin Schrauwen, David Verstraeten, and Jan Van Campenhout. "An overview of reservoir computing: theory, applications and implementations." 2007.

[SWB07]   Thomas Serre, Lior Wolf, Stanley Bileschi, Maximilian Riesenhuber, and Tomaso Poggio. "Robust object recognition with cortex-like mechanisms." *Pattern Analysis and Machine Intelligence, IEEE Transactions on*, **29**(3):411–426, 2007.

[SYY11]   Woodrow L Shew, Hongdian Yang, Shan Yu, Rajarshi Roy, and Dietmar Plenz. "Information capacity and transmission are maximized in balanced cortical networks with neuronal avalanches." *The Journal of Neuroscience*, **31**(1):55–63, 2011.

[TFF08]   Antonio Torralba, Robert Fergus, and William T Freeman. "80 million tiny images: A large data set for nonparametric object and scene recognition." *Pattern Analysis and Machine Intelligence, IEEE Transactions on*, **30**(11):1958–1970, 2008.

[TFM96]   Simon Thorpe, Denis Fize, Catherine Marlot, et al. "Speed of processing in the human visual system." *nature*, **381**(6582):520–522, 1996.

[TFS08]   Paul Tiesinga, Jean-Marc Fellous, and Terrence J Sejnowski. "Regulation of spike timing in visual cortical circuits." *Nature Reviews Neuroscience*, **9**(2):97–107, 2008.

[TGL11]   Christof Teuscher, Cristian Grecu, Ting Lu, and Ron Weiss. "Challenges and promises of nano and bio communication networks." In *Networks on Chip (NoCS), 2011 Fifth IEEE/ACM International Symposium on*, pp. 247–254. IEEE, 2011.

[TH08]   Christof Teuscher and Anders A Hansson. "Non-traditional irregular interconnects for massive scale SoC." In *Circuits and Systems, 2008. ISCAS 2008. IEEE International Symposium on*, pp. 2785–2788. IEEE, 2008.

[THN05]   K Terabe, T Hasegawa, T Nakayama, and M Aono. "Quantized conductance atomic switch." *Nature*, **433**(7021):47–50, 2005.

[Tur50]   Alan Turing. "Mind-A Quarterly Review of Psychology and Philosophy." *Vol. LIX*, (236), 1950.

[Tur92]   AM Turing. "Intelligent Machinery, report for the National Physical Laboratory, 1948.", 1992.

[TVH02]   James M Tour, William L Van Zandt, Christopher P Husband, Summer M Husband, Lauren S Wilson, Paul D Franzon, and David P Nackashi. "Nanocell logic gates for molecular computing." *Nanotechnology, IEEE Transactions on*, **1**(2):100–109, 2002.

[Ull07]   Shimon Ullman. "Object recognition and segmentation by a fragment-based hierarchy." *Trends in cognitive sciences*, **11**(2):58–64, 2007.

[Van95]   Tim Van Gelder. "What might cognition be, if not computation?" *The Journal of Philosophy*, **92**(7):345–381, 1995.

[VSd07]   David Verstraeten, Benjamin Schrauwen, Michiel dHaene, and Dirk Stroobandt. "An experimental unification of reservoir computing methods." *Neural Networks*, **20**(3):391–403, 2007.

[WA07]   Rainer Waser and Masakazu Aono. "Nanoionics-based resistive switching memories." *Nature materials*, **6**(11):833–840, 2007.

[Wer07]   Gerhard Werner. "Metastability, criticality and phase transitions in brain and its models." *Biosystems*, **90**(2):496–508, 2007.

[WKT07]   Zhongchang Wang, Takuya Kadohira, Tomofumi Tada, and Satoshi Watanabe. "Nonequilibrium quantum transport properties of a silver atomic switch." *Nano letters*, **7**(9):2688–2692, 2007.

[WS81]   TA Witten Jr and Leonard M Sander. "Diffusion-limited aggregation, a kinetic critical phenomenon." *Physical review letters*, **47**(19):1400, 1981.

[WXM06]   Xiaogang Wen, Yu-Tao Xie, Wing Cheung Mak, Kwan Yee Cheung, Xiao-Yuan Li, Reinhard Renneberg, and Shihe Yang. "Dendritic nanostructures of silver: facile synthesis, structural characterizations, and sensing applications." *Langmuir*, **22**(10):4836–4842, 2006.

[XBW10]   Zhi Xu, Yoshio Bando, Wenlong Wang, Xuedong Bai, and Dmitri Golberg. "Real-time in situ HRTEM-resolved resistance switching of Ag2S nanoscale ionic conductor." *ACS nano*, **4**(5):2515–2522, 2010.

[XH05]   Younan Xia and Naomi J Halas. "Shape-controlled synthesis and surface plasmonic properties of metallic nanostructures." *MRS bulletin*, **30**(05):338–348, 2005.

[XRC09]   Qiangfei Xia, Warren Robinett, Michael W Cumbie, Neel Banerjee, Thomas J Cardinali, J Joshua Yang, Wei Wu, Xuema Li, William M Tong, Dmitri B Strukov, et al. "Memristor- CMOS hybrid integrated circuits for reconfigurable logic." *Nano letters*, **9**(10):3640–3645, 2009.

[YCY11]   Hongjun You, Feng Chen, Shengchun Yang, Zhimao Yang, Bingjun Ding, Shuhua Liang, and Xiaoping Song. "Size Effect on Nanoparticle-Mediated Silver Crystal Growth." *Crystal Growth & Design*, **11**(12):5449–5456, 2011.

[YTL12] Rui Yang, Kazuya Terabe, Guangqiang Liu, Tohru Tsuruoka, Tsuyoshi Hasegawa, James K Gimzewski, and Masakazu Aono. "On-demand nanodevice with electrical and neuromorphic multifunction realized by local ion migration." *ACS nano*, **6**(11):9515–9521, 2012.

[ZAD10] WS Zhao, G Agnus, V Derycke, A Filoramo, JP Bourgoin, and C Gamrat. "Nanotube devices based crossbar architecture: toward neuromorphic computing." *Nanotechnology*, **21**(17):175202, 2010.